

ENHANCING A SIMPLE WATER-BASED PHOTOVOLTAIC-THERMAL (PVT)
SOLAR COLLECTOR USING CFD ANALYSIS

by

Marwan Hicham Osman

A Thesis presented to the Faculty of the
American University of Sharjah
College of Engineering
In Partial Fulfillment
of the Requirements
for the Degree of

Master of Science in
Mechanical Engineering

Sharjah, United Arab Emirates

July 2019

Approval Signatures

We, the undersigned, approve the Master's Thesis of Marwan Hicham Osman.

Thesis Title: Enhancing a Simple Water-Based Photovoltaic-Thermal (PVT) Solar Collector Using CFD Analysis.

Signature	Date of Signature (dd/mm/yyyy)
_____ Dr. Mehmet Fatih Orhan Associate Professor, Department of Mechanical Engineering Thesis Advisor	_____
_____ Dr. Mohammad Omar Hamdan Associate Professor, Department of Mechanical Engineering Thesis Co-Advisor	_____
_____ Dr. Rachid Mohamed Chebbi Professor, Department of Chemical Engineering Thesis Committee Member	_____
_____ Dr. Bassam Abdel Jaber Abu-Nabah Associate Professor, Department of Mechanical Engineering Thesis Committee Member	_____
_____ Dr. Mamoun Abdel-Hafez Head, Department of Mechanical Engineering	_____
_____ Dr. Lotfi Romdhane Associate Dean, College of Engineering	_____
_____ Dr. Naif Darwish Acting Dean, College of Engineering	_____
_____ Dr. Mohamed El-Tarhuni Vice Provost for Graduate Studies	_____

Acknowledgement

I would like to acknowledge my gratitude and render my warmest thanks to my advisors Dr. Mehmet Fatih Orhan and Dr. Mohammad Omar Hamdan for helping me throughout all stages of this journey. Their friendly guidance and expert advice made this work possible.

I would also wish to express my gratitude to the examination committee Dr. Rachid Mohamed Chebbi and Dr. Bassam Abdel Jaber Abu-Nabah for extended discussions and valuable suggestions.

My completion of this project could not have been accomplished without my family who had the greatest indirect contribution to this work. Also, a warm thanks to my friends for supporting me and Special thanks to Eng. Abdulrahman Al-Khaldi and Eng. Mustafa Al-Akshar for the fruitful discussions and assistance.

I would like to acknowledge and thank the American University of Sharjah for allowing me to conduct my research and providing assistance throughout all stages of the work.

Dedication

To my family ...

Abstract

Photovoltaics thermal collectors are gaining more attention due to their promising potential to pave the way for the penetration of solar energy in modern day power generation technologies. PVTs' flexibility, manufacturability, high efficiency, and multi-output nature inspired many innovative designs and design improvements available in the literature. PVT solar collectors conventionally attach PV cell(s) to a solar thermal collector to simultaneously generate electrical and thermal energies from the same solar input. The advantages of PVTs are twofold. First, extraction of the generated heat from the PV cells to be utilized in end-user applications, most often space heating or direct hot water (DHW). Second, maintaining the PV cells at a reasonable operating temperature, which reflects on the cells' conversion efficiency and longevity. This study aims to design a PVT system and optimize its operation to maximize overall efficiencies using a zero-dimensional model along with a detailed Computational Fluid Dynamics (CFD) analysis of the thermal collector. The PVT performance can be investigated by determining its thermal and electrical characteristics. The approach taken in this study to analyze the PVT collector is separated into two main sections, energy and exergy analyses in which the thermal, electrical and overall efficiencies are evaluated. The zero-dimensional model involves controlling heat convection of the PV to study the trade-off between high water outlet temperature and electrical conversion efficiency. A detailed CFD analysis is conducted to evaluate the performance of a workable design for the PVT hybrid system. Then, the CFD analysis is used to calculate the overall convection heat transfer for a PVT system. By applying the mathematical model, the effect of flow rate and the inlet temperature on the energy and exergy efficiency has been tested. It was observed that the overall efficiency and exergy of the PVT increase as the mass flow rate increased. This study demonstrated that, the optimum inlet water temperature to maximize the overall exergy generated by the system at any operating conditions can be achieved. Nevertheless, the performance of the PVT was tested at different thermal conductivity and collector geometries to see the effect on the overall exergy and energy efficiency.

Keywords: *Solar energy; Solar collectors; Photovoltaics thermal (PVT); Photovoltaic cells.*

Table of Contents

Abstract	6
List of Figures	8
List of Tables	10
Abbreviations	11
Chapter 1. Introduction	13
1.1. Overview	13
1.2. Thesis Objectives	15
1.3. Research Contribution.....	16
1.4. Thesis Organization.....	16
Chapter 2. Theoretical Background and Literature Review	17
2.1. Limitation of PV Systems	17
2.2. Cooling Techniques for PV Panel.....	18
2.2.1. Passive cooling techniques.	18
2.2.2. Active cooling methods.	21
2.3. PVT Principles and Performance	24
2.4. Flat Plate PVT Collector Classification	27
2.4.1. PVT water collector.	28
2.4.2. PVT air collector.....	43
2.4.3. Combination of water and/or air PVT collector.	50
Chapter 3: System Description and Numerical Simulation	54
3.1. Assumptions	55
3.2. Grid Generation and Solution Procedure	56
3.3. Mesh Independence and Model Validation.....	58
3.4. CFD Results and Overall Convection Coefficient Calculation.....	63
Chapter 4: Analysis.....	67
Chapter 5: Results and Discussion.....	72
Chapter 6: Conclusions	84
References.....	86
Vita.....	93

List of Figures

Figure 1. Classification of solar energy systems.	14
Figure 2. I-V curve of a PV module with different cell/ modules temperatures [1]... 18	18
Figure 3. Configuration of panel B, showing the air channel between the PV panel and the roof (Adopted from [10]).	19
Figure 4. Thermosyphon effect used on PVT system [14].	20
Figure 5. Forced air cooling [19].	22
Figure 6. Water cooling technique (Adopted from [22]).	23
Figure 7. Typical PV system components (Adopted from [31]).	25
Figure 8. Types of PVT collectors (Adopted from [38]).	27
Figure 9. Schematic diagram of PVT water based system (Adopted from [36]).	29
Figure 10. PVT water collector with absorber underneath the solar panel [47].	30
Figure 11. Single pass PVT air collector.	43
Figure 12. Schematic diagram of PVT air based system (Adopted from [36]).	44
Figure 13. Cross-section of unglazed PVT air (a): (i) with tedlar and (ii) without tedlar and (b): (i) glazed with tedlar and (ii) without tedlar (Adopted from [83]).	45
Figure 14. Cross-section of a single pass PVT air collector with Compound Parabolic Concentrator (CPC) and fins (Adopted from [86]).	46
Figure 15. Cross-section of PVT air collector with rectangular shape absorber collector design (Adopted from [39]).	46
Figure 16. Single pass PVT with finned of double duct PVT air heaters (Adopted from [87]).	47
Figure 17. Single pass PVT with rectangular tunnel design [88].	47
Figure 18. Cross-section of double pass PVT solar collector.	48
Figure 19. Cross-section of double pass PVT solar collector with fins (Adopted from [90]).	49
Figure 20. Cross-section of double pass PVT solar collector with fins and CPC (Adopted from [90]).	49
Figure 21. Cross-section of the PVT experiment model (Adopted from [51]).	51
Figure 22. Cross-section of PVT collector models (Adopted from [92]).	52
Figure 23. Cross-section of bi-fluid PVT (water and air) collector [93].	53
Figure 24. Schematic representation of the cooling channel attached to the PV.	54
Figure 25. Methodology of the study.	56
Figure 26. CFD meshing of the rectangular duct.	57
Figure 27. Mesh independence study by checking outlet velocity and inlet pressure.	59
Figure 28. Mesh independence study by inspecting outlet temperature.	60
Figure 29. Variation of Nusselt number through the duct.	61
Figure 30. Variation of friction coefficient along the duct.	62
Figure 31. The pressure across the duct.	62
Figure 32. The convection coefficient of the PV and inlet pressure against the thickness of the channel.	63
Figure 33. The overall convection coefficient at different thermal conductivity of the solid material.	64
Figure 34. Dimensions of the cooling channel.	64
Figure 35. The overall convection coefficient at different wall thickness, t (mm).	65

Figure 36. The overall convection coefficient of PV against different W/H ratio.	65
Figure 37. Reynolds number at different W/H ratio.	66
Figure 38. The overall convection coefficient of PV against different a/b ratio.	66
Figure 39. The overall solar irradiance reaching the PV.	67
Figure 40. The PV temperature at different irradiation for different mass flow rate...	72
Figure 41. Variation of energy efficiencies (Thermal, Electrical and Overall) with mass flow rate under 1000 W/m ²	73
Figure 42. Variation of exergy efficiencies (Thermal, Electrical and Overall) with mass flow rate under 1000 W/m ²	73
Figure 43. Variation of energy efficiencies (thermal, electrical, and overall) with the inlet temperature of water.	74
Figure 44. Variation of exergy efficiencies (thermal, electrical, and overall) with the inlet temperature of water.	75
Figure 45. Overall exergy efficiency at different inlet water temperature and operating conditions for mass flow rate of 0.04 kg/s.	77
Figure 46. Overall exergy efficiency at different inlet water temperature and operating conditions for mass flow rate of 0.011 kg/s.	77
Figure 47. Exergy efficiency at different thermal conductivity.	78
Figure 48. Energy efficiency at different thermal conductivity.	78
Figure 49. Energy efficiency at different wall thickness, t(mm).	79
Figure 50. Exergy efficiency at different wall thickness, t(mm).	79
Figure 51. Exergy efficiency at different W/H.	80
Figure 52. Energy efficiency at different W/H.	80
Figure 53. Electrical efficiency at different wall thickness (t) and a/b ratios.	81
Figure 54. Overall efficiency at different wall thickness (t) and a/b ratios.	81
Figure 55. Thermal efficiency at different wall thickness (t) and a/b ratios.	82
Figure 56. Thermal exergy at different wall thickness (t) and a/b ratios.	82
Figure 57. Electrical exergy at different wall thickness (t) and a/b ratios.	83
Figure 58. Overall exergy at different wall thickness (t) against different a/b ratios ..	83

List of Tables

Table 1. Current and Future solar energy plants in UAE (Adopted from [6]).....	15
Table 2. Summary of recently published articles on PVT systems.	38
Table 3. Fluid (water) properties used in the simulation.	55

Abbreviations

A_c	Cross-sectional area of the duct (m ²)
A_{PV}	PV area (m ²)
C_p	Specific heat (J/kg.K)
D_h	Hydraulic diameter
\dot{E}	Electrical energy produced by the PV
f	Darcy friction coefficient
h	Convection coefficient (W/m ² .K)
h_w	Heat transfer coefficient of the flowing air
I	Total irradiance (W/m ²)
k	Thermal conductivity (W/m.K)
k_f	Fluid thermal conductivity (W/m.K)
\dot{m}	Mass flow rate (kg/s)
Nu	Nusselt number
P	Pressure
p	Wetted perimeter
\dot{Q}	Rate of heat transfer
\dot{Q}_u	Useful heat gain
\dot{Q}_{conv}	Amount of heat lost by forced convection.
\dot{Q}_{Rad}	Amount of heat lost by Radiation.
T_s	Surface temperature (K)
T_m	Mixed cup temperature (K)
T_o	Outlet temperature (K)

T_i	Inlet temperature (K)
T_a	Ambient temperature (K)
T_{ref}	Reference temperature (K)
T_{sun}	Sun's temperature (K)
ΔT_{LMT}	Log mean temperature
$U_{overall}$	Overall convection coefficient of the PV
\dot{W}_p	Pumping power
ρ	Density (kg/m ³)
μ	Dynamic viscosity (kg/m.s)
τ	Shear stress
η	Overall efficiency of the collector
η_{th}	Thermal efficiency of the collector.
η_{ele}	Electrical efficiency of the PV.
η_{ref}	Reference efficiency.
$\eta_{exe,ele}$	Electrical exergy efficiency.
$\eta_{ex,th}$	Thermal exergy efficiency.
η_{exe}	Overall exergy efficiency.
σ	Stefan-Boltzmann constant (W/m ² .K ⁴)
ε_{PVT}	Thermal emissivity of the PVT
β	Temperature coefficient (K ⁻¹)

Chapter 1. Introduction

In this chapter, the definition of the PVT is introduced. Also, the benefits of the PVT compared to the standalone PV is discussed. Then the objectives along with the contributions of this research are listed. Finally, the organization of this thesis report is presented.

1.1. Overview

The important role of energy remains indubitable in human's life. Nowadays, energy plays a very important role in people's activities in many forms such as communication, transportation, and more. Energy development has been directly connected to success and growth of our civilization. It is the human desire to enhance the prosperity of their families that drives the energy demand. With a specific end goal to make their lives wealthier, gainful, more secure, and healthier, new and clean technologies should be formed. Changes in atmosphere due to the use of fossil fuel have driven nations to seek better alternatives for energy, particularly sustainable sources.

One of the most promising sustainable energy sources is solar energy, which is the most abundant energy resource. The overall solar irradiation reaching the planet per year is around 5.46×10^{24} J [1]. To get a clue of what the sun energy is capable of, it is enough to understand that within the years 2005-2010 the annual world energy consumption was approximately 5×10^{20} J [2]. This indicates that only 0.01% of the overall annual solar energy reaching the earth is enough to satisfy the need of the globe. The energy consumption in the Arabian Gulf countries is expanding rapidly and the countries started looking towards other sources of energy, which are most likely renewable sources for meeting the rising demands. As for United Arab Emirates (UAE), the best renewable energy source is solar energy according to its geographic conditions [3]. Meanwhile, UAE produces electricity from fossil fuel like oil and gas, which is considered as non-renewable source of energy and one day it will be depleted. The human actions resulting from energy consumption and the pollution produced have led to dramatic changes in the atmosphere, such as global warming, damage to the ozone layer, and the melting of ice at the two poles [4]. Global warming and pollution can be limited in the future by using clean and renewable energies such as solar energy.

A promising system that can reduce the dependence on fossil fuel is the use of photovoltaic (PV). In recent years and due to cheaper technique of fabrication of PV, PVs have penetrated the energy market in great extent. In recent years, many projects have been constructed in gulf region and many projects had been evaluated for coming years as shown in Table 1. To maximize the benefit of PV, a combination between photovoltaic and solar thermal unit (PVT) is used to simultaneously produce both electricity and heat. PV is considered one of the most promising and growing solar energy technology[3]. Nevertheless, many research works have been done on PVT systems to enhance their efficiency and performance. As shown in Figure 1, PVT is a hybrid collector, which combine both solar PV and thermal collectors in order to maximize the electrical efficiency of the PV cell and to utilize the captured thermal energy.

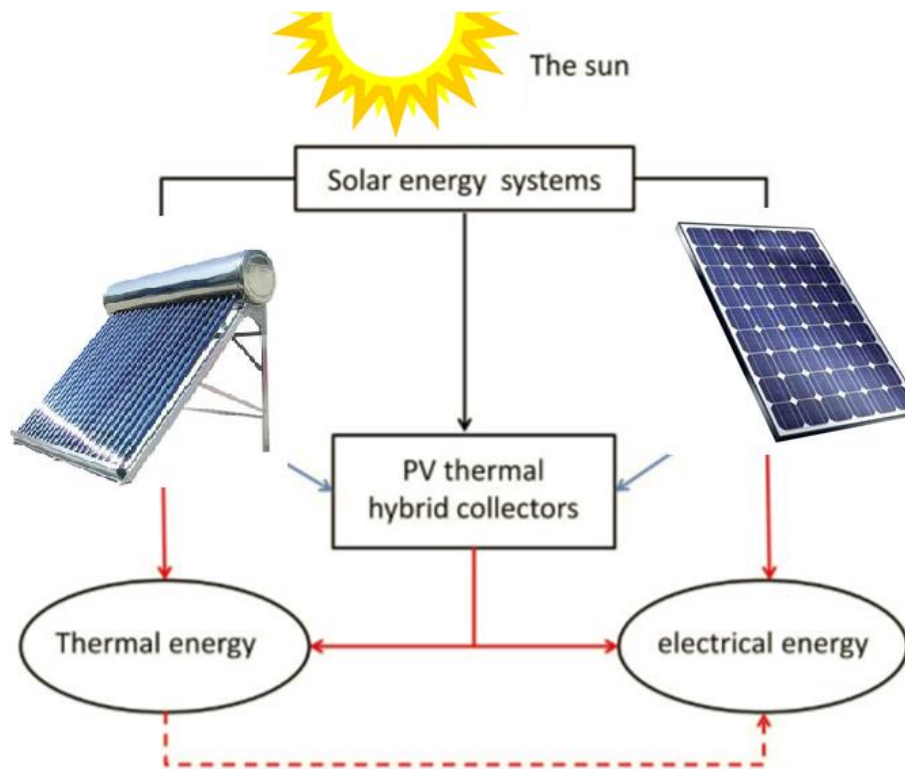


Figure 1. Classification of solar energy systems.

Photovoltaic main purpose is to convert energy produced by sunlight to electrical energy. The PV scheme consists of solar cells, which are considered as the smallest unit and they are connected in parallel and series to make a PV module. The PV cell material allows photons, light particles, to knock its electrons lose from atoms,

which generates a flow of electricity. PV units are also connected in parallel and series to make PV arrays.

PV power plants usage have rapidly increased in the world. The European Union (EU) has announced a plan to increase the portion of renewables in energy generation to at least 30% by 2030, with this percentage growing to 100% in 2050 [5].

Table 1. Current and Future solar energy plants in UAE (Adopted from [6]).

	Project	Year	Installed capacity
Abu Dhabi	1. Masdar City [PV]	2013	10 MW
	2. Shams 1 [CSP]	2013	100 MW
	3. Noor 1 [PV]	2020	100 MW
	4. Noor 2 [PV]	2020	150 MW
Dubai	1. Phase 1: Dubai Solar Park [PV]	2013	13 MW
	2. Rooftop building [PV]	2013	4 MW
	3. Phase2: Dubai Solar Park [PV]	2020	130 MW

1.2. Thesis Objectives

In this research, the performance of the PVT is investigated. This study aims to design a PVT system and optimize its operation to maximize overall efficiencies using a zero-dimensional model along with a detailed CFD analysis of the thermal collector. The performance of the PVT can be expressed in term of efficiency either electrical or thermal. The objectives of this research are as follows:

- To investigate the performance of the PVT by determining its thermal and electrical characteristics.
- To study the effect of different parameters on the overall convection heat transfer coefficient, $U_{overall}$.
- To study the trade-off between high water outlet temperature and electrical conversion efficiency.
- To conduct a sensitivity analysis on PVT affecting parameters.

1.3. Research Contribution

The contributions of this research work can be summarized as follows:

- Propose an overall study of the PVT performance by conducting a parametric analysis to well understand the effect of different parameters on PVT.
- Propose an overview on how to enhance the performance of the PVT by determining its thermal and electrical characteristics. The analysis is separated into two sections, energy and exergy analyses.

1.4. Thesis Organization

The rest of the thesis is organized as follows: Chapter 2 provides background about PVT collectors and their types. Moreover, related works to this research are discussed. The system description and the simulation results using CFD are discussed in Chapter 3 along with the Mesh independence study and model validation. Chapter 4 presents the analysis of the PVT performance. As for Chapter 5, it discusses the results obtained from this study. Finally, Chapter 6 concludes the thesis and outlines the future work.

Chapter 2. Theoretical Background and Literature Review

In this section, the shortage in performance of PV modules, because of high operating temperature is explained. In addition, the necessity of developing PVT collectors is identified. The idea of PVT collectors and their types are stated in detail. A brief literature review regarding the design and energetic balance of PVT collectors is showed.

2.1. Limitation of PV Systems

Each kind of solar cells within the PV systems contains a specific cut-off absorption wavelength equivalent to the cells band gap energy. Any incident photon having a wavelength longer than the cut-off wavelength will not be absorbed by the PV cells, which means photons of longer wavelength (their energy is below the band gap energy) do not generate electron hole pairs to supply electricity, however the photons dissipate their energy as heat within the cells. Most of solar cells convert 8 to 20 % of the solar irradiations into electricity depending on the type of cells and therefore the operating conditions. In general, greater than 50 % of the solar energy is converted to heat [1]. As a result, the PV cells temperature may increase to more than 30 °C above the ambient temperature depending on the way heat is carried away from the cell (which depend on cell thermal conductivity and surrounding medium convection capabilities). Increasing the cells temperature ends up in reducing voltage at open circuit (VOC) and therefore reducing the electrical efficiency of the cells. Figure 2 illustrate an example of the current-voltage (I-V) curves of a PV module under same solar irradiance and different cell temperature. For example, by increasing the cell temperature from the ambient value of 25 °C to 85 °C, the V_{OC} drops by 18 % that affects negatively the system's electrical performance,[7] .

Cooling the PV modules with a fluid stream (coolant) is a good strategy to improve the modules performance. Hence, enhancing the heat removal from PV cell will enhance the PV performance and will improve the overall energy produce of the PV [1]. Scientists have explored different techniques to cool PV including passive and active methods as will be discussed in coming sections.

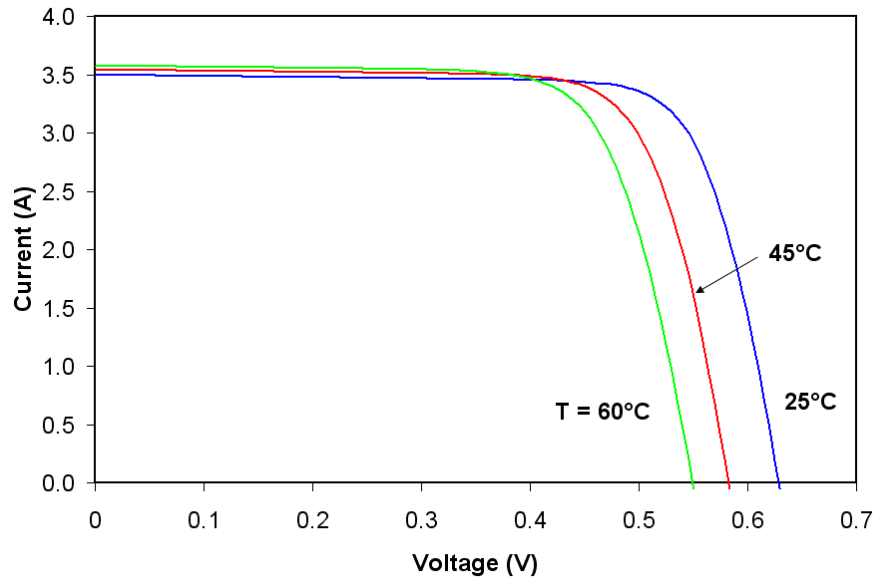


Figure 2. I-V curve of a PV module with different cell/ modules temperatures [1].

2.2. Cooling Techniques for PV Panel

Different cooling techniques have been suggested in PV exploitation, as cited in [8]. The main advantage of cooling is to achieve a higher electrical output. Nevertheless, cooling needs a separate system to achieve the desired cooling. The construction and maintenance of that system can be costly and there is an opportunity that the cost of system maintenance could outweigh the benefits of the developed electrical yield. Hence, there is a strong need to have a proper optimized cooling system that enhance the overall system performance. There are two types of cooling classification which active cooling, which consumes energy (pump, fan, etc.,) and passive cooling, which uses natural convection/conduction to allow heat extraction.

2.2.1. Passive cooling techniques. Passive cooling is a technique that uses no power consumption device to cool the system. In PVT applications, passive cooling consists of three main sections: air cooling, water cooling and conductive cooling. Generally, the conductive and air passive cooling are almost the same, but the main alteration is that the nature of heat transfer mechanism from PV panel is conductive. Cuce et al. [9] studied polycrystalline PV cells under specified conditions. In this study, two PV cells were tested, the first PV model consist of fins fabricated from aluminum acting like a heat sink, as for the second PV model it has no Fins attached. The irradiance applied was between 200 to $800 W/m^2$. The results showed an improvement

of 9 % in electrical efficiency owing to the use of heat sink as a passive cooling technique.

R. M. Hernandez et al.[10] indicated that the flow channel depth below the PV cells has important effect on passive cooling. In this study, Two PV panels A and B were compared, in which panel A is considered as reference panel (without any plate underneath), Figure 3 shows the configuration of panel B which is positioned on a steel plate with adjusting a space between the two surfaces. This arrangement was tested by changing the width of the channel, given by the aspect ratios (b/L) 0.0525, 0.0675, and 0.0825. In the three cases, panel B is hotter than the isolated panel A, so due to the increase in PV surface temperature, the electrical performance of the system dropped. It showed that, for an aspect ratio of 0.085, the PV module (Panel B) heats up by 5-6 °C when compared with a PV on a regular stand (panel A). Also, they have noticed that the difference in temperature increases with the increase of insulation. In other words, passive flow channels might negatively affect the PV cooling.

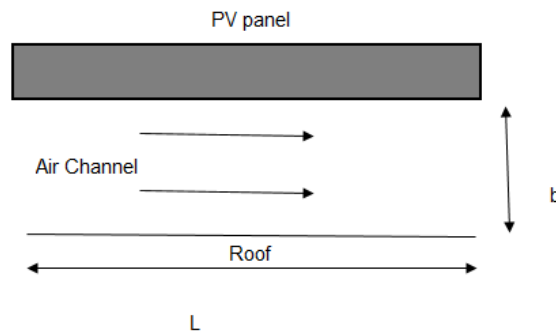


Figure 3. Configuration of panel B, showing the air channel between the PV panel and the roof (Adopted from [10]).

Other type of conductive passive cooling is phase change material (PCM) cooling. Even though this can not be considered as cooling, it has the ability of keeping the same temperature. But, it is counted as a conductive passive cooling because of the fact that no additional power is needed to cool the system, which the heat is mostly dissipated by conduction [3]. The authors in [11] showed that, a reduction of 15 °C relative to the reference case can be reached by selecting the correct PCM material, for a duration of 5 hours, and at solar radiation of 1,000 W/m². PV modules with minimal power of 65 W were used with PCM material with thickness of 50 mm from the back,

and with vertical aluminium fins to improve conduction. The results showed that the power gain was greater by 9.7 % than that from a reference PV module. Maiti et al.[12] used a V-shaped reflective panel to achieve total concentration of 2000 W/m² (2 suns). A 0.133 m² surface of PV panel was used with 10 W of small power. Using PCM material of 5.5 kg mixed with turning shavings led to a drop in the highest temperature from 85 °C to 65 °C. The growth in efficiency attained was 55 %. Though, a PCM material of 5.5 kg for 0.133 m² of surface below 2 suns is significantly higher mass of material than in [11].

Water passive cooling technique is more efficient, due to the thermal properties of water in which it has higher thermal conductivity and specific heat than the air. Some studies conducted with front and back cooling. Rosa-Clot et al. [13] used a submerged method to cool the mono-crystalline PV unit in water. The outcome had sizeable success and PV temperature was conserved at uniform temperature. The study found, under same solar radiation, that submerged photovoltaic solar panel has produced a relative efficiency increase of 20 %, compared with non-submerged one. Another important finding was that, submerged PV performance dropped with depth since solar spectrum changes at different water depths. Yet, at a 4 cm water depth, relative efficiency has increased by 11 %.

El-Seesy et al. [14] conducted an experiment to cool a polycrystalline silicon PV using a thermosyphon effect, Figure 4. The total area of the PV module was 0.26 m², along with a sheet fabricated from copper and tubing mounted on the backside of the unit, and 80 liters of water capacity of thermosyphon water system. The results showed an increase of 19% in relative efficiency when compared to PV without cooling.



Figure 4. Thermosyphon effect used on PVT system [14].

Chandrasekar et al. [15] studied a system of monocrystalline PV module to cool it using capillary effect. The capillary effect was formed by infolding the cotton wick spirally at the back of the unit and submerged in fluid. Nano fluid capillary cooling was also tested, but it failed to improve the cooling effect in comparison with water [15]. The maximum growth in efficiency increased to 10.4 % when compared to a non-cooled module. Han et al. [16] compared and discussed the immersion in different variety of cooling fluids. The immersion was in isolation liquid, de-ionized water and three more different organic liquids. The irradiance was improved to 10, 20 and 30 suns, where 1 sun is equals to 1000 W/m^2 . An improvement on relative efficiency of 15 % was reported in that study. Conversely, a concentration of 30 suns needs a considerable amount of cooling, which can clearly be done with passive liquid cooling. Abdulgafar et al. [17] studied a system of polycrystalline PV cell at 0.12 W and 15 cm^2 submerged in de-ionized water at different depths. The results showed an interesting outcome, in which at the lowest depth level of 1 cm the highest power was obtained. As for the efficiency, it was observed that at depth of 6 cm the highest efficiency of 22% was obtained. The reason behind this outcome was due to immersing the pyrometer which is used for detecting solar irradiance in water. The study reported an increase in relative efficiency with the decrease in irradiance, although the power obtained by the non-immersed PV was higher than immersed PV. Also, the mass of the PV module is very low compared to the amount of water used for cooling, therefore this will be difficult to implement in large-scale PV systems.

2.2.2. Active cooling methods. Active cooling techniques can be considered as those techniques that continuously consume power in order to cool the PV module. Most of the methods used are based on air or water cooling. Therefore, main consumption system is pump or fan, which is needed for maintaining fluid flow. In general, active cooling result in more generated power and more accessible thermal energy, but when power usage is considered, a thought rises whether cooling system can support itself. In addition to, active cooling system can be used in applications of concentrated PV cells, because of the ability to use low amount of fluid which can be described by fluid-to-cell mass ratio. Therefore, the power consumption needed to uphold the system had decreased. Teo et al. [18] studied four different PV units with a surface area equals to 0.78 m^2 . Special flow channel was manufactured and CFD study was used to optimize its shape. Total efficiency increased from 9% to 14% which mean

an increase in relative efficiency of 55% at specific irradiance. Optimal air flow beneath the panel is 0.055 kg/s, though no ambient temperature was given. This information is reliable only for this specific case.

Farhana et al [19] conducted a study on two different PV systems with an area of 0.924 m². As shown in Figure 5, the researchers investigated the effect of using air as a coolant on the PV system. It consists of two systems, standalone PV compared to PV with cooling system. There was no information mentioned about mass flow of the air. Instead, using the given fan specification the mass flow obtained in this study was approaching 0.035 kg/s. Outcomes illustrate a maximum relative efficiency increase of 8.9 % and a decrease in temperature of maximum 12 °C.



Figure 5. Forced air cooling [19].

As for active cooling, two distinct methods can be applied [3]: front side and back side cooling. Hosseini et al. [20] formed a thin water film at front side of a monocrystalline PV panel and had significant total efficiency increase of 1%. Total area of panel was 0.44 m² and the maximum water flow was around 1 L/min. The pump selected consumes 0.25 hP. A reduction in temperature of 20 °C was achieved. Du et al. [21] studied the performance of a concentrated 0.152 m² surface area of PV module. The intensity of the concentration was at 8.5 suns. Cooling method used was backside cooling via two aluminum pipes on aluminum mounting. The increase of the peak efficiency was 0.8 % for mass flow of 0.035 kg/s of water which represent 10% increase

in relative efficiency. Maximum surface temperature of the PV obtained was around 60 °C.

Bahaidarah et al. [22] attempt to cool down a 1.24 m² surface area of monocrystalline PV unit from back side, through closed casing in which a flow of water is established, Figure 6. In this study, the power consumed by the pump was around 0.5 hP and the maximum mass flow rate of water obtained was 0.06 kg/s. The results showed an improvement in maximum efficiency of 2.8% compared to standalone PV module, the improvement in efficiency considered as major compared to the size of the PV, and a reduction in PV surface temperature by 10 °C.

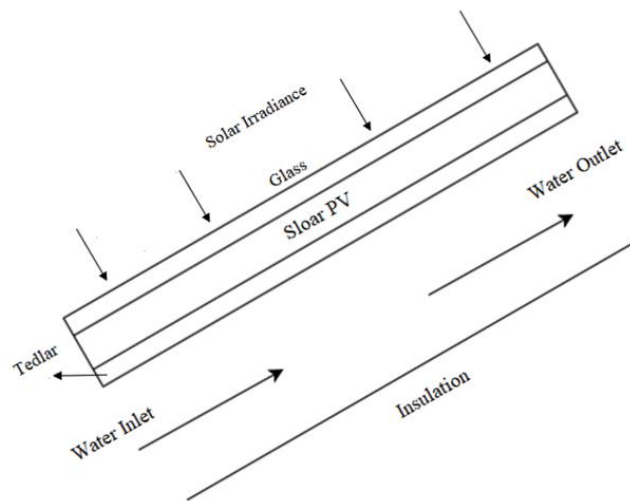


Figure 6. Water cooling technique (Adopted from [22]).

Dorobantu et al. [23] investigated the performance of PV unit with a surface area of 0.56 m² by washing it using water of 0.03 kg/s. This study focused on measuring the improvement in power produced which reached 4 W. The outcomes indicate that the PV temperature reduced by 12.5 °C on the back side and 8 °C on front side. Pump consumption was not declared, it is only lay emphasis on that increased power yield is sufficient to cover the pumping cost.

Moharram et al. [24] Attempt to cool a 1.25 m² area of PV unit on the front side by using water as a coolant. The power consumed by the pump was around 1 hP and the mass flow rate of water was 0.48 kg/s. The outcomes showed that the cooling rate was 2 °C/min in which the cooling was plotted each 5 minutes with a pause of 15

minutes. The improvement in efficiency was almost 1.5 %. Sun et al. [25] cooled a concentrated mono-crystalline PV cell array of 0.014 m², irradiated by 9.1 suns. The used Cooling liquid was dimethyl silicon oil. Mass flow was varying between two ranges 0.19 and 0.95 kg/s. The surface temperature of the PV cell was maintained, depending on mass flow rate, between 20 °C to 32 °C, the total efficiency obtained was ranging, depending on the time of the year, from 12.5 % and 13.74 %. That efficiency is fairly close to efficiency of non-concentrated cell array, which is 13.94 %. Hereafter, there was a small decrease in efficiency because of higher sunlight concentration. Also, insignificant cell degradation was observed after 270 days of direct immersion. Smith et al. [26] investigated the increase in power yield for concentrated cells by spraying water to cool the front side. Monocrystalline PV panels were used, without panel specifications. Another group of panels was also measured as a test group. Concentration factor was absent. Water flow was at maximum of 0.116 kg/s. Net power gain for regular water cooling, when pump consumption is taken into account, was 4.6%. The power development was 24 % when ice water was used (2.5 °C at the entrance). When light concentration and ice water cooling was joined, power rise was 43 % larger than that of the control group.

In [27], a cooling technique from both back and front side is checked. Water flow is changing and its maximum value was 0.0625 kg/s. Water is applied in jet form, which improves the cooling outcome, according to [28] . Outcomes are showing a relative rise in efficiency of 14.8 %, 19.1 %, and 20.4 % for backside, front side and simultaneous back and front cooling.

2.3. PVT Principles and Performance

Photovoltaic thermal collector system, as stated by Zondag [29], consist of two main systems, the photovoltaic panel which is used to convert radiation from the sun into electrical power, and thermal collector which convert the solar radiation absorbed by the collector into heat. Bhargava et al. [30] cited that the hybrid system is functioned merely by the solar radiation.

In general, PV systems have different configurations [31]: grid connected, standalone, tracking systems and hybrid. Regularly, a PV system consist of a PV module/array, charge controller and maximum power point tracking MPPT, inverter, and battery (optional), as shown in Figure 7. PV has received progressively more and

been used in many applications. Many researchers have studied many different designs of PV attempting to improve their efficiency and increase the range of useful applications. Solar systems consist of two main categories: photoelectric and thermal. However, a third category had been suggested which combine PV and thermal collectors to produce heat and electricity.

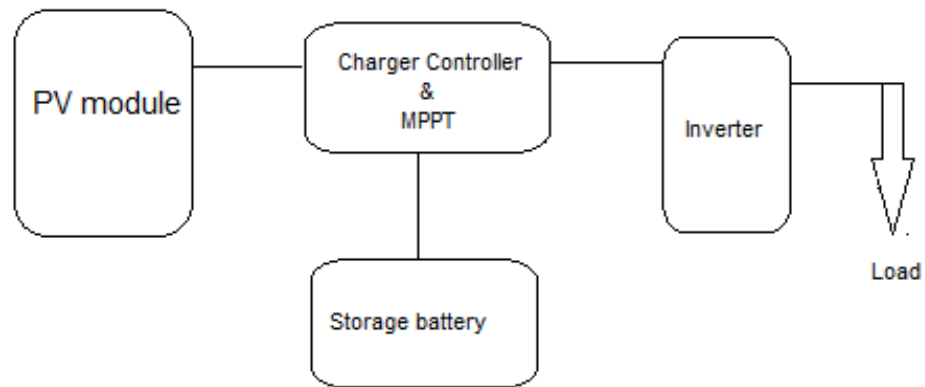


Figure 7. Typical PV system components (Adopted from [31]).

Many studies [32] had a conclusion about the relation between the PV surface temperature and the open circuit voltage which revealed that the open circuit voltage will drop as the surface temperature increase which led to a drop in the electrical efficiency of the PV. The overall efficiency of the system has improved as the cooling system attached to the PV unit.

Moreover two main fluids is used to cool down the PV in Hybrid PVT system which are air or water and in some applications a combination of air and water is applied [33]. The efficiency estimation of the PVT plays an important role in determining the amount of the electricity produced compared to the heat removed from the collector. The waste heat recovery escalate the total efficiency of the system and makes it bigger than any individual Photovoltaic (PV) system [34]. Although investigation into hybrid systems begins in the 1970s, they are at the early developmental stages and will be an effective and productive substitute to solo PV systems because of their larger electrical production and lower cost [35]. The main advantages of PVT system are the following. The solar energy technology or substitute as photovoltaic and solar thermal technology has many advantages and disadvantages equating to others energy. The potential advantages such as [36]:

- It works on quiet environment.
- High performance system.
- Clean technology – does not produce a radioactive material. highly credible system with life span between 20 and 30 years.
- Low maintenance system.

The disadvantages:

- Non-uniform cooling.
- less efficiency, and longer payback period;
- production and installation cost—expensive and high cost;
- not appropriate for integration with present roof system;
- Need bigger space for separate systems (electricity production hot and water).

PV and thermal solar collectors use unlike range of the solar spectrum. The solar cells use visible light waves, while collector uses infrared waves. Engaging the two systems in cycle will result in much effective usage of the full solar spectrum [37].

- 1- The most vital basic cost of the system is the installation cost, which is divided between the two systems and decrease the total cost compared to mounting two individual systems.
- 2- The total space required for installation will be less than that for each system separately.
- 3- The PVT system has the benefit of increasing the isolation of construction and the surface shading throughout summer, dropping the thermal load.
- 4- The building's architect will be able to make a wonderful appearance of the buildings compared to using two separate systems, where the PV panels will be the only outside front.

We can conclude from the above that the significance of hybrid PVT systems depends on the possibility of increasing the produced electricity to a pleasing level with the recovery of some amount of the thermal losses that could be useful for other applications.

2.4. Flat Plate PVT Collector Classification

There are three main classifications of the flat plate collector in a PVT which are air, water, and a combination of air and/or water collector. Moreover, the collectors of the PVT can be indicated by the absorber below the flat plate. Some designs of flat plate collector can be integrated with glass cover, glazed or unglazed, encapsulated materials, solar cell, and absorber collector below. The absorber collector plays important role in PVT system. It cools the PV cell or module down, instantaneously gathering the thermal energy produced in the form of either hot water or hot air. As this process happens, the efficiency of the PV cell or module increases.

Aste et al. [38] stated that, between all types of PVT solar collectors, the utmost popular PVT collector is the PVT air collector; yet, this type of collector has less applications compared to the water collectors. Zondag et al. [39] has explained the types of PVT collector. As shown in Figure 8, the collector consists of sheet and tube [1], channel [2], free flow [3] and two-absorber types [4].

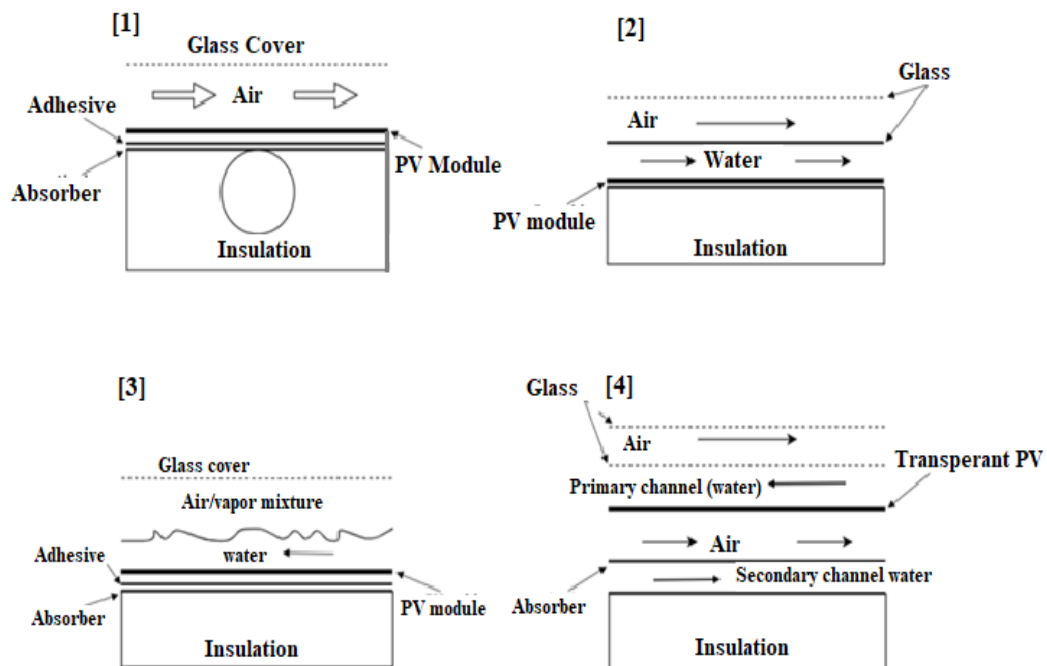


Figure 8. Types of PVT collectors (Adopted from [38]).

The medium or the fluid used in the collector can be noticed by its flow pattern, i.e. air and water or water/air combination. The water collector can be indicated by the flow pattern of water but as for air collector, depending on the formation of the flow the air type can be indicated, according to the absorber collector the air can be distributed above, beneath, or at both sides. It can be classified as single pass or double pass. Garg and Agarwal [40] stated that collectors are usually designed with pump and the circulation can be forced or natural.

The PVT systems can be connected in either grid-connected or standalone which is somehow similar to the connection of the PV units. The system of grid-connected is usually works in parallel and interconnected with the electric utility grid. The main component of grid-connected PVT systems is the converter/inverter, or PCU, power conditioning unit, and thermal storage. In the other hand, the stand-alone systems are designed to supply certain loads of electrical DC or AC, it is usually working sovereign of the electrical utility grid. Talavera et al. [41] conducted a study on the both previous mentioned systems, and a conclusion was made on the basis in which some conditions regarding the economics are achieved which is that the grid-connected systems are much profitable.

2.4.1. PVT water collector. The difficulties of having two separate standalone systems, PV and solar collector, shown in many aspects such as low PV efficiency, architectural uniformity and limited space for the installation of detached system, these factors were the key that inspired many researchers to combine the two systems into one which is called hybrid PVT system. Bazilian et al. [42] stated that the PV cell has many disadvantages but the most affecting one is the low efficiency alongside with the high cost of the unit or installation. It was mentioned that around 6 or 8% of the total solar irradiance reaching the PV is converted into electricity and the rest is dissipated as heat into the PV or lost to the surroundings due to radiation or natural convection. Figure 9 depicts a water-based PVT collector integrated with auxiliary heater, thermal storage and converter/inverter (grid-connected).

Zondag et al. [43] stated some advantages of using PVT instead of standalone system. It was mentioned that by using PVT collector will enhance the electrical efficiency of the system by reducing the surface temperature due to cooling technique. Moreover, PVT offer more architectural uniformity by aesthetical design and lastly,

reduced the usage of space on roof will decrease the payback period. Tiwari and Sodha [44] mentioned that by combining PV and solar collector into one will affect positively on the efficiency gain. In addition to many experiments and simulation studies have been done to explain the PVT water collector system. Moreover, Christandonis [45] conducted a simulation study on the performance of the PVT collector used for domestic heating, it was directed in Island of Rhodes. In this study, a comparison has been done between the PV-TC system and conventional solar collector system. The results showed that the overall efficiency of the conventional collector is 9% higher than the efficiency of PV-TC.

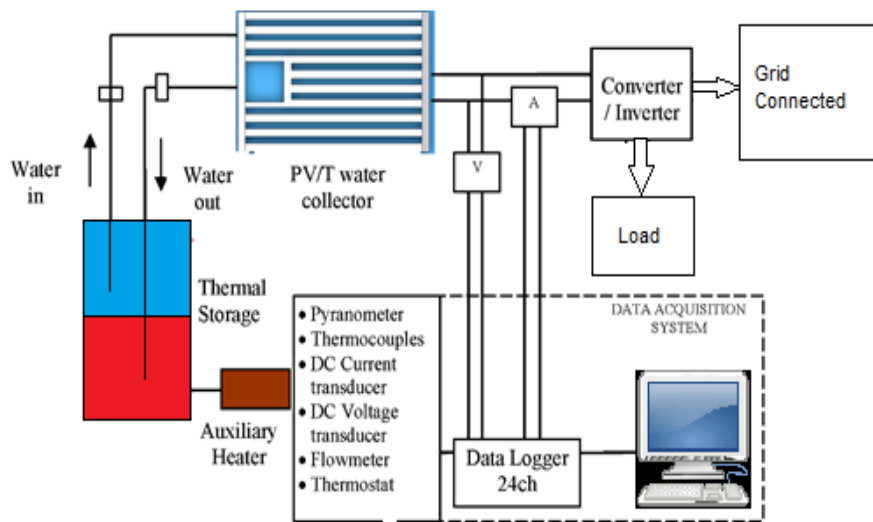


Figure 9. Schematic diagram of PVT water based system (Adopted from [36]).

According to the performance of cell materials, many researchers [46] from Mexico have built and tested a collector with different panel materials such as c-Si, a-Si and CuInSe₂. In this study, the thermal contact between the panel and the collector had been investigated. They agreed that a special design including heat removal should be completed which has the ability to produce more heat and enhance the thermal and electrical efficiency. Figure10 depicts a complete water PVT collector design with an absorber collector beneath the PV cell (solar panel).

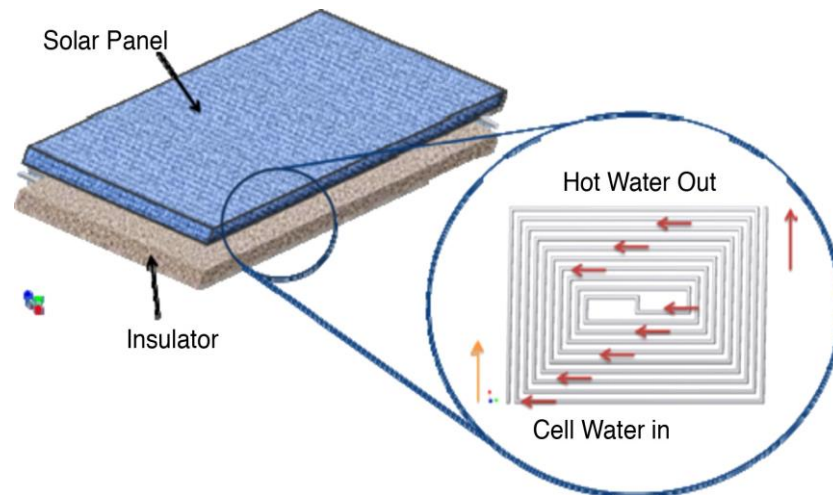


Figure 10. PVT water collector with absorber underneath the solar panel [47].

Hybrid PVT systems have the capability to produce thermal and electrical form of energy at the same time by collecting solar radiation produced by sunlight. The basic form of this module made of an open solar collector with a plate surface equipped with PV cells surface. The cells of the Photovoltaic absorb sunlight and use part of it to yield electricity, although the remaining share is moving to the coolant (liquid or air) through the collector. The heated fluid is used in different heat applications either low or medium such as domestic hot water, space heating, drying, etc. The PVT system efficiency affected by many factors such as the type of PV used, the fluid type used for cooling, the system dimensions, and operational factors such as the type of used application, flow rate, and indeed the weather conditions.

The most used fluid for cooling the PVT systems is water because of its availability, low price and cooling features [48]. Make up the PVT collector of identical parts for those used in the water flat plate solar collector with one and only modification in which the transparent glass located at the upper part of the flat collector replaced with plank PV mounted on top of the collector. The PV panel is positioned on the collector by the use of adhesive material that helps thermal energy and consists of an absorption layer of Tedlar and ethylene vinyl acetate [49]. The existence of the collector under the PV aims to extract heat from it, and thus elaborate the output voltages and current. In addition, it uses the extracted heat to heat up the water for different usage, such as water heating, domestic or space heating [50].

Tripanagnostopoulos et al. [51] used PV modules made of polycrystalline and amorphous silicon in PVT system. The results involved the estimation of the impact of the heat extractor fluids, reflector types and glazing. The study assured that in all cases, water was tolerable for use as a heat extractor fluid compared to air. The electrical efficiency produced was fairly high as a result of the high thermal efficiency of water.

Kiran and Devadiga [52] examined the performance of PVT system cooled by water. The PVT system electrical efficiency without cooling was 7.58% and 8.16% with cooling but with the added thermal efficiency of 50.80% removed from the panel. The summation of electrical and thermal energy was 58.97%. This total efficiency attained from the system was greater than the abilities of the individual stand-alone PV panel and solar water collector.

Dubey and Tiwari [53] assessed the performance of incompletely covered water-based flat plate collectors linked in series by theoretical modeling. The water was forced to circulate in the collectors using a DC motor driven by the PV unit. The examination showed that the fully covered collector by PV module was better than the partially covered collector in term of electric power generation and the opposite for hot water requirements.

Ibrahim et al. [54] studied a spiral flow absorber with a multicrystal PV module used for BIPVT, Building integrated photovoltaic/Thermal, applications. The study inspected the efficiency of the hybrid system when a single glazing polycrystalline silicon PV module attached to the flat plate absorber beneath it. The fluid used to remove heat from the system was water. The performance investigation indicated an enhancement in thermal efficiency of the system by 55–62%. The progress in the thermal energy was due to growth in solar radiation. The highest electrical efficiency attained was 11.4%.

Jahromi et al. [55] conducted an exergy and economic analysis for a specific collector in different cities in Iran with adjustable insolation levels. In this study, a MATLAB model had been produced and compared to an experimental study on the same collector to check the validity of the model. The results presented good outcomes where the maximum exergies attained were 9.7%, 9.6%, and 9.6% for Tabriz, Shiraz, and Esfahan, respectively. The Net Present Value (NPV) technique was used to

complete the economic analysis for the studied cities in Iran. The examination exposed that the given system is economically feasible.

Palaskar and Deshmukh [56] proposed flat reflectors of aluminum sheets with a spiral flow heat exchanger in a PVT system. The experimental setup in Mumbai, India. The researchers used forced water as a working fluid of the system with a given mass flow rate of 0.042 kg/s to flow through the heat exchanger. The attained electrical and thermal efficiencies of the system were 12.40% and 71.40%, respectively.

Alzaabi et al. [57] Conducted an experiment on a water-based PVT to enhance the electrical performance of the PV panel. The experiment was conducted in UAE during spring in 2014. The results obtained from the study showed that the output electrical power of the system was improved by 5% compared to standalone PV unit. The thermal efficiency of the given system was between 60% and 70%.

Saitoh et al. [58] conducted an experiment to study the performance of a hybrid PVT system. The results of the experiment showed that the electrical energy is ranging between 10% to 13%, and the thermal energy obtained was ranging from 40% to 50%. When a comparison was made between a solar collector and an individual PV with the PVT collector, the results presented that the exergy efficiency achieved by hybrid system is higher.

Palaskar and Deshmukh [59] Conducted an experiment to predict the effect of a special type of absorber, spiral flow PV absorber, on the Hybrid PVT system. The experiment was conducted under Mumbai climate condition. The results showed an enhancement in which the highest thermal efficiency obtained was around 68.2% while the highest electrical efficiency reached was 12.9%.

Mojumder et al. [60] studied four different types of PVT collector by determining the efficiency variations in the different systems. The different in the studied systems is the shape of the thin metallic sheet, trapezoidal, flat, saw tooth forward and saw tooth backward contained within the collector. The efficiency was affected significantly due to the difference in the metallic sheet air channel. The lower efficiency achieved from this investigation was by the share of the flat metallic sheet scheme. Then again, the maximum efficiency accomplished by the backward saw tooth and forward saw tooth while the trapezoidal metallic sheet was lower.

Haddad et al. [61] conducted an experiment on a hybrid water-based PVT collector to study the improvement of thermal performance of the system. The water was pumped to circulate in the heat exchanger to decrease the surface temperature of the PV panel and to extract hot water for domestic application. The highest thermal efficiency attained was 42%. The researcher was not disturbed with improvements in the system's electrical efficiency and did not mention it.

Rosa-Clot et al. [62] examined non-concentrating liquid-cooled PVT collectors. The system used c-Si, crystalline silicon, cells. The examination exhibited that the major benefit of system characterizes a retrofit of existing PV plants. This collector can be placed on the upper part of PV panels and the water will act as a filter and remove the infrared. PVT and PV systems were mounted at two different locations in Italy, Enna and Pisa. The PVT and PV electrical efficiency were found to be 13.19% and 8.77%, respectively. The maximum thermal efficiency achieved for the hybrid PVT system was 62%.

Al-Nimr and Al-Ammari [63] directed a simulation study for a PVT distillation system. The studied system made of a PVT cell located at the bottom of a single slope basin solar still. The system performance was executed using a mathematical model. The simulation results were compared with other results attained in experimental and theoretical studies and exhibited an excellent agreement. The effect of some factors such as the ambient temperature, solar radiation, condensing chamber, and wind speed were examined for the projected system. The highest overall efficiency produced by the system was 57%.

Daghigh et al. [64] conduct a simulation in Malaysia using (TRNSYS) to assess monthly the PVT water heater performance. The results indicate that the temperature of water in March, useful heat gain, and produced electricity reached their maximum values. In July the parameter stated above reached its minimum values. In the same time, if you increase the area of the collector it will have the same effect on these parameters as March operation for a certain limit, collector area 7 m².

Tse et al. [65] used a technical simulation program to show the benefits of the PVT system on the solo PV module. An economic study was made to state the advantages of the system installation. The study revealed the real potential of PVT

technologies in Hong Kong. The highest electrical efficiency produced was 16% while the researchers did not investigate the system's thermal efficiency.

Brottier et al. [66] conduct an experiment that explored the performance and reliability of two different solar systems for DHW, domestic hot water, near Lyon. The two systems made of an unglazed PVT collector. The means used could deliver 91% of the requirements of hot water for the period from May to September for 4 people.

Yazdanifard et al. [67] directed a simulation of a flat plate hybrid water-based PVT system with glass cover to examine the effect of many parameters on the performance of this module. These parameters consist of climate parameters such as solar radiation and design parameters such as the pipes number, packing factor, Reynolds number, pipes dimensions, and length of the collector. The outcomes agreed well with the obtainable data. The conclusion obtained from the study shows that the glazed PVT system has bigger energy efficiency compared to unglazed one, whereas the efficiency of exergy depends on Reynolds number, the length of the collector, and the packing factor. The highest obtained electrical and thermal efficiency of the system was 17% and 70%, consequently.

Daghigh et al. [68] attempt to increase the efficiency of a BIPVT system using a new design idea of a water-based PVT collector. The simulation for a crystalline silicon (c-Si) system and an amorphous silicon (a-Si) PVT system in Malaysia. The thermal efficiency of the PVT system was 72%, the electrical efficiency was 4.9% and the total efficiency was 77%. For the crystalline silicon PVT system, the thermal, electrical, and overall efficiencies were 51.0%, 11.6%, and 63.0%, respectively.

Starke et al. [69] investigated two different hybrid CSP+PV systems. The power produced and its cost study were executed. The study considered different climate conditions in the Atacama Desert, Chile. The study intended to optimize and estimate the storage capacity and the power generated from the CSP plants with the capacity variation of the PV plant. The Simulation program (TRNSYS) was used in the research. The simulation results showed that using the hybrid CSP+PV plants in the Atacama Desert is very applicable because of the high solar irradiation levels. Electrical and thermal system efficiencies were not evaluated.

Khanjari et al. [70] investigated the effect of the addition of nanofluid to water used in cooling PVT system. This addition of nanofluid was to enhance water thermal conductivity. A computational fluid dynamic, CFD, simulation study three different types of fluids, namely pure water, alumina-water nanofluid, and Ag-water nanofluid. The influence of the volumetric concentration of the nanoparticle on the system performance was investigated in this research. It was found that the nanoparticles volumetric ratio is directly proportional to the efficiency and the heat transfer coefficient. The maximum heat transfer coefficient attained was 43% for Ag-water nanofluid, and 12% for alumina-water. The electrical energy with aluminum nanofluid was 8–10% greater than pure water. The development in the example of Ag-water nanofluid was 28–45% more than for pure water.

Fudholi et al. [71] studied a water-based PVT system under solar radiation varying from 500 to 800 W/m² by determining the electrical and thermal effectiveness. The results indicate that the highest thermal efficiency attained was 68.4% and the maximum electrical efficiency was 13.8%.

Hassani et al. [72] examined the exergy life cycle for three different variables nanofluids-based PVT arrangements theoretically. The system performance of the proposed study was compared to a typical PV and PV/ T system. The outcomes showed that the life cycle exergy for the nanofluid-based PVT system performance is better compared to standard PV and PVT systems. This conclusion was shown in the exergetic efficiency of the system in which the maximum exergetic and electrical efficiency obtained were 12% and 12%, respectively.

Al-Shamani et al. [73] directed a review article to estimate the advantages of nanoparticles used in cooling PVT systems. The case defines the analytical, numerical, simulation, and experimental efforts in this area. The investigation focused on the effect of some parameters such as, absorber plate type, covered and uncovered PVT collectors, and absorber design arrangements types on the PVT performance. The results indicated that the coverless PV/ T collector had the maximum total exergy. Furthermore, it exposed that the electrical and thermal efficiencies of the in any PVT systems will be improve when nanofluids added to water.

Al-Shamani et al. [74] tested, designed, and fabricated a PVT system were conducted in Malaysia. In these study different Nano fluids, types (TiO₂, SiO₂, and SiC) were used as coolant fluids. The outcomes specified that the highest thermal efficiency of 81.73% was attained by SiC nanofluid-based PVT system with an electrical efficiency of 13.52%.

Hussein et al. [75] conducted an experiment in Iraq to investigate the effect of using nanofluids, Zn-H₂O, at five different concentration (0.1, 0.2, 0.3, 0.4, and 0.5%) on the performance of the water-based PVT hybrid system. The results showed that the optimum concentration ratio is at 0.3% in which the cell temperature dropped from 76° C to 58° C, the electrical and thermal efficiency reached were 7.8 % and 63%, respectively.

Nasrin et al. [76] conducted a simulation along with an indoor experiment of a PVT system by controlling the operating conditions and parameters to enhance the performance of PVT hybrid system by the use of water/MWCNT nanofluid. At mass flow rates 0.5 L/min, inlet temperature of 32 ° C and at radiation varies from 200 to 1000 W/m², the numerical results agreed with the experimental measurements. The overall efficiency obtained numerically and experimentally at 1000 W/ m² irradiation were 89.2 and 87.65% respectively.

Ahmed et al. [77] conducted an experiment in Kirkuk city to study the effect of reflectance mirrors, glass cover and the mounted angle of the lower reflector on the performance of water-based PVT hybrid system. The results stated that the reflectance mirrors increased the cell temperature, in which the temperature reaches 92.7 ° C when using the upper and lower reflectance mirrors with a glass cover, but the temperature reaches 76.1 ° C by using the lower mirror and it reaches 71.35 ° C without the use of the mirrors. As for the total efficiency, it reaches 81.03 % due to the use of two reflectors and the daily average with and without glass of the total efficiency was 58.95% and 49.97% respectively.

Evola and Marletta [78] analyzed a water-based PVT in term of performance by using the analysis of first and second law of thermodynamics. What was interesting in the paper is that, by using the second law of thermodynamics, it can be identified for any operating condition an optimum value for the inlet temperature that can maximize

the exergy efficiency of the system. It was shown that low inlet temperature is more desirable for energy efficiency.

Yazdanpanahi et al. [79] conducted an exergic analysis experimentally and numerically on a water-based PVT system. The numerical results were in good agreement with the experimental ones. The maximum exergy efficiency obtained was 13.95% at a mass flow rate equals to 0.002 kg/s.

Aberoumand et al. [80] studied the effect of implementing Ag/water nanofluid as a coolant for three different flow regimes, laminar, transient, and turbulent in PVT system. They used different concentration of Ag/water nanofluid, 2 wt% and 4 wt%. The results showed that, increasing the concentration of nanofluids and as the flow moves toward turbulent region the exergy efficiency will increase. The study showed that at 4 wt% concentration, the exergy efficiency improved by 30% compared to the result obtained by using only water as a coolant.

Water based PVT considered as one of the most efficient systems in which it can be integrated into buildings without affecting its architectural design. However, with the tremendous quantity of research been conducted in this field, as illustrated in Table 2, there are some areas must be investigated carefully. Enhancing the thermal efficiency by adding Nano material to the water is a critical research area that is not completely investigated. Table 2 indicates that this field is rich in research work. Most of these studies investigated the improvement of thermal efficiency while the variation in the electrical efficiency was limited. As for the thermal efficiency, the difference was clear due to variable fluid flow rates and speed. Also, the rate of heat transfer between water and runoff channels linked to the PV cell differs from one reference to another. The usage of water for cooling PV systems is the ideal method compared to air-cooling because of the high specific heat of water.

Table 2. Summary of recently published articles on PVT systems.

Year	Type of system	Electrical efficiency (%)	Thermal Efficiency (%)	Highlights	Author	Country
2002	Water	-	70%	In this research, a polycrystalline and amorphous silicon PV modules were used in a hybrid PVT system. The aim of the experiments was to estimate the impact of the cooling fluids used to cool the system and the effect of some variables as the reflector types and glazing. The study showed that the most efficient fluid was water compared to air in all cases.	Tripanagnostopoulos et al. [51]	Greece
2011	Water	8.88%	90%	The study used TRNSYS simulation program to estimate the performance of water-based PVT in Malaysia. The results designated that the water temperature in March, useful heat gain, and produced electricity reached their maximum values while in July the earlier mentioned parameters reached their minimum values.	Daghigh et al. [64]	Malaysia
2013	Water	9.25%	30%	The experiment showed how the system's efficiency was affected by four different shapes of thin metallic sheets attached to the collector. The used shapes were the flat, the trapezoidal, the saw tooth forward, and the saw tooth backward. The system efficiencies were affected significantly where the lowest efficiency achieved was for the flat metallic sheet system and the maximum efficiencies were the forward saw tooth and the backward saw tooth.	Mojumder et al. [60]	Bangladesh
2014	Water	11.4%	55–62%	The study investigated a multicrystal photovoltaic unit used for BIPVT application performance. The system entailed of a single glazing sheet of polycrystalline silicon PV attached to a flat plate collector. The cooling fluid of the system was Water. The system thermal energy efficiency was about 55–62%. The maximum attained electrical efficiency was 11.4%	Ibrahim et al. [54]	Malaysia

Year	Type of system	Electrical efficiency (%)	Thermal Efficiency (%)	Highlights	Author	Country
2014	Water	8.16%	50.8%	Kiran and Devadiga examined the performance of a water-based PVT system. The electrical efficiency 8.16% with cooling and 7.58% without cooling but with additional thermal efficiency of 50.80% extracted from the PV panel.	Kiran and Devadiga [52]	India
2014	Water	15–20%	60–70%	In this study a design of a Hybrid Photovoltaic Thermal system was proposed, and the cooling fluid used was water to enhance the electrical efficiency of the PV panels. The experiment was conducted in Al-Sharjah, UAE in April/ 2014. The results showed that the electrical power increased from 15% to 20% compared to individual PV panel. The attained system thermal efficiency was between 60 to 70%.	Alzaabi et al. [57]	UAE
2014	Nanoparticles + water	-	-	This article showed the advantages of using nanofluids in coolant fluids of PVT systems. It was concluded that the coverless PVT collector has the maximum total exergy. Also, it discovered that the addition of nanofluids to coolant fluid (water) in any PVT systems will improve the thermal and electrical efficiencies of the system.	Al-Shamani et al. [73]	Malaysia
2015	Water	9.7 %	54.7 %	The study investigated the economic feasibility and exergy of a particular collector at three cities in Iran with different insolation level. The results showed a good agreement and the maximum exergies achieved were 9.6%, 9.6%, and 9.7% for Shiraz, Esfahan, and Tabriz cities, respectively.	Jahromi et al. [55]	Iran
2015	Water	-	42%	An experiment been conducted on a hybrid water-based PVT collector to study the improvement of thermal performance of the system. The highest thermal efficiency attained was 42%. The researcher was not disturbed with improvements in the system's electrical efficiency and did not mention it.	Haddad et al. [61]	Algeria

Year	Type of system	Electrical efficiency (%)	Thermal Efficiency (%)	Highlights	Author	Country
2015	Water	12.4%	71.4%	A flat reflectors of aluminum sheets with a spiral flow heat exchanger in a PVT system had been tested. A mass flow rate of 0.042 kg/s to flow through the heat exchanger. The attained electrical and thermal efficiencies of the system were 12.40% and 71.40%, respectively.	Palaskar and Deshmukh [56]	India
2016	Water	13.19%	62%	Non-concentrating liquid-cooled PVT collectors was examined. This collector can be placed on the upper part of PV panels and the water will act as a filter and remove the infrared. The PVT and PV electrical efficiency were found to be 13.19% and 8.77%, respectively. The maximum thermal efficiency achieved for the hybrid PVT system was 62%.	Rosa-Clot et al. [62]	Italy
2016	Distillation	-	57 %	A simulation study for a PVT distillation system was conducted. The studied system made of a PVT cell located at the bottom of a single slope basin solar still. The effect of some factors such as the ambient temperature, solar radiation, condensing chamber, and wind speed were examined for the projected system. The highest overall efficiency produced by the system was 57%.	Al-Nimr and Al-Ammari [63]	Jordan
2016	CSP+PV	-	-	This study examines the power generation and economic for two hybrid CSP+PV systems was directed depending on the climate conditions at Atacama Desert, Chile. The results designated that using the hybrid CSP+PV plants is very good due to the high solar irradiation levels. The study didn't calculate the thermal and electrical efficiencies.	Starke et al. [69]	Chile
2016	Water	16 %	-	This study used a technical simulation program to show the benefits of the PVT system on the solo PV module. An economic study was made to state the advantages of the system installation. The highest electrical efficiency produced was 16% .	Tse et al. [65]	Hong Kong

Year	Type of system	Electrical efficiency (%)	Thermal Efficiency (%)	Highlights	Author	Country
2016	Water	17 %	70 %	The researchers directed a simulation of a flat plate hybrid water-based PVT system with glass cover to examine the effect of many parameters on the performance of this module. These parameters consist of climate parameters such as solar radiation and design parameters such as the pipes number, packing factor, Reynolds number, pipes dimensions, and length of the collector. The outcomes agreed well with the obtainable data. The conclusion obtained from the study shows that the glazed PVT system has bigger energy efficiency compared to unglazed one, whereas the efficiency of exergy depends on Reynolds number, the length of the collector, and the packing factor.	Yazdanifard et al. [67]	Iran
2016	Nano fluid with PVT	13.2 %	55 %	The study examined the influence of adding nanofluid to water used in cooling PVT system. CFD simulation study employed three types of fluids which were pure water, Ag-water nanofluid, and Alumina-water nanofluid. The study originates that increasing the nanoparticles volumetric ratio increased the heat transfer coefficient and the efficiency	Khanjari et al. [70]	Iran
2016	Nano fluid with PVT _v	13.5 %	81.73 %	The researchers tested, designed, and fabricated a PVT system were conducted in Malaysia. In these study different Nano fluids, types (TiO ₂ , SiO ₂ , and SiC) were used as coolant fluids. The outcomes specified that the highest thermal efficiency of 81.73% was attained by SiC nanofluid-based PVT system with an electrical efficiency of 13.52%.	Al-Shamani et al. [74]	Malaysia
2017	Nano fluid with PVT	7.8%	63%	An experiment conducted to investigate the effect of using nanofluids, Zn-H ₂ O, at five different concentration (0.1, 0.2, 0.3, 0.4, and 0.5%) on the performance of the water-based PVT hybrid system. The results showed that the optimum concentration ratio is at 0.3% in which the cell temperature dropped from 76° C to 58° C, the electrical and thermal efficiency reached were 7.8 % and 63%, respectively.	Hussein et al. [75]	Iraq

Year	Type of system	Electrical efficiency (%)	Thermal Efficiency (%)	Highlights	Author	Country
2018	Water	-	-	An experiment conducted in Kirkuk city to study the effect of reflectance mirrors, glass cover and the mounted angle of the lower reflector on the performance of water-based PVT hybrid system. The results stated that the reflectance mirrors increased the cell temperature, in which the temperature reaches 92.7 ° C when using the upper and lower reflectance mirrors with a glass cover, but the temperature reaches 76.1 ° C by using the lower mirror and it reaches 71.35 ° C without the use of the mirrors. As for the total efficiency, it reaches 81.03 % due to the use of two reflectors and the daily average with and without glass of the total efficiency was 58.95% and 49.97% respectively	Ahmed et al. [77]	Kirkuk
2018	Nano fluid with PVT	-	79.2%	A simulation along with an indoor experiment of a PVT system by controlling the operating conditions and parameters to enhance the performance of PVT hybrid system by the use of water/MWCNT nanofluid. At mass flow rates 0.5 L/min, inlet temperature of 32 ° C and at radiation varies from 200 to 1000 W/m ² , the numerical results agreed with the experimental measurements. The overall efficiency obtained numerically and experimentally at 1000 W/ m ² irradiation were 89.2 and 87.65% respectively.	Nasrin et al. [76]	Malaysia

2.4.2. PVT air collector. In PVT air collectors, air is circulated through the collector rather than water. This kind of collectors is recommended for applications wherever heated air is needed. PVT air collectors provides some benefits in which they are cheaper and simpler compared to PVT water collectors [81], in which a fan used rather than a pump. Moreover, there's no risk of freezing, or boiling at extreme climatic conditions. On the opposite hand, PVT air collectors suffer from some major disadvantages for example having lower thermal performance characteristics compared to water kinds because of lower heat capacity and thermal conductivity of air compared to water. Moreover, lower density of air affects the transfer volume to be ominously higher than that of water-based PVT kinds. Thus, pipes with higher volume and bigger bulk are required that is not appropriate for applications with low offered space and is not esthetically likable. Despite these disadvantages, PVT air collectors are appropriate selections for hot air applications because of their lower price. Figure 11 shows a one pass flat plate PVT collector, in which the air is circulated in a duct at the rear of PV modules to remove heat.

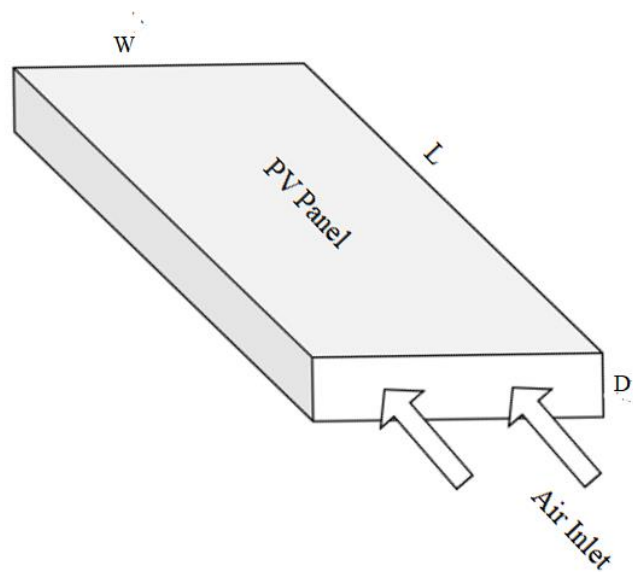


Figure 11. Single pass PVT air collector.

Air-based PVT collectors may also be covered by glass or uncovered, in which the covered collector has an extra glass over the PV units to decrease heat loss from the

highest of the collector [8]. Diversity of air-based PVT collector designs as well as single pass or double-pass, wall-mounted or roof mounted have stated in the literature.

As shown in Figure 12, the thermal energy is created from the derived heat in the form of hot air or water from the PVT collector. Hot air created from this collector, during this case, it is used in several applications such as agricultural/herbs drying as cocoa, ginseng, and beans.

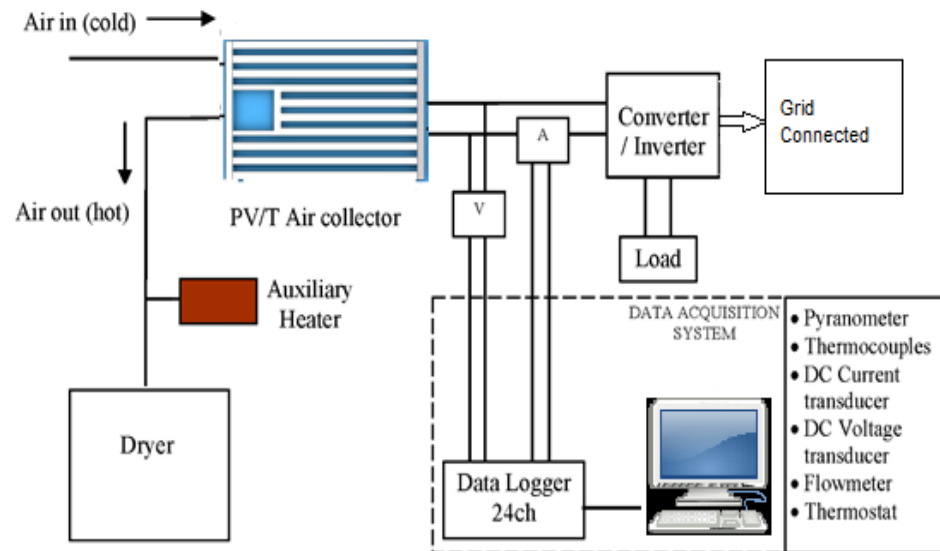


Figure 12. Schematic diagram of PVT air based system (Adopted from [36]).

The agriculture/herb drying is crucially vital to the food industries. With the unstable condition of hot and wet climate, particularly in tropical countries, the PVT air collector has become the finest way to get superior quality of drying product. Othman et al. [82] mentioned that the usage of dryers of solar PVT air collector can improve the wealth creation and nation building along with sustainable development for the country. As in Figure 13, Tiwari and Sodha [83] have performed analysis on the general performance of unglazed and glazed PVT air collector with or without tedlar. The numerical computations are meted out for composite climate in New Delhi, Asian country in which the results are compared. From their observation, they determined that the glazed hybrid PVT with no tedlar provides the most effective performance compared to all configurations being assessed.

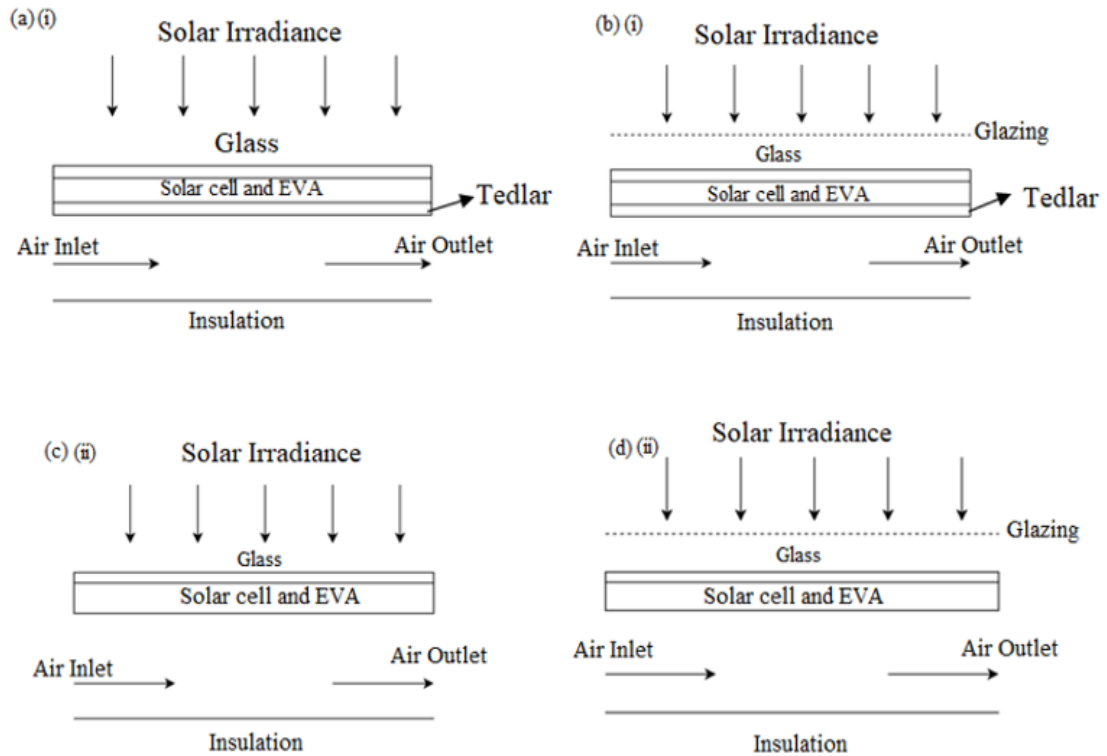


Figure 13. Cross-section of unglazed PVT air (a): (i) with tedlar and (ii) without tedlar and (b): (i) glazed with tedlar and (ii) without tedlar (Adopted from [83]).

Solanki et al. [84] had test the performance of the PVT air collectors by conducting indoor simulation. They established a system for thermal and electrical of solar air PVT heater that related in series. The experimental results display that the thermal efficiency achieved is 42% and electrical efficiency produced is 8.4%. Studied performed by Sopian et al. [85] demonstrate that the double pass PVT solar collector accomplished higher efficiency in compare to single pass PVT solar collector.

2.4.2.1. Single pass PVT air collector. Alfegi et al. [86] have executed mathematical model of single pass PVT air collector with compound parabolic concentrator (CPC) and fins. The model focused on each side (top and bottom sides) of the collector to predict the thermal and combined PVT performance. As shown in Figure 14, the working fluid, air, flows between uppermost glasses of the collector to the bottommost plates of the absorbent material. Results at irradiance of 400 W/m^2 shows that the combined PVT efficiency improved from 26.6% to 39.13% at mass flow rates differs from 0.0316 to 0.09 kg/s.

A comparison study has been done to analyse the effect of mass flow rates on the thermal and electrical efficiencies of the PVT collectors [39]. As shown in Figure 15, a solo pass rectangular tunnel absorber collector has been designed and compared with spiral flow collector as in Figure 4. The solo pass rectangular tunnel has been designed to produce hot air and electricity whereas the spiral flow has been designed to produce electricity and hot water. Each absorber was mounted beneath the flat plate single glazing sheet of Pc-si PV module. The experiment results indicate that the single flow collector produces combined PVT efficiency of 64% with electrical efficiency of 11% and maximum power output of 25.35 W and solo pass rectangular tunnel collector produced combined PVT efficiency of 55% with electrical efficiency of 10% and highest power output of 22.45 W.

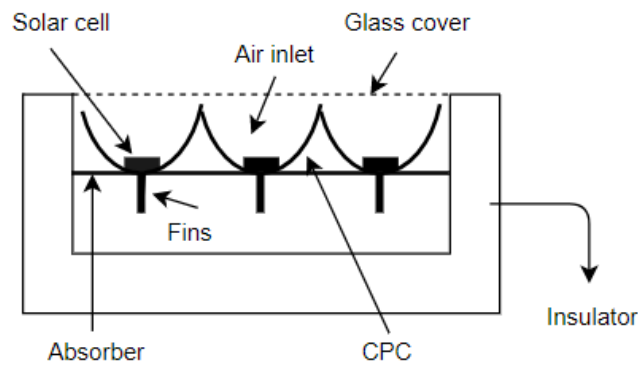


Figure 14. Cross-section of a single pass PVT air collector with Compound Parabolic Concentrator (CPC) and fins (Adopted from [86]).

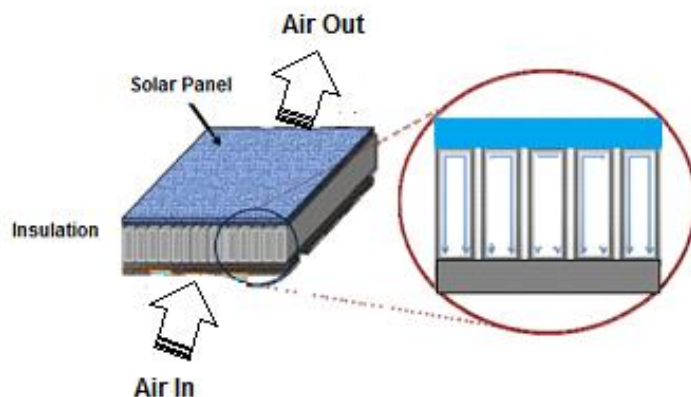


Figure 15. Cross-section of PVT air collector with rectangular shape absorber collector design (Adopted from [39]).

The performance result of the air rate of flow for single pass, double duct PVT with finned, has been investigated [87]. Figure 16 shows the experiment with PV cells placed on topmost of the fin. The experiment has been conducted to study the impact of the flow rate of the system. Results show that with the fin connected beneath, the PV increased its efficiency from 49.135% to 62.823% at mass flow rates numerous from 0.0316 to 0.09 kg/s, solar radiation of 600 W/m² with 35.8 C as inlet temperature.

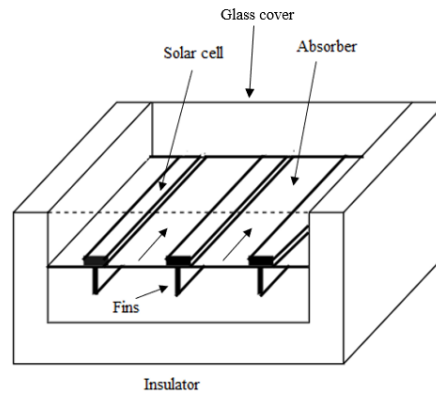


Figure 16. Single pass PVT with finned of double duct PVT air heaters (Adopted from [87]).

An experiment on one pass PVT with rectangle shaped tunnel absorber has been developed [88]. The rectangle tunnel, as shown in Figure 17, operated as an absorber collector has been mounted beneath the PV panel. The major purpose of the experiment is to recognise the appropriate air flow which will increase the efficiency of the PV module. The results indicate that at solar irradiance of 817.4 W/m² the system overall efficiency was 64.72%, as for the thermal efficiency it was 54.70% at mass flow rate and ambient temperature of 0.0287 kg/s and 25.8C, respectively. They determined that the PVT with rectangular absorber tunnel indicates improved performance compared to conventional PVT system.

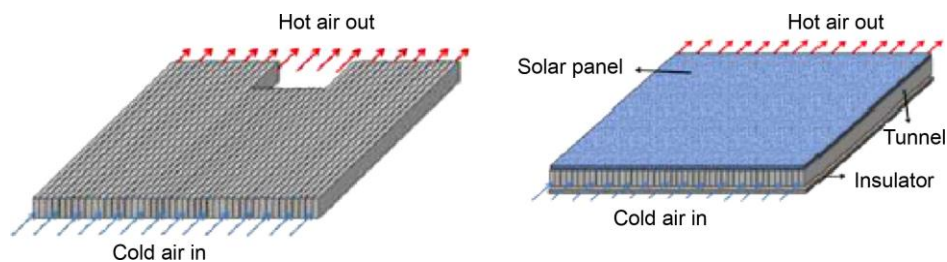


Figure 17. Single pass PVT with rectangular tunnel design [88].

2.4.2.2. Double pass PVT air collector. As shown in Figure 18, a double pass air-based PVT collector appropriate for drying applications has been tested [89]. They said that the steady state solution to define the outlet and mean PV panel temperature has been obtained depending on differential equations of the higher and lower channels of the collector. The outcomes from the experiment express that the thermal efficiency is 60% and the mass flow rate equals to 0.036 kg/s, solar radiation of 800 W/m² and the temperature increased to 188.8C. The performance of the collector with fins is more enhanced by fixing the parabolic concentrator to the collector.

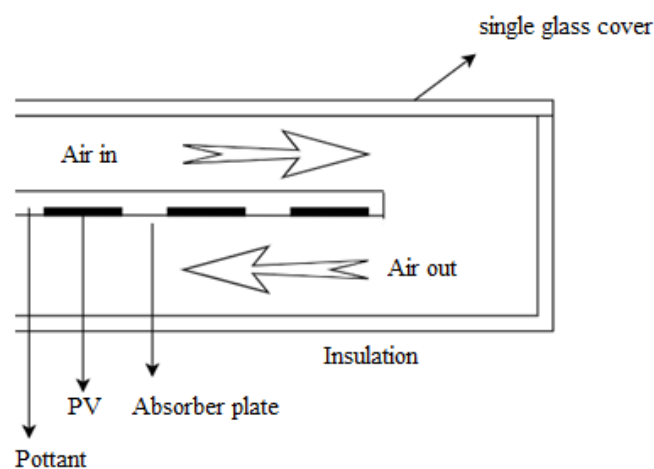


Figure 18. Cross-section of double pass PVT solar collector.

Performance analysis was conducted on a double pass PVT air collector with fins has been studied [90]. In their study, the concentrating reflectors are accustomed to escalating the power created from the solar cell. They verified that by using fins at the rear of the collector can enhance the heat transfer of the collector. As shown in Figure 19, the collector made of three main components: glass cover located at the top, panel with PV cells and absorbent collector at the bottom. Air was flow through the top part of glass shield and PV panel and flowing through the lower part of PV panel. The fins have been designed and made up of aluminum sheet to rise the capability of absorbing heat from PV cells therefore escalate the collector efficiency.

Othman et al. [90] studied the performance of a double pass PVT air collector with fins integrated with compound parabolic concentrator (CPC) at different operating conditions. The addition of CPC to the system effect positively on the electrical and

thermal energy produced by the hybrid PVT. They added fins to the collector to encounter the problem with low performance of solar cells at high operational temperatures. As shown in Figure 20, the airflow behavior, perform as the same manner of the collector with fins however with CPC, the solar radiation is increased. Fins connected beneath the PV cells help removed the heat from PV cells.

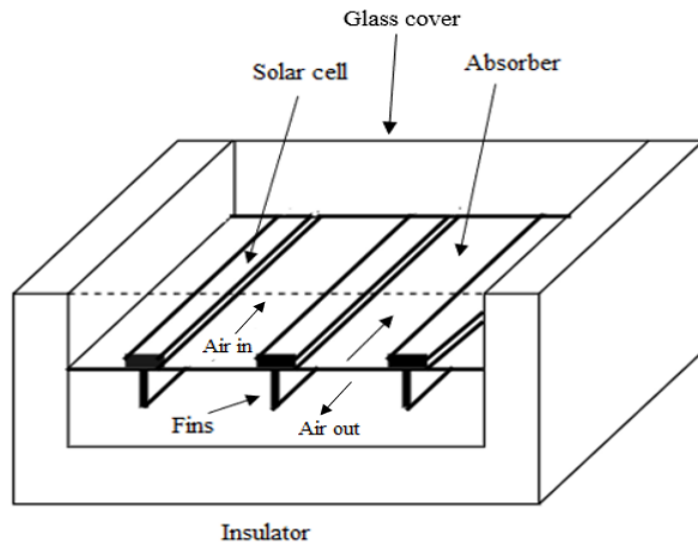


Figure 19. Cross-section of double pass PVT solar collector with fins (Adopted from [90]).

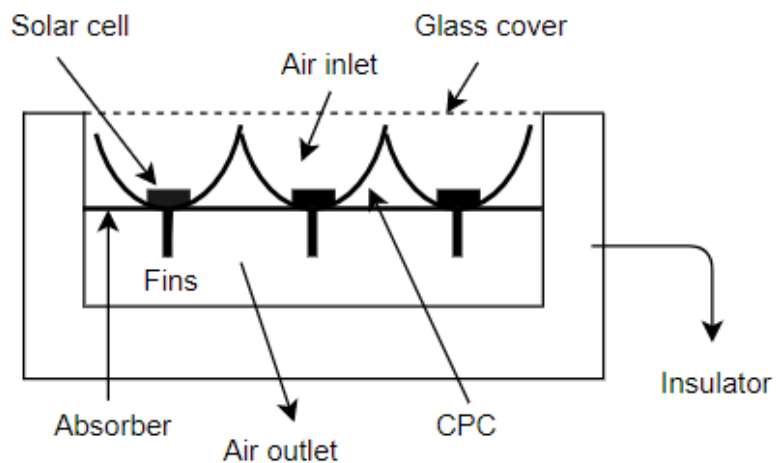


Figure 20. Cross-section of double pass PVT solar collector with fins and CPC (Adopted from [90]).

2.4.3. Combination of water and/or air PVT collector. Classification of the PVT collector, water and/or air, can be defined by the flow pattern of the coolant. Firstly, in water collectors some parameters should be taken into consideration such as channel, sheet and tube, and type of the absorber. Secondly, the essential parameters to take into consideration in air collectors is the flow pattern. It can be located on top, beneath or both side of the absorber collector and can be in single or double pass collectors.

Extra comparative study has been prepared by Zondag et al. [39]. The concepts of channel PVT, sheet-and-tube, free flow and two-absorber PVT-collectors are examined. The results illustrate that the combined PVT collectors deliver the efficiency of over 50%. A thermal efficiency of 52%, 58%, 65% were attained for the following systems, uncover collector, single cover sheet and tube, channel above the PV, respectively. Moreover, Zondag and van Helden [91] executed another research on PVT system that utilized the heat. They investigated the performance of different PVT types for roof domestic applications. The types of the PVT that had been studied are with or without cover, water or air type, open or closed loop systems. They determined that the performance of PVT water collectors is better than air-based PVT collectors and the covered closed loop systems performed better than uncovered closed loop systems.

2.4.3.1 Two-absorber. A relative experiment of PVT has been achieved by Tripanagnostopoulos [51]. Studied and compared four different configurations of PVT by conducting an outdoor experiment at different type of PV, a-Si and pc-Si modules. As shown in Figure 21, the four PVT used in this experiment was glazed or unglazed air-based PVT and glazed or unglazed water-based PVT. The outcomes of this study showed that the pc-Si module is better than a-Si module by comparing the electrical efficiency. Also, the electrical efficiency obtained by the water-based PVT is better than the other systems by 13.3%. This experimental work also demonstrated that when the PV is cooling, the electrical efficiency increases and simultaneously increase the overall efficiency.

Tonui and Tripanagnostopoulos [8] did another experiment to enhance PVT solar collector with heat extraction by natural or forced air circulation. In this experiment, the study includes the possibility of producing electricity and heat energy from commercial PV module adopted as an air-based PVT solar collector either with

natural or forced flow. One more development of combination of air and water type of hybrid PVT collector has been designed by Tonui and Tripanagnostopoulos [92].

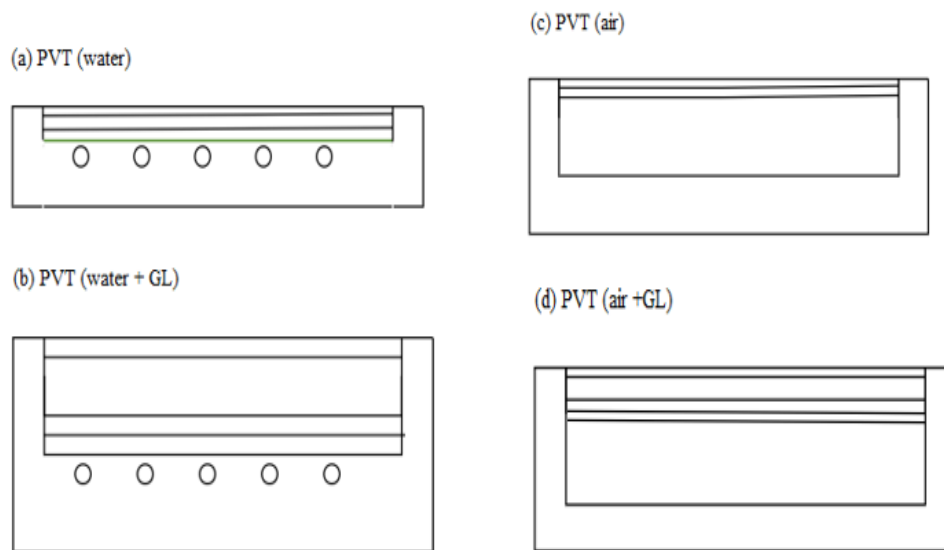


Figure 21. Cross-section of the PVT experiment model (Adopted from [51]).

As depicts in Figure 22, they investigated a combination of water and air PVT collector to enhance the system performance and produce hot air and water to use in variety of applications. In one of the designs of PVT a flat sheet fabricated from metal with a finned wall attached at the back side of the air channel. In this experiment, they examined the effect of the channel length, channel depth and mass flow rate on thermal and electrical efficiency for both air and water. They said that the PVT water-based collector is more efficient than the air-based PVT collector owing to the thermo-physical properties of water which is better than air, which usually low with the maximum thermal efficiency attained, is about 52% and 9–10% for the electrical efficiency, giving the total efficiency of about 61–62%.

A basic steady state two-dimensional mathematical model of bi-fluid hybrid PVT (water and air) collector with an absorber collector made of metal has been developed and created by Assoa et al. [93]. They designed a channel made of a ribbed sheet steel collector. Simulation has been performed and compared it with the experiment.

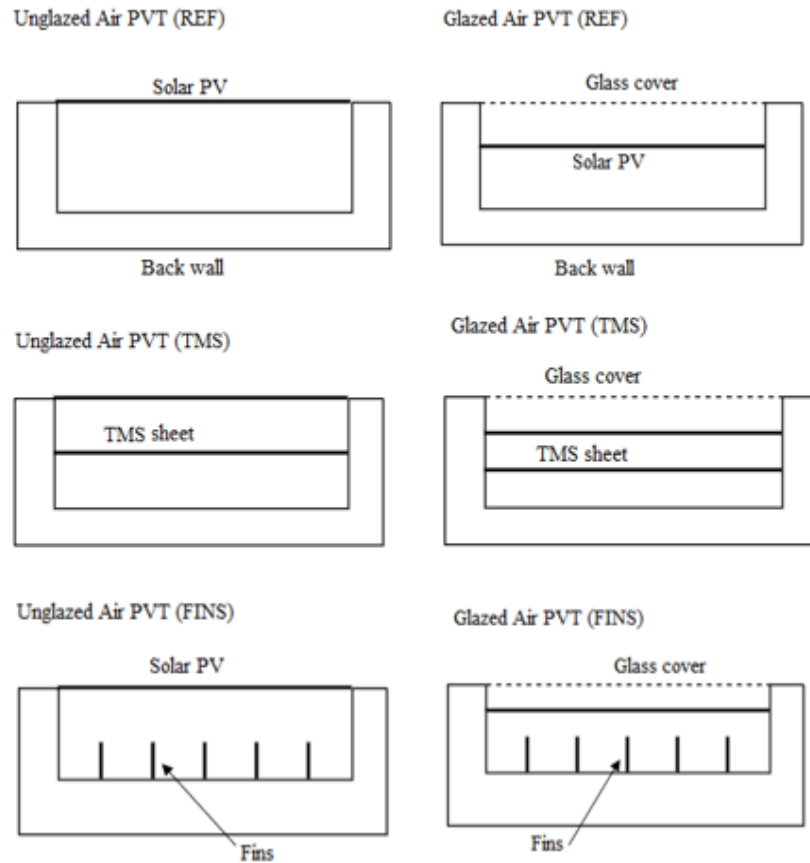


Figure 22. Cross-section of PVT collector models (Adopted from [92]).

The experiment, as shown in Figure 23, consists of an air-based PV collector with ribbed sheet steel absorbent material. The PV module is made from a material called polycrystalline (240-millimetre 1980 mm) is mounted through a skinny layer of highly versatile polyvinyl fluoride film and later mounted to the rib. The rib includes insulation layer of polystyrene and enclosed with skinny reflective layer and circulation pipe for water circulation. They determined that the collector flow rate have influenced on the air based solar collector behaviour thanks to some thermal losses exist between the collector and therefore the water based solar collector. They recommended enhancing the bi-fluid PVT collector design by study on the insulation material and enhancing the design of the collectors. The study of the performance of the solar collector showed that the thermal efficiencies were able to reach around 80% depending on the length of the collector and mass flow rate.

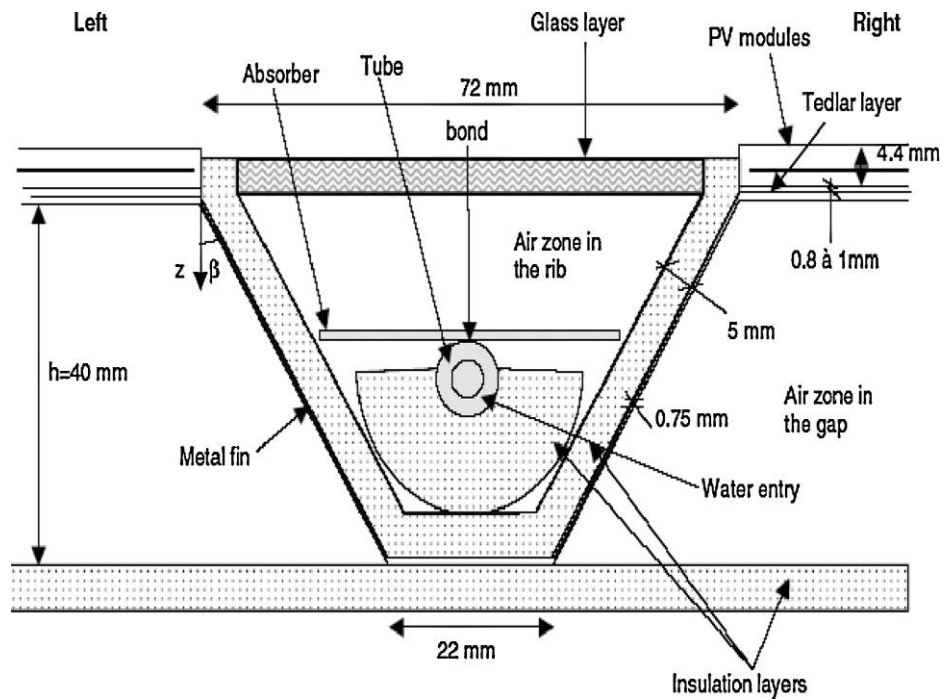


Figure 23. Cross-section of bi-fluid PVT (water and air) collector [93].

Fraisse et al. [94] investigated the Energy performance of PVT water collectors applied to the combined systems. The combined systems, in fact, are the addition of PV modules with thermal, that later combined with ‘‘Direct Solar’’ floor. During this study, hot water was supplied to the house. The study has been conducted in France, with no PV glass cover, created efficiency was 10% which is better than the regular standalone module with a 6%.

Chapter 3: System Description and Numerical Simulation

Figure 24 depicts a brief description of the PVT system used in this study. The system consists of a photovoltaic plate at the top with a thermal collector at the bottom consist of many miniature aluminum channels. The miniature cooling channels are rectangular with a width of (a) and a height of (b) and are fabricated inside the aluminum block with a height of (H). A unit block used to assemble the channel is also presented in Figure 24 with a width of (W).

To explore the performance of the proposed system, a numerical simulation has been conducted using a commercial software (ANSYS-Fluent). ANSYS-Fluent is a computational fluid dynamics (CFD) tool that uses finite volume techniques to solve the governing equations that capture the problem physics.

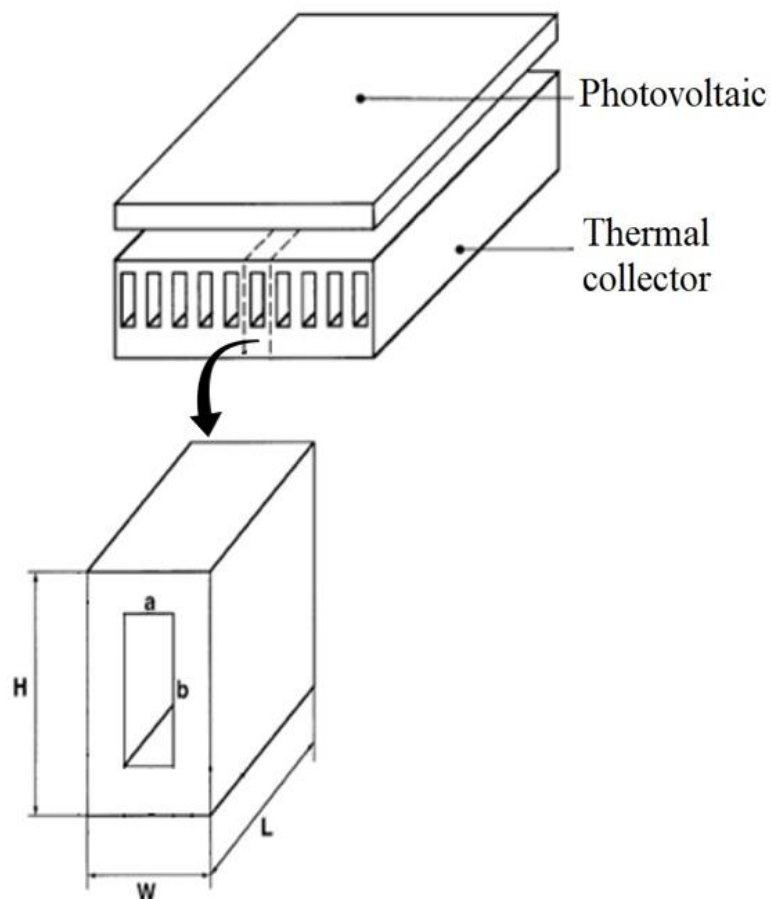


Figure 24. Schematic representation of the cooling channel attached to the PV.

3.1. Assumptions

To achieve the anticipated heat transfer, the fluid in this application is forced by external means like a pump through a non-circular flow section. This method is called forced convection. The flow regime applied in this study is laminar flow in which the Reynold number is less than the critical value of 2100. Laminar flow usually occurs at low velocities or high viscosities.

The boundary conditions applied in this study include a specified velocity at the inlet and zero-gauge pressure at the outlet. Also, the inlet and ambient temperatures were preliminary CFD input data. To enhance the overall performance of the system, all channel walls were adiabatic, and the no-slip condition was applied. At stationary solid boundary,

$$u = 0, \text{ at the boundary} \quad (1)$$

The fluid velocity relative to the boundary is equal to zero. This is the no-slip condition.

In this simulation, the energy model had been considered and the surface conditions were fixed. The heat generated from the solar irradiance absorbed by the PV is applied to the heat transfer equations which is transmitted by heat convection. The free convection and radiation heat transfer across the surfaces was zero. Table 3 depicts the properties of the coolant (water) used in the numerical simulation.

Table 3. Fluid (water) properties used in the simulation.

Property	Value	Unit
Density	998.2	kg/m ³
Thermal conductivity	0.6	W/m.K
Specific heat	4182	J/kg.K
Dynamic viscosity	0.001003	kg/m.s

3.2. Grid Generation and Solution Procedure

The generation of the grid in any numerical simulations plays a very important role. In this study, a uniform structured mesh is generated in 3D for a rectangular duct using the commercial software ANSYS (CFD). Figure 25 illustrates the methodology used in this study.

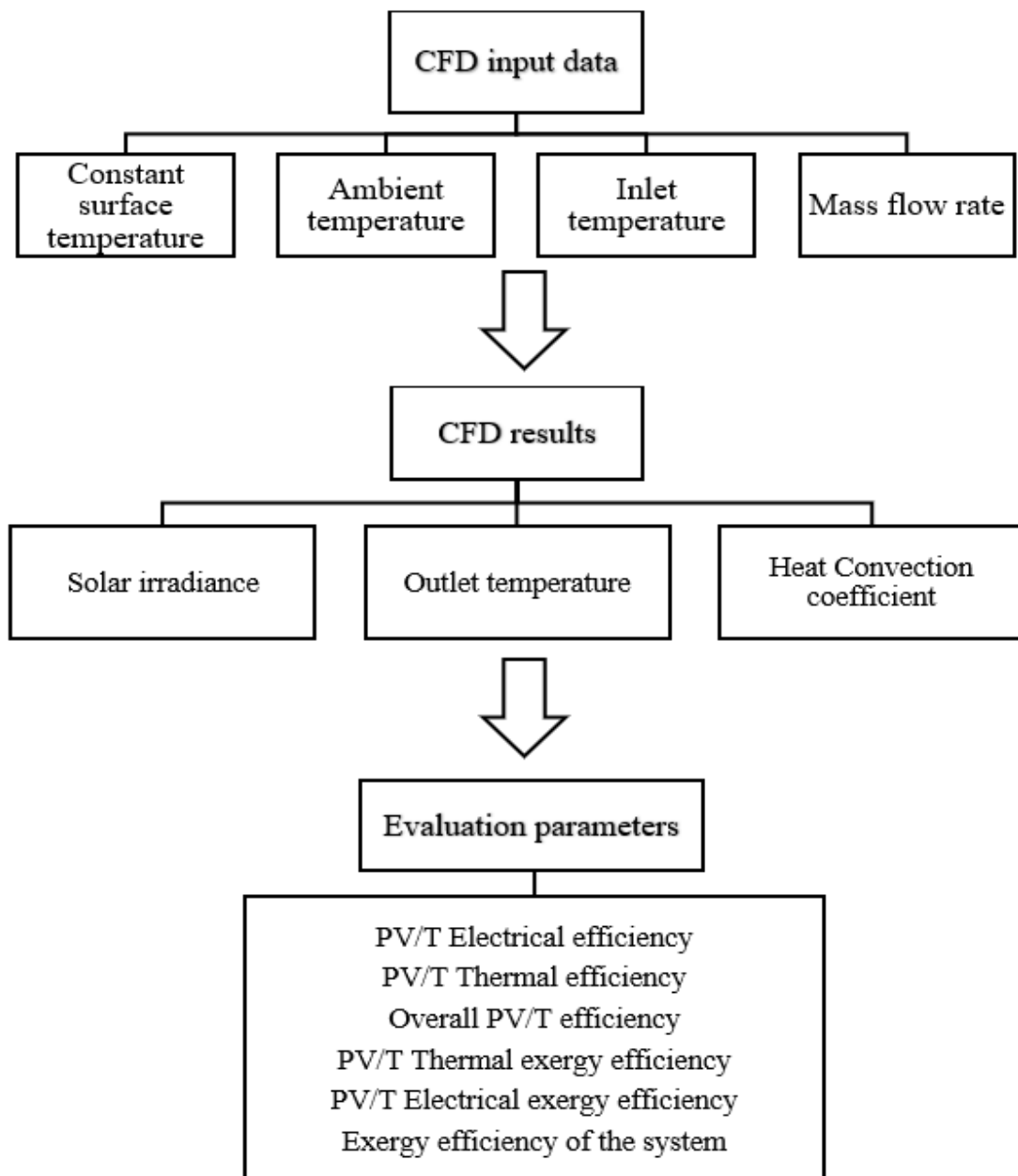


Figure 25. Methodology of the study.

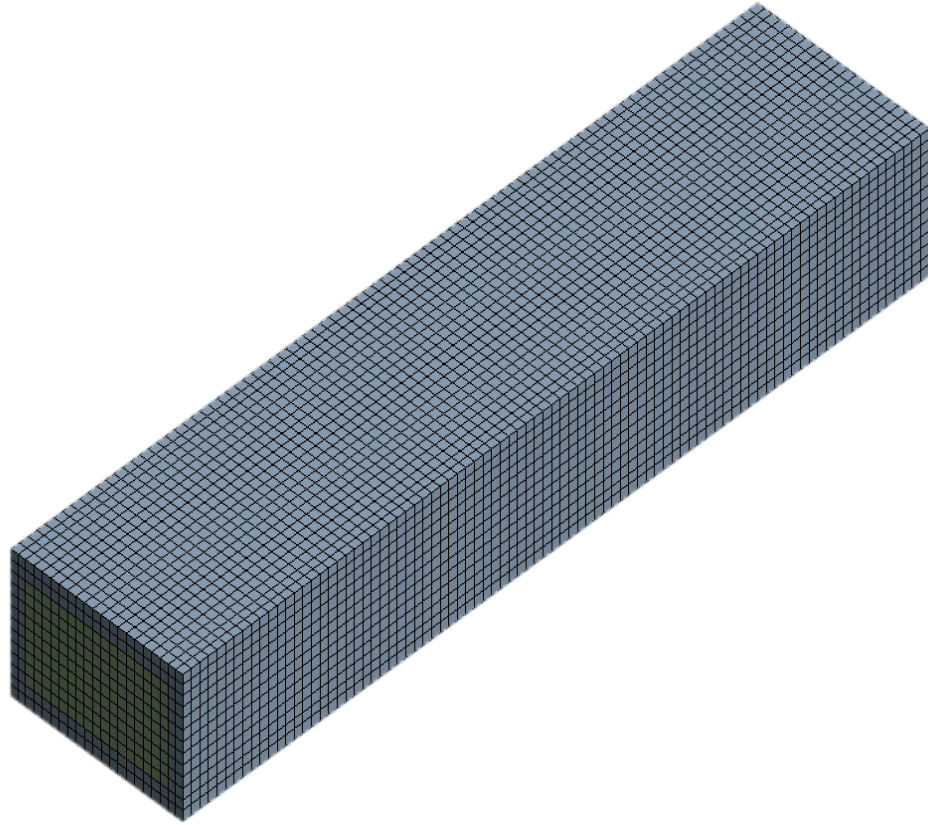


Figure 26. CFD meshing of the rectangular duct.

Figure 26 shows the applied mesh for the rectangular absorber. To accomplish the objectives of this study different methods and approaches were taken into consideration in which CFD tool is used along with the energy balance equation to study the performance of the suggested system.

The governing equations of CFD used in this study for 3D, steady state, and incompressible flow are the Navier-stoke equations and the energy equation. By applying the conservation of mass, momentum and energy, the following equations can be derived [95].

The continuity equation is,

$$\frac{\partial u}{\partial x} + \frac{\partial v}{\partial y} + \frac{\partial w}{\partial z} = 0 \quad (2)$$

The momentum equation is,

x-component:

$$\rho \left(u \frac{\partial u}{\partial x} + v \frac{\partial u}{\partial y} + w \frac{\partial u}{\partial z} \right) = -\frac{\partial P}{\partial x} + \mu \left(\frac{\partial^2 u}{\partial x^2} + \frac{\partial^2 u}{\partial y^2} + \frac{\partial^2 u}{\partial z^2} \right) \quad (3)$$

y-component:

$$\rho \left(u \frac{\partial v}{\partial x} + v \frac{\partial v}{\partial y} + w \frac{\partial v}{\partial z} \right) = -\frac{\partial P}{\partial y} + \mu \left(\frac{\partial^2 v}{\partial x^2} + \frac{\partial^2 v}{\partial y^2} + \frac{\partial^2 v}{\partial z^2} \right) \quad (4)$$

z-component:

$$\rho \left(u \frac{\partial w}{\partial x} + v \frac{\partial w}{\partial y} + w \frac{\partial w}{\partial z} \right) = -\frac{\partial P}{\partial z} + \mu \left(\frac{\partial^2 w}{\partial x^2} + \frac{\partial^2 w}{\partial y^2} + \frac{\partial^2 w}{\partial z^2} \right) \quad (5)$$

Equations (2)-(5) are the Navier-Stokes equations used to solve 3-dimensional steady state flow in a duct, where u, v and w are the fluid velocity components, P is the fluid pressure, ρ is the fluid density, and μ is the fluid dynamic viscosity.

Also, the energy equation is,

$$\rho C_p \left(u \frac{\partial T}{\partial x} + v \frac{\partial T}{\partial y} + w \frac{\partial T}{\partial z} \right) = k \left(\frac{\partial^2 T}{\partial x^2} + \frac{\partial^2 T}{\partial y^2} + \frac{\partial^2 T}{\partial z^2} \right) \quad (6)$$

where, C_p , k and T denote the specific heat capacity, the thermal conductivity and temperature, respectively.

3.3. Mesh Independence and Model Validation

To check the validity of the numerical results obtained by ANSYS, a fully developed laminar flow was tested by obtaining the Nusselt number and Darcy friction coefficient throughout the rectangular duct. The boundary conditions applied in this study include the PV surface temperature set at 50 °C and the inlet temperature and velocity of the coolant, water, are set to be 25 °C, and 0.1 m/s, respectively. Figure 24 illustrates the dimensions of the studied channel in which W, H , and a , are equal to 12 mm, 7 mm, and 10 mm, respectively. The height b was estimated to be $0.5a$. As for the depth (L) it will be evaluated after calculating the entrance length using Equation (8).

$$Re = \frac{\rho V D_h}{\mu} \quad (7)$$

$$L_e = 0.05 Re D_h \quad (8)$$

where, ρ is the fluid density, V is the average velocity, μ is the fluid dynamic viscosity, and D_h is the hydraulic diameter expressed as,

$$D_h = \frac{4A_c}{p} \quad (9)$$

where, A_c is the cross-sectional area of the duct and p is the wetted perimeter.

A Reynolds number of 666.8 that indicates a laminar flow regime was obtained under the conditions above and at a hydraulic diameter of 0.0067 m. The entrance length, L_e , of 0.22 m was evaluated at the given Re and D . Also, a rectangular duct depth (L) of 2 m was used in the numerical simulation.

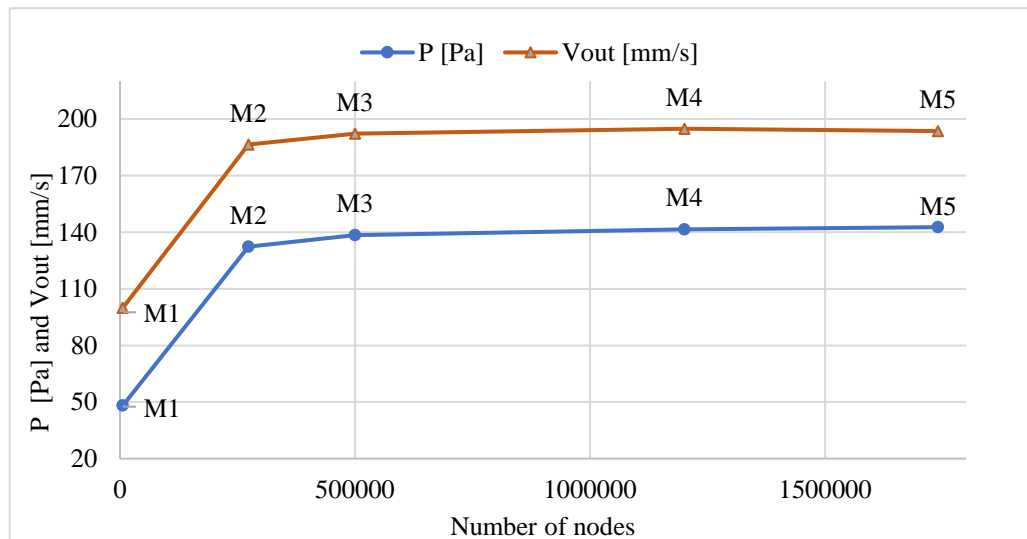


Figure 27. Mesh independence study by checking outlet velocity and inlet pressure.

One of the important aspects of numerical simulation is mesh generation which may lead to inaccurate results if the cells number is not enough or may result in longer solver runs if the cells are too many. Generally, each mesh should provide specific requirements which can be achieved through the right selection of the appropriate meshing technology. In this study, a 3D mesh independency test was applied using CFD. As illustrated in Figures 27 and 28, different mesh sizes were tested, to investigate the effect of the mesh size on the simulation results, by investigating three main parameters: inlet pressure, outlet velocity and outlet temperature.

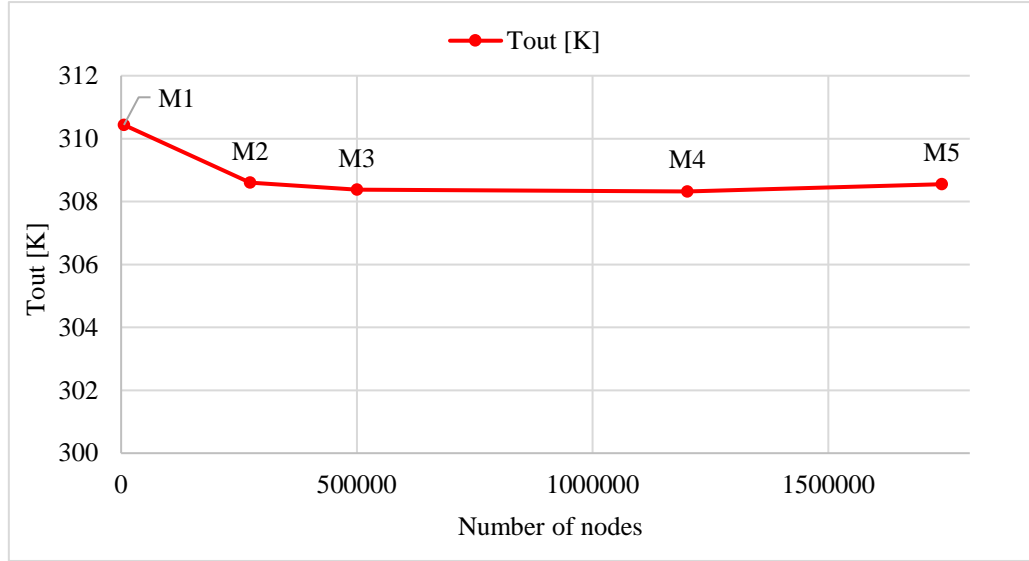


Figure 28. Mesh independence study by inspecting outlet temperature.

The results shown in Figures 27 and 28 clearly illustrate that the results of the CFD simulation depend on the number of mesh nodes. The results obtained for M1 and M2 are enough to show how the mesh can affect the solution, but it is noticeable that the values of the investigated parameters (P , V_{out} , and T_{out}) remain almost unchanged with a small deviation for meshes M3, M4, and M5. Due to slight differences the selected mesh used to carry out the numerical analysis of the proposed study is M4.

As the mesh size of the model was selected, M4, the validation of the numerical results was obtained by finding the Nusselt number, Nu , and the Darcy friction coefficient, f . The thermal conductivity of aluminum, k , was set to a very high value to ensure that the surface temperature of the fluid is almost the same as the surface temperature of the absorber. In this study, a constant surface temperature was assumed and set as a boundary condition. The methodology of calculating Nu and f using CFD was by dividing the fluid domains of the model into cross sections in which the results are collected at each plane cross section. The Nusselt number along the rectangular duct was obtained using Equation (10),

$$Nu = \frac{hD_h}{k_f} \quad (10)$$

where h and k_f are the heat convection coefficient and the fluid thermal conductivity, respectively. The heat convection coefficient was estimated using the heat transfer rate to the fluid inside the rectangular duct which can be expressed by Equation (11),

$$\dot{Q} = hA_s(T_s - T_m) \quad (11)$$

where A_s is the surface area of the plane cross-section, T_s is the surface temperature, T_m is the mixed cup temperature estimated from CFD simulation by mass flow average setup at different cross-section throughout the duct.

The variation of the Nusselt number across the duct in laminar flow for the constant surface temperature case is shown in Figure 29. It is noticeable that the Nusselt number and thus the heat transfer convection coefficient, h , are very high in the entrance region and then reach a constant value which indicates that the flow is fully developed. In literature [96], the value of Nusselt number for constant surface temperature and fully developed laminar flow equal to 3.39 for an aspect ratio a/b of 2.

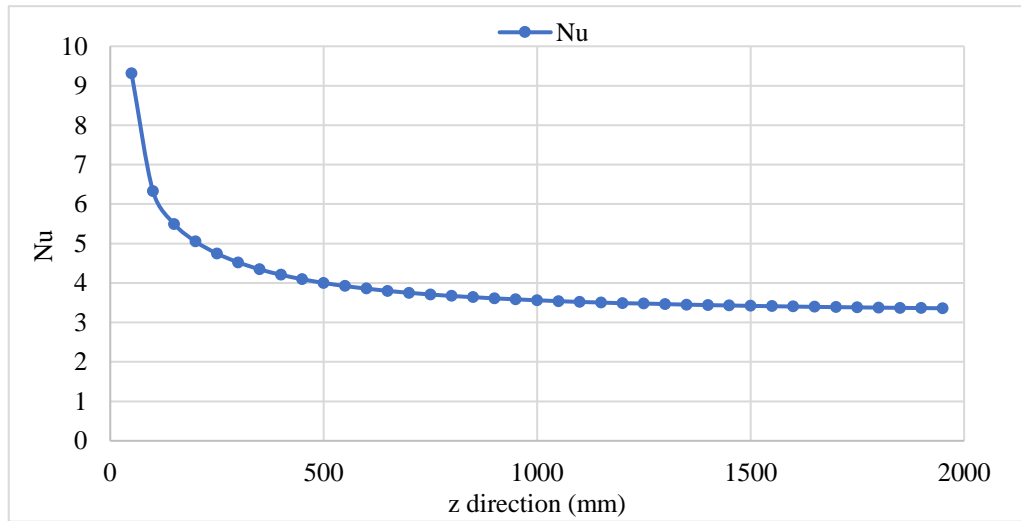


Figure 29. Variation of Nusselt number through the duct.

The Darcy friction coefficient, f , was estimated in this study to ensure that the results obtained from the numerical simulation are reliable. The value was obtained at different plane cross-section using the relation below,

$$f = \frac{8\tau}{\rho V_{inlet}^2} \quad (12)$$

$$\tau = \frac{\Delta P A_c}{A_s} \quad (13)$$

where, ΔP is the pressure difference between two consecutive cross-sections in the fluid domain, A_c is the cross-sectional area, and A_s is the surface area per unit length.

Figure 30 shows the variation of the friction coefficient throughout the duct, it shows that the friction coefficient is very high at the entrance region then it settles down to almost a constant value along the rectangular duct. Also, it is noticeable from Figure 31 that the pressure drop across the duct reaches a constant slope which indicates that the flow becomes fully developed state.

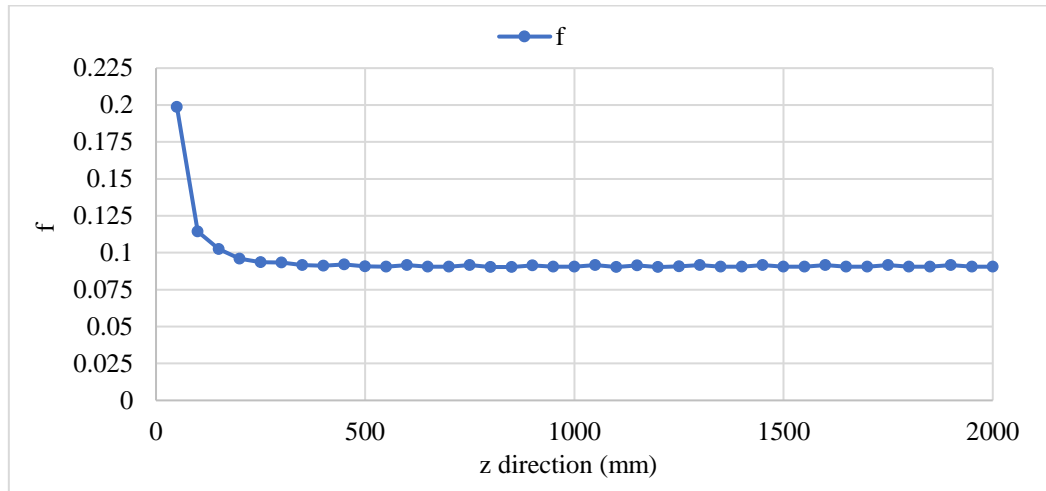


Figure 30. Variation of friction coefficient along the duct.

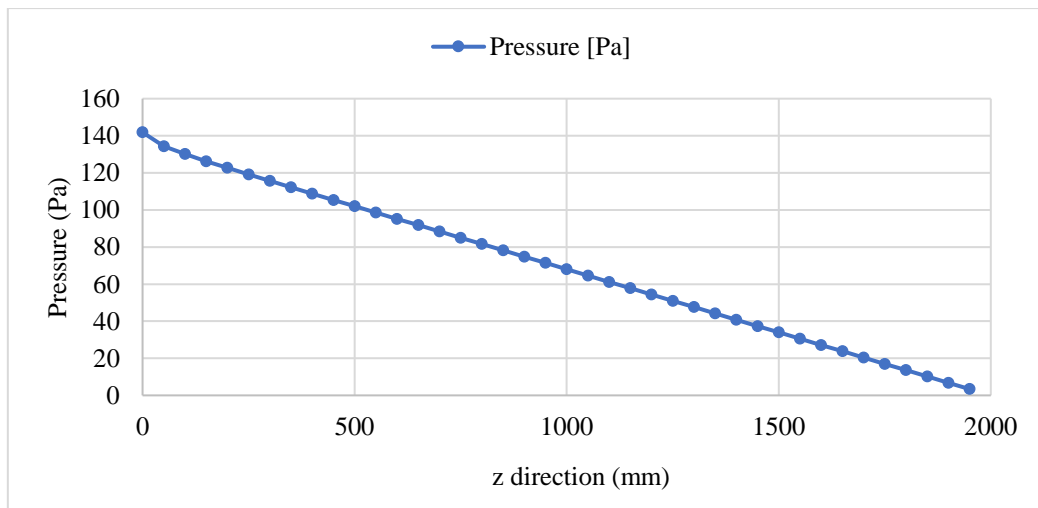


Figure 31. The pressure across the duct.

In the literature [96], the value of the friction factor at fully developed laminar flow regime for a/b equals to 2 is given by Equation (14),

$$f = \frac{62.2}{Re} \quad (14)$$

The value obtained by Equation (14) for Darcy friction coefficient, f , is 0.093.

3.4. CFD Results and Overall Convection Coefficient Calculation

To fully define the performance of the PVT collector one more parameter must be defined. The overall convection coefficient of the PVT can be expressed by the relation below,

$$\dot{m}c_p[T_o - T_i] = U_{overall}A_{PV}\Delta T_{LMT} \quad (15)$$

where, $U_{overall}$ is the overall convection coefficient of the PV, \dot{m} is the mass flow rate, ΔT_{LMT} is the log mean temperature difference stated by Equation (20), A_{PV} is the PV area. The value of $U_{overall}$ was studied by changing the thickness of the channel to select the highest U_{PV} can be obtained set as a parameter for the PV.

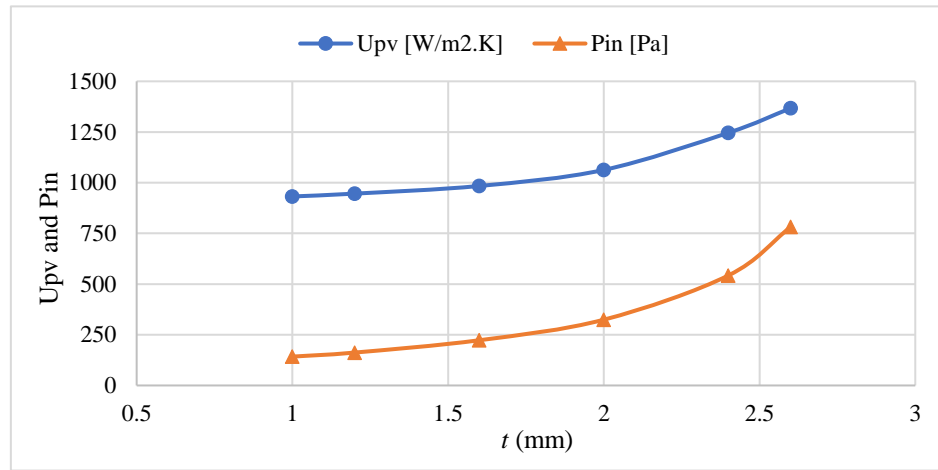


Figure 32. The convection coefficient of the PV and inlet pressure against the thickness of the channel.

Figure 32 depicts the effect of the channel on the value of the PV overall convection coefficient. A point of interest in the analysis of PVT overall convection coefficient is the pressure across the duct since it is related directly to power consumed by the pump or a fan to maintain flow. It showed that the pressure and the overall convection coefficient will increase with the wall thickness (t) shown in Figure 34, it is not better to select higher thickness because of the pressure, since it requires higher pump energy to achieve higher pressure. The pump power should not exceed the electrical energy extracted from the PV, otherwise the system will not consume energy rather than produce it.

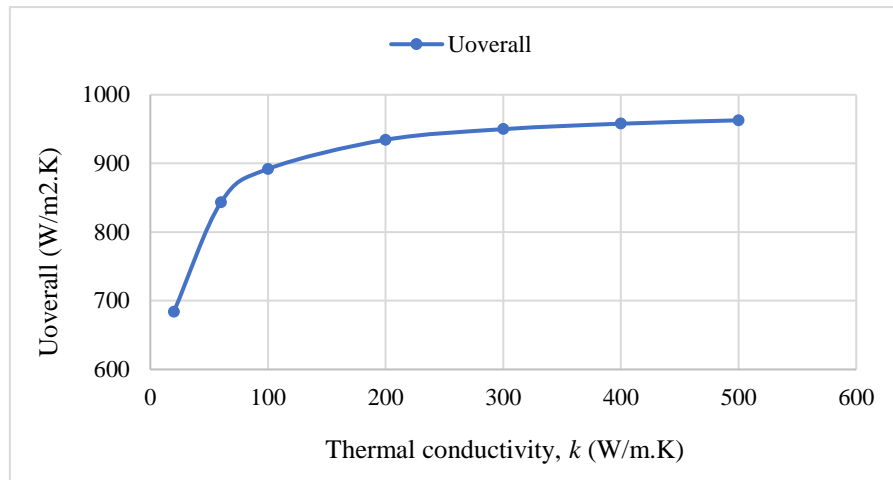


Figure 33. The overall convection coefficient at different thermal conductivity of the solid material.

The overall convection coefficient of the PV was calculated at different thermal conductivity as shown in Figure 33. The study was performed on a rectangular channel with specified cross section in which a , b , are 5 mm and 10 mm respectively. The thickness was set to 1 mm in all directions. The results showed that as the thermal conductivity increase the overall convection coefficient will increase. Also, the outcomes indicate that the overall convection coefficient will change slightly at higher thermal conductivity compared to the values at lower thermal conductivity.

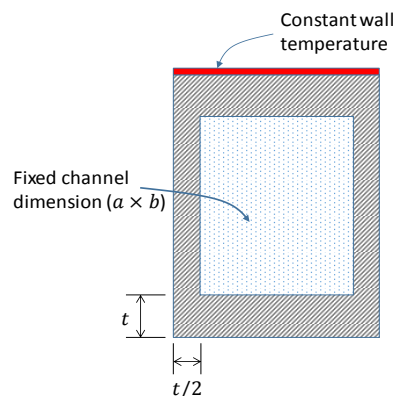


Figure 34. Dimensions of the cooling channel.

Figure 35 depicts the effects of the wall thickness of the cooling channel on the overall convection coefficient of the PV. The study was conducted at different wall thickness based on Figure 34 in which a , b , are set to 5 mm and 10 mm, respectively. The mass flow rate remains the same. The outcomes showed that the overall convection coefficient decrease as the wall thickness of the cooling channel increases.

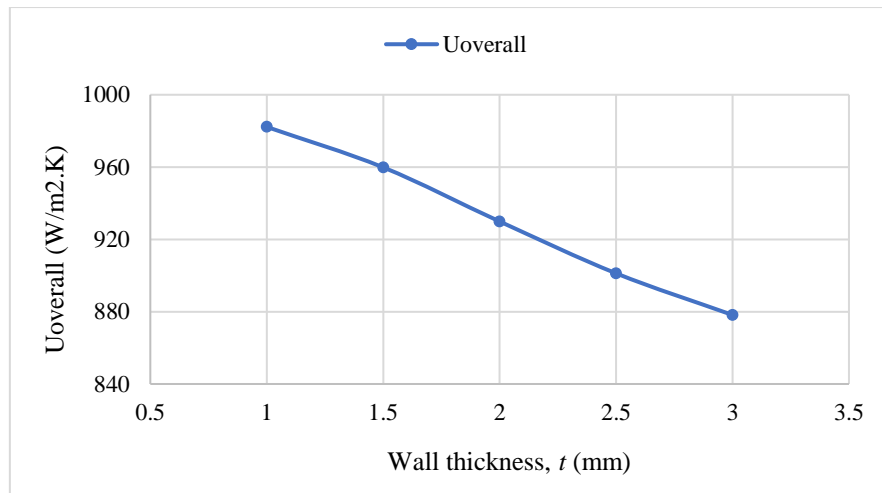


Figure 35. The overall convection coefficient at different wall thickness, t (mm).

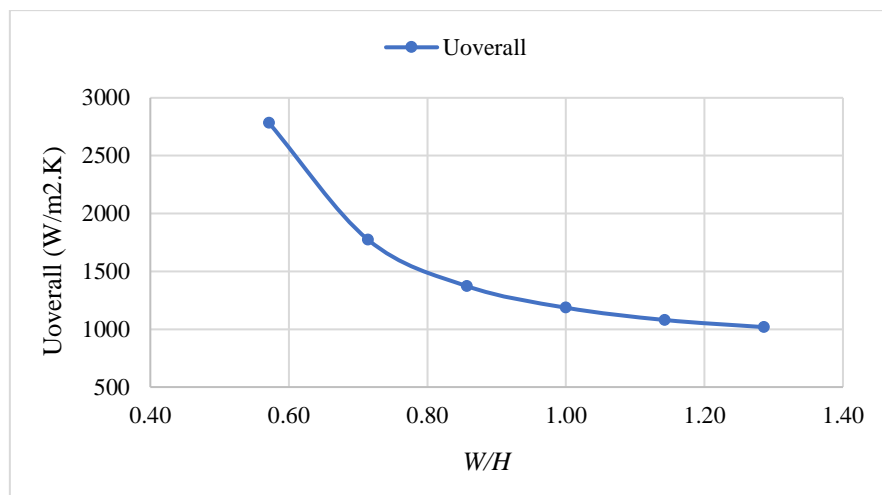


Figure 36. The overall convection coefficient of PV against different W/H ratio.

The overall convection coefficient of the PV can be affected by many parameters. The study conducted in Figure 36 was to check the effect of different values of W/H on the $U_{overall}$. In this Figure, the H value was fixed to 7 mm and the value of W was changing. The thickness, t , was fixed to 1 mm in all directions and a was set to 5 mm. The results obtained showed that the PV overall convection coefficient will drop with the increase of the W/H ratio. The mass flow rate increases as the W/H increase due to fixing the thickness and the height of the cooling channel and increasing the W . The velocity for all readings was fixed to 0.1 m/s, to make sure that the fluid regime is maintained in the laminar region, the Reynolds number was obtained as shown in Figure 37.

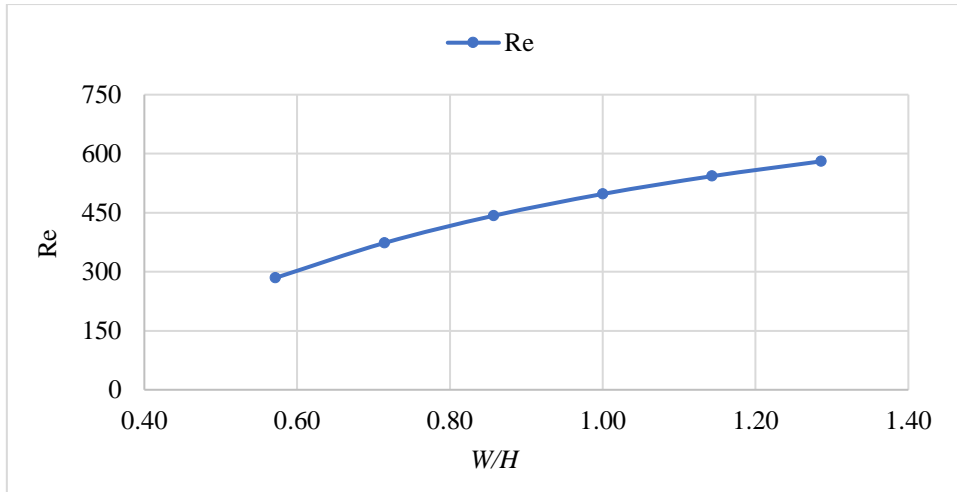


Figure 37. Reynolds number at different W/H ratio.

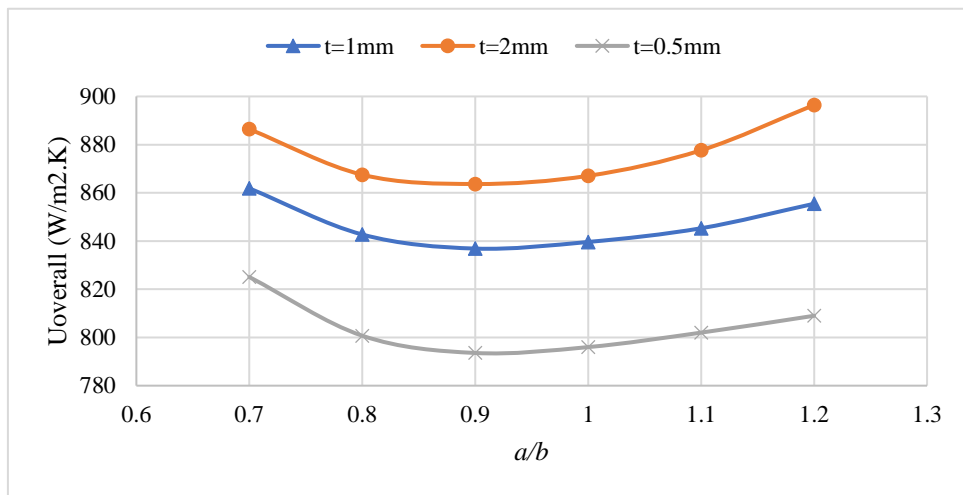


Figure 38. The overall convection coefficient of PV against different a/b ratio.

Figure 38 was conducted at Re , b , of 800 and 10 mm at different thickness, t , to show the effect of the a/b ratio on the PV overall convection coefficient at different wall thickness. In order to maintain the same Reynolds number, the velocity is calculated at specified values of a/b by calculating the new hydraulic diameter, D_h . The results obtained were interesting in which the overall convection coefficient takes a parabolic shape in which its minimum value was obtained at a/b of 0.9 for all thicknesses. The minimum value of $U_{overall}$ was obtained at a thickness of 0.5 mm at a/b of 0.9 and as the thickness increases the graph is shifted upward by maintaining the minimum value of $U_{overall}$ at a/b of 0.9.

Chapter 4: Analysis

As illustrated in Figure 39, the overall solar irradiance (I) is getting absorbed by the photovoltaic which release this energy in form of electrical power (\dot{E}), thermal energy (\dot{Q}_u) and heat lost to the surrounding (\dot{Q}_{lost}). The PVT performance can be explained by the combination of efficiency expressions involving thermal efficiency, η_{th} , and electrical efficiency, η_{ele} . These expressions indicate the amount of thermal and electrical gain from the solar irradiation absorbed by the PV. The total efficiency of the PVT, η , is obtained to assess the overall performance of the PVT [71],

$$\eta = \eta_{th} + \eta_{ele} \quad (16)$$

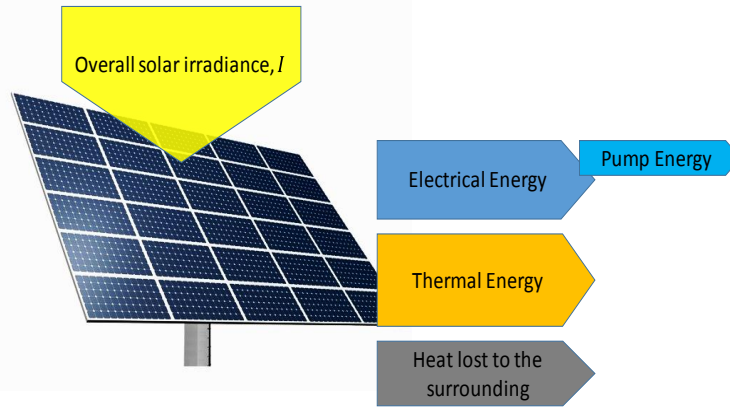


Figure 39. The overall solar irradiance reaching the PV.

The thermal performance of the PVT depends on different design parameters and working conditions. This system was constructed on single configuration of constant surface temperature, ambient temperature, and mass flow rate. The thermal efficiency of flat plate PVT solar collector is the ratio of useful thermal energy, \dot{Q}_u , to overall solar irradiance, I , can be estimated as,

$$\eta_{th} = \frac{\dot{Q}_u}{IA_{PV}} \quad (17)$$

where, A_{PV} is the PV area and \dot{Q}_u is the useful heat gain absorbed by the solar collector can be expressed as a combination of average mass flow rate, \dot{m} , heat capacity of the fluid, c_p , and temperature difference between inlet and outlet temperature of the working fluid, T_i and T_o , respectively. It is given as,

$$\dot{Q}_u = \dot{m}c_p[T_o - T_i] \quad (18)$$

It is essential to state one more equation to describe the thermal performance of the absorber. To achieve this aim, the model proposed in Figure 24 is treated as heat exchanger with constant surface temperature. From Newton's law of cooling, the heat transfer rate to the fluid through a duct is calculated using CFD and it can be given by the following relation,

$$\dot{Q}_u = U_{overall}A_{PV}\Delta T_{LMT} \quad (19)$$

where, U_{PV} is the heat convection coefficient of the PV, A_{PV} is the PV surface area, and ΔT_{LMT} is the log mean temperature difference which is given by Equation (20) where, T_s is the PV surface temperature,

$$\Delta T_{LMT} = \frac{T_i - T_o}{\ln\left(\frac{T_s - T_o}{T_s - T_i}\right)} \quad (20)$$

The thermal performance of the PVT is basically expressed as the collector efficiency defined as the useful heat gain to the solar irradiance absorbed by the collector. The useful energy gain, \dot{Q}_u , depends on the energy losses from the top, bottom, and edge of the collector owing to convective and radiative heat transfer process.

The edge losses can be ignored for a good designed collector with small ratio of collector perimeter to area [97]. The edge and bottom losses of PVT collector are always existing, but their influence is not noteworthy compared to top losses. The losses due to radiation in the equivalent background environment [98] is shown by Equation (21):

$$\dot{Q}_{Rad} = \sigma \varepsilon_{PVT} A_{PV} (T_s^4 - T_a^4) \quad (21)$$

where, T_s is the PV temperature, T_a is the ambient temperature assumed to be 300 K, σ is the Stefan-Boltzmann constant, $5.67 \times 10^{-8} W/m^2K^4$, ε_{PVT} is the thermal emissivity of the PVT which is assumed to be 0.9. The forced convection from the front surface of the PVT can be expressed as,

$$\dot{Q}_{conv} = h_w A_{PVT} (T_{PVT} - T_a) \quad (22)$$

The heat transfer coefficient (h_w) of the flowing air over the collector depends primarily on the wind velocity (v) which is given by Watmuff et al. [99]:

$$h_w = 2.8 + 3v \quad (22.1)$$

The electrical efficiency of the PV model is proposed by Zondag et al. [43] in which it depends linearly on the surface temperature of the PV, it is expressed as,

$$\eta_{ele} = \eta_{ref} [1 - \beta(T_{cell} - T_{ref})] \quad (23)$$

Depending on the PV material and operation conditions, the reference efficiency (η_{ref}) and the temperature coefficient (β) vary between different studies [100]. In this study the reference efficiency and the temperature coefficient are assumed to be 0.2 and 0.004 K⁻¹ [101], respectively. The reference temperature (T_{ref}) is set at 298 K. The pumping power should be taken into consideration since it will consume electrical energy. it is calculated using the following relation:

$$\dot{W}_p = \frac{1}{\rho} \dot{m} \Delta P \quad (24)$$

The total energy can be expressed as,

$$I = \dot{E} + \dot{Q}_u + (\dot{Q}_{conv} + \dot{Q}_{Rad}) \quad (25)$$

The model designated previously is basically built on the basis first law of thermodynamics which concern the PVT energy performance. Therefore, using that approach the collected electrical and thermal energy of the system can be associated under a metric criterion, with no reference to their actual thermodynamics quality [78].

Moreover, by stating the second law of thermodynamics it would show the proper assessment of the quality of the energy flux. Serving this aim, the main concept of exergy should be applied. It measures the maximum useful work that can be attained in a process that takes the system to equilibrium with the environment.

The analysis of exergy for PVT systems usually trails the same track. Basically, the exergy balance equation of the system should be considered, hence it is expressed as,

$$\Delta\dot{X}_{sys} = \dot{X}_{in} - \dot{X}_{out} - \dot{X}_{dest} \quad (26)$$

where, \dot{X}_{in} , \dot{X}_{out} , and \dot{X}_{dest} are inlet exergy, outlet exergy, and destroyed exergy due to irreversibility, respectively. $\Delta\dot{X}_{sys}$ in this case is equal to zero since the system is in steady state, so the equation will be simplified to,

$$\sum \dot{X}_{in} - \sum \dot{X}_{out} = \sum \dot{X}_{dest} \quad (27)$$

The input energy of any solar systems (PVT) is the sun's solar irradiance that reaches the system [102]. Hence, the inlet exergy of the PVT system can be assumed to be the exergy of radiation.

$$\dot{X}_{in} = \dot{X}_{sun} \quad (28)$$

In literature many relationships to calculate solar radiant energy had been proposed. The most supported relation is presented by Petela [103] which is expressed by Equation (29),

$$\dot{X}_{solar,in} = I \cdot A_{PV} \cdot \left[1 - \frac{4}{3} \left(\frac{T_a}{T_{sun}} \right) + \frac{1}{3} \left(\frac{T_a}{T_{sun}} \right)^4 \right] \quad (29)$$

where, T_a is the ambient temperature and T_{sun} is the sun's temperature equals to 6000 K. As for the output exergy of the system, \dot{X}_{out} , it is stated as the summation of thermal exergy and electrical exergy as given by Equation (30),

$$\sum \dot{X}_{out} = \sum \dot{X}_{th} + \sum \dot{X}_{ele} \quad (30)$$

As highlighted in the literature review, several works had already stated the exergy analysis for water-based and air-based PVT collectors. In this study, Equation (31) is based on the Gouy-Stodola Theorem [104]. It basically measures the increase of thermal exergy in fluid related to its temperature alteration between T_{in} and T_{out} .

$$\dot{X}_{th,out} = \dot{m} \cdot c_p \cdot \left[(T_{out} - T_{in}) - T_0 \ln \left(\frac{T_{out}}{T_{in}} \right) \right] \quad (31)$$

where, c_p and T_0 are the specific heat of the water and reference temperature at which the exergy of thermal power is zero (dead state), respectively.

Actually, dead state temperature (T_0) is usually assumed to be equal to the variable outdoor temperature as stated by Chow et al. [105]. Though, Pons [106] suggested that it is not right to consider T_0 as a variable parameter which will produce thermodynamics contradictions. Moreover, the constant T_0 is assumed. The constant value for T_0 varies between different studies amongst the authors and it is assumed in this study to be 298 K.

As for the electrical exergy of the system which is considered as pure exergy. By obtaining the PV electrical efficiency (η_{ele}) from Equation (32), the electrical exergy can be expressed as,

$$\dot{X}_{ele} = \dot{E}_{ele} = \eta_{ele} \cdot I \cdot A_{PV} \quad (32)$$

Eventually, the exergy efficiency of electricity production ($\eta_{exe,ele}$) and heat recovery ($\eta_{exe,th}$) can be given by Equation (33) and Equation (34):

$$\eta_{exe,ele} = \frac{\dot{X}_{ele}}{\dot{X}_{solar,in}} \quad (33)$$

$$\eta_{exe,th} = \frac{\dot{X}_{th}}{\dot{X}_{solar,in}} \quad (34)$$

The total exergy efficiency (η_{exe}) of the system can be expressed as the summation of the thermal and electrical exergy efficiency stated by Equation (35):

$$\eta_{exe} = \eta_{exe,ele} + \eta_{exe,th} \quad (35)$$

Chapter 5: Results and Discussion

The approach taken in this study to analyze the PVT collector are separated into two main sections, energy and exergy analyses in which the thermal, electrical and overall efficiencies are evaluated. In this section, the mathematical model mentioned earlier is applied to the prototype of the PVT collector described in Figure 24.

The effect of mass flow rate on the PVT performance is investigated (Figures 40-42). The mass flow rate through the selected channels indirectly affects PV unit cooling. The effect of mass flow rate on the PV surface temperature at various solar irradiance levels is shown in Figure 40. The results showed that the PV temperature drops as the mass flow rate increase at all solar irradiance. At same mass flow rate the PV temperature increase as the solar radiation increases. Figures 41-42 was conducted under different conditions at which the values for the flow rate used in this study ranges between 0.01 to 0.05 kg/s applied under solar irradiance of 1000 W/m² and at inlet temperature equals to 298 K. Figure 41 shows the electrical, thermal and overall efficiencies of the system. It is noticeable that the thermal efficiency has increased from 45.6 % to 71.45% at flow rate of 0.01-0.05 kg/s. On the other hand, the electrical efficiency of the absorber is almost constant.

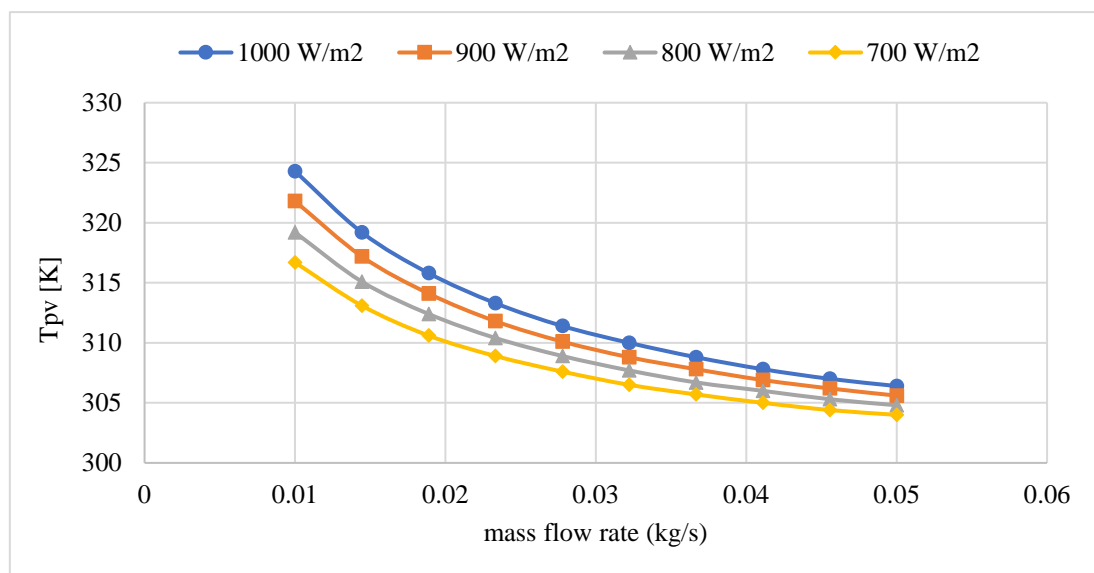


Figure 40. The PV temperature at different irradiation for different mass flow rate.

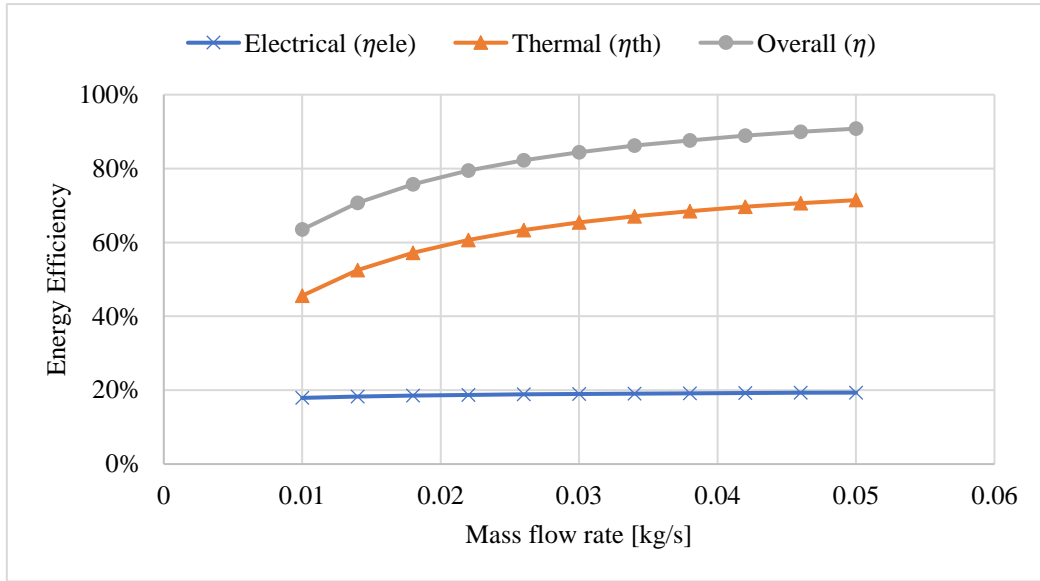


Figure 41. Variation of energy efficiencies (Thermal, Electrical and Overall) with mass flow rate under 1000 W/m^2 .

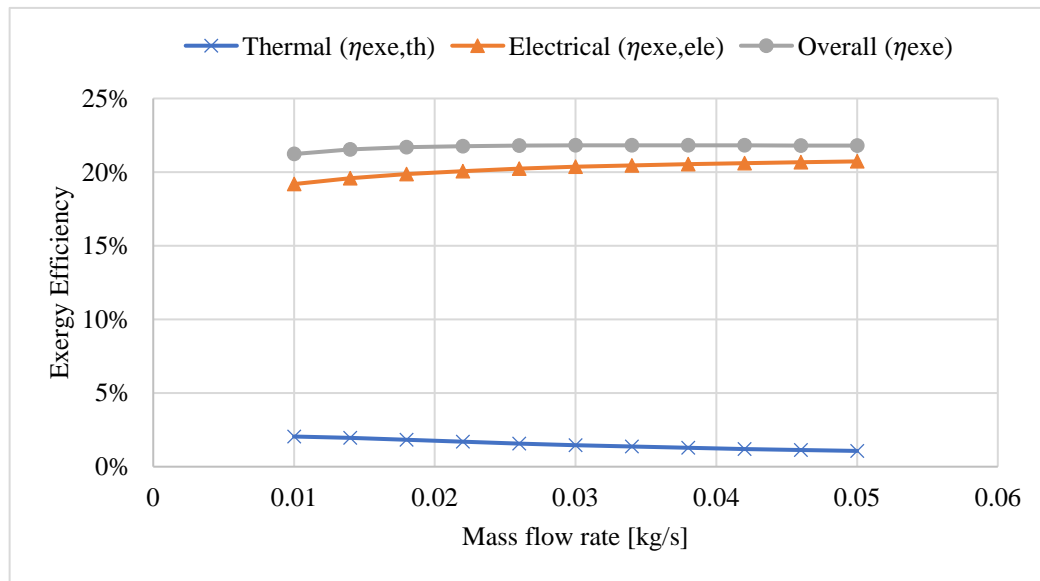


Figure 42. Variation of exergy efficiencies (Thermal, Electrical and Overall) with mass flow rate under 1000 W/m^2 .

The energy efficiency depends on the first law of thermodynamics with no reference to the actual thermodynamics' quality of the different energy forms, electrical and thermal, formed by the PVT collector. To serve the quality concept of different energy forms, exergy (available energy) has been defined as mentioned in previous sections. Figure 42 depicts the effect of mass flow rate on the exergy efficiency (Thermal, electrical and overall efficiencies). It can be observed that the trends for

thermal and electrical efficiencies are opposite, in which the thermal exergy efficiency increases while the electrical exergy efficiency decreases at low mass flow rate.

The effect of inlet temperature of water on the PVT performance is inspected (Figures 43-46). The temperature of the coolant at the selected channels affects PV unit cooling. The effect of T_{in} on the collector is shown in Figures 43-46. The values for the inlet temperature used in this study ranges from 25 °C to 47 °C applied under solar irradiance of 1000 W/m² and at flow rate equals to 0.02 kg/s. Figure 43 shows the electrical, thermal and overall efficiencies of the system. It is noticeable that the thermal efficiency decreased from 59 % to 36% at T_{in} of 25 - 47 °C. While, the electrical efficiency of the absorber is almost constant. The overall efficiency shows the same trend as the thermal efficiency. It is predictable that the overall efficiency won't reach to 100% due to losses.

Figure 44 illustrates the effect of inlet temperature on the exergy efficiencies (thermal, electrical and overall). It can be observed that the trends for thermal and electrical efficiencies are opposite, in which the electrical exergy efficiency increases while the thermal exergy efficiency decreases at low T_{in} . The combination of the thermal and electrical curves shows a very interesting result at which when the PVT operates at inlet temperature it would get optimal performance for T_{in} in the range of 34 °C and 37 °C. Therefore, it is not recommended to operate the PVT collector at very low temperatures.

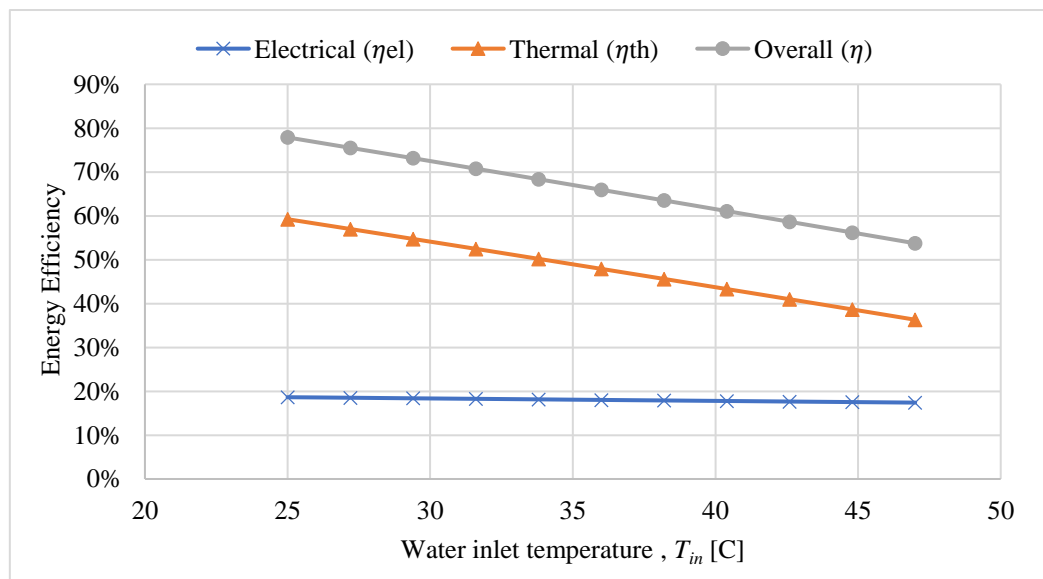


Figure 43. Variation of energy efficiencies (thermal, electrical, and overall) with the inlet temperature of water.

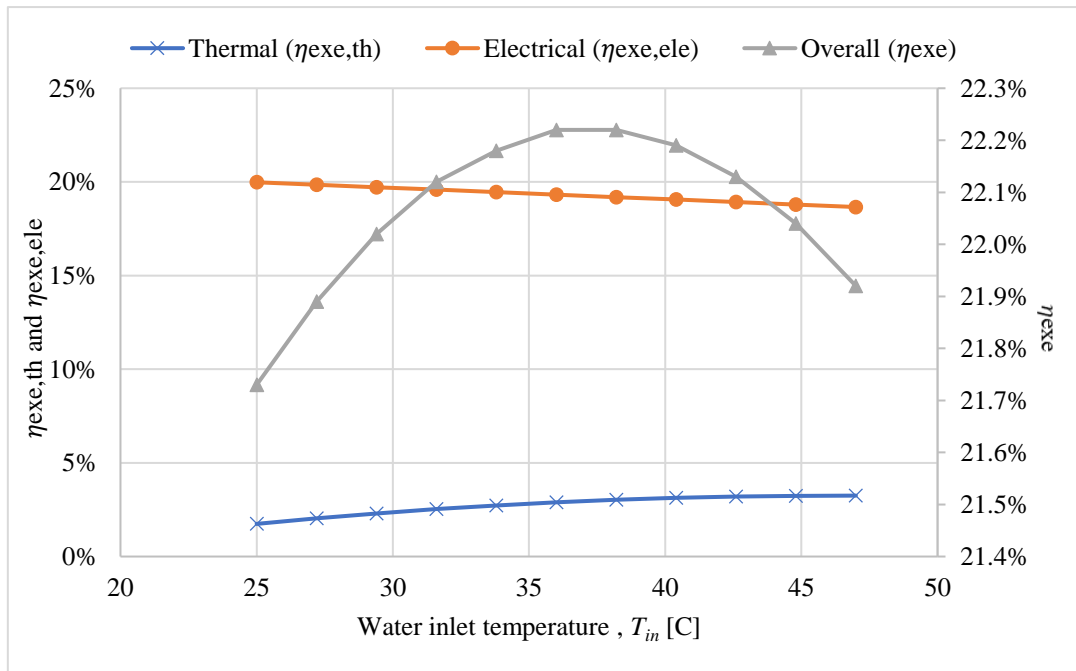


Figure 44. Variation of exergy efficiencies (thermal, electrical, and overall) with the inlet temperature of water

Figure 45-46 show clearly a maximum in exergy efficiency at specific value of inlet water temperature. The study conducted for two different mass flow rates (0.04 and 0.011 kg/s) belonging to the same operating conditions. Three combination of solar radiation and ambient temperature were tested. The results showed that under any conditions it is possible to identify an optimum inlet water temperature that will maximize the overall exergy efficiency of the system. The obtained optimum inlet water temperature is feasible since it can be managed i.e. the optimum inlet temperature ranges from 299 K at 400 W/m² and 308 K, to 314 K at 900 W/m² and 288 K. It is noticeable that the mass flow rate has almost no effect on the optimum inlet temperature obtained.

The effect of thermal conductivity of solid channel on the exergy and energy efficiency was investigated in Figures 47-48. The geometry of the collector used in this study was the same geometry used in Figure 33. The thermal conductivity ranges from 20 to 500 W/m². K. The outcomes obtained from Figure 48a showed an increase in the electrical efficiency from 10.8% to 13.3% as the thermal conductivity increases. As for thermal efficiency, it drops down from 85% to 83.8% with the increase of the thermal conductivity. Figure 48b showed the overall efficiency of the collector which increases

with the increase of thermal conductivity. Moreover, the exergy analysis was conducted, and the results were shown in Figure 47. The outcomes of this study showed an increase in the electrical and overall exergy with the thermal conductivity. The thermal exergy shows a very small change as the thermal conductivity of the material increases.

The PVT performance depends on the collector geometry. Some studies been conducted to investigate the effect of different collector geometries on the PVT performance. As illustrated in Figures 49-50, the energy and exergy efficiency are investigated at different wall thickness, t . The mass flow rate in this study was fixed and the flow channel dimension ($a \times b$) was set to (5 mm x 10 mm). The results obtained in Figures 49a and 49b show an increase in electrical efficiency and decrease in thermal efficiency as the wall thickness (t) increases. This outcome led to a decrease in the overall efficiency of the PVT. Figure 50 depicts the analysis of exergy efficiency which showed an increase in electrical and a decrease in thermal exergy as the wall thickness (t) increase. These outcomes led to an increase in the overall exergy of the PVT.

Figures 51-52 investigate the effect of different W/H on the PVT performance. The study was conducted by fixing H to 7 mm and change W value. The wall thickness was fixed to 1 mm at all directions and the mass flow rate is changing with W . Figure 51 depicts the effect of W/H on the exergy efficiency. The results showed an increase in the electrical exergy and a decrease in the thermal exergy with the increase in the W/H ratio. Whilst, the overall exergy decreased from 24.5% to 21.8%. The obtained results from Figure 52 shows an increase in the electrical efficiency with the increase of W/H due to an increase in the mass flow rate which will decrease the surface temperature of the PV as mentioned in Figure 40. According to Equation (23), as the PV surface temperature drops the electrical efficiency will be enhanced. On the other hand, as the W/H increase the thermal efficiency will drop from 81.9% to 78.9%. Due to the increase in electrical and decrease in the thermal efficiency the overall efficiency of the PVT increased.

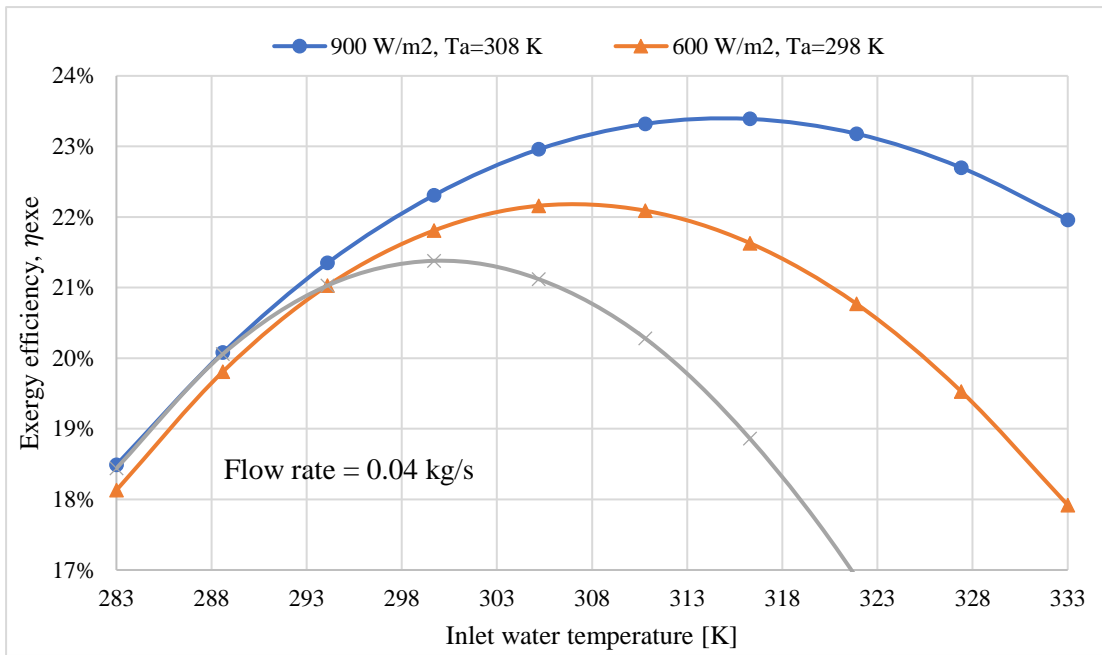


Figure 45. Overall exergy efficiency at different inlet water temperature and operating conditions for mass flow rate of 0.04 kg/s.

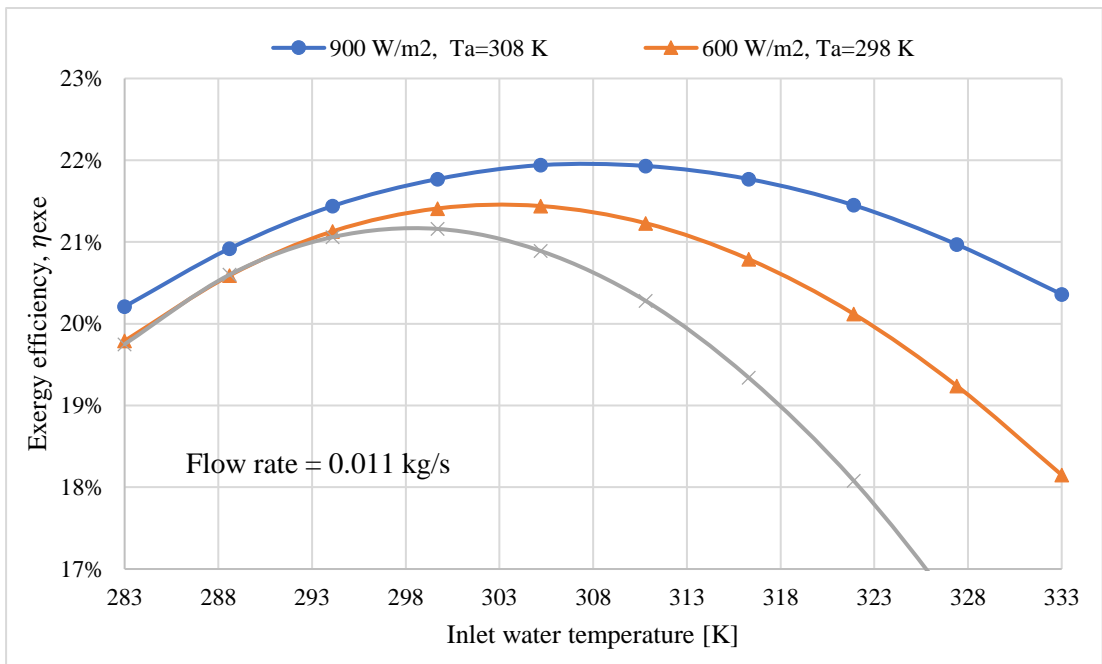


Figure 46. Overall exergy efficiency at different inlet water temperature and operating conditions for mass flow rate of 0.011 kg/s.

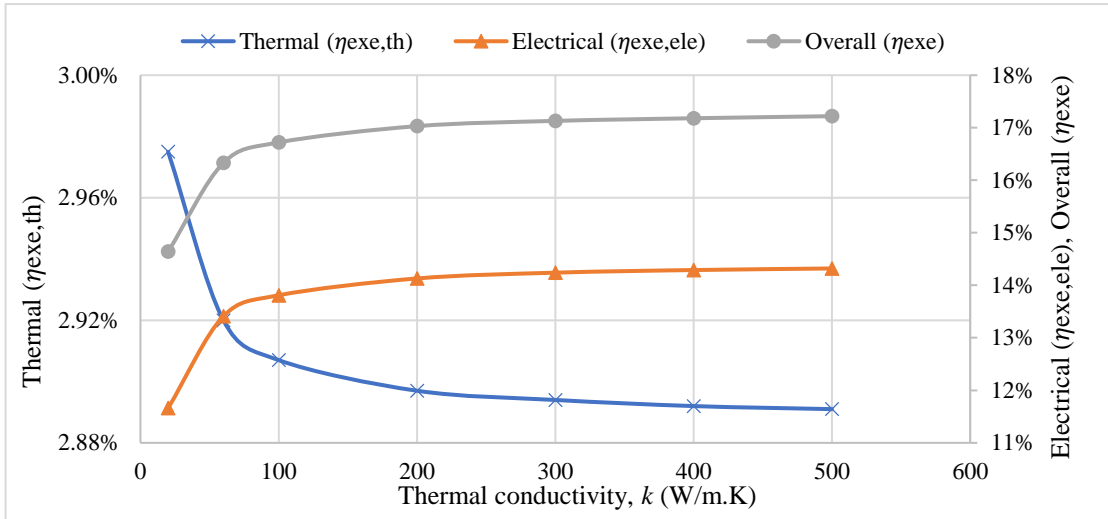
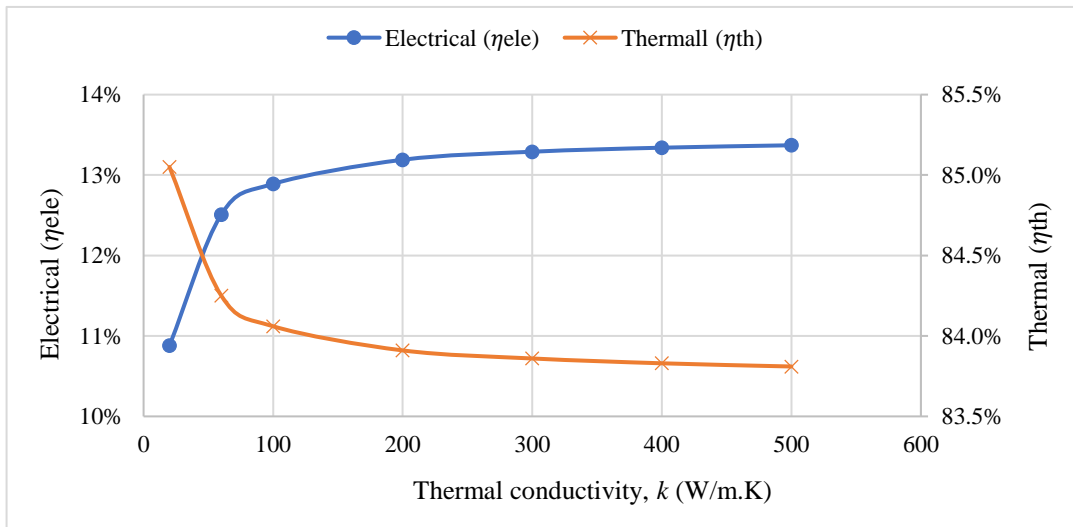


Figure 47. Exergy efficiency at different thermal conductivity.

a.



b.

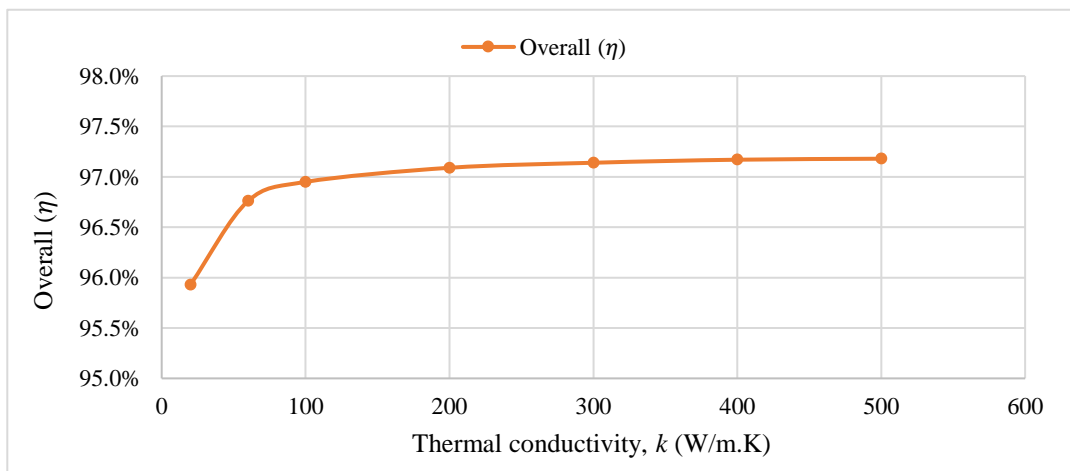


Figure 48. Energy efficiency at different thermal conductivity.

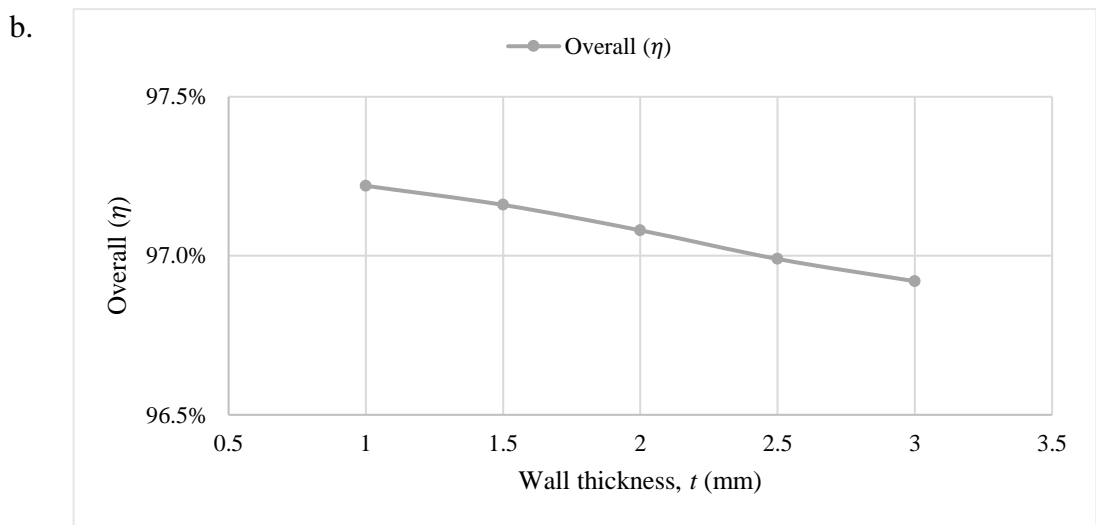
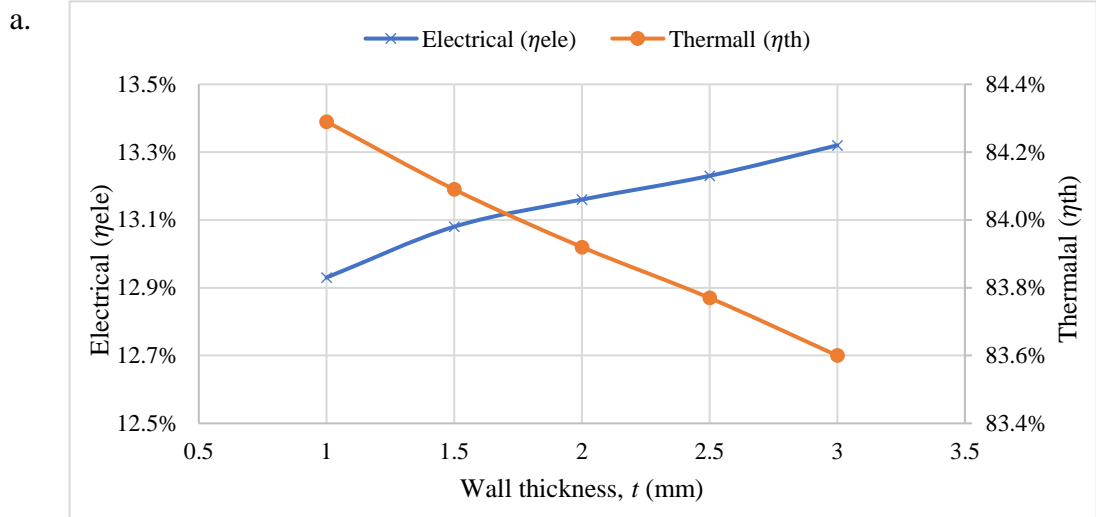


Figure 49. Energy efficiency at different wall thickness, t (mm).

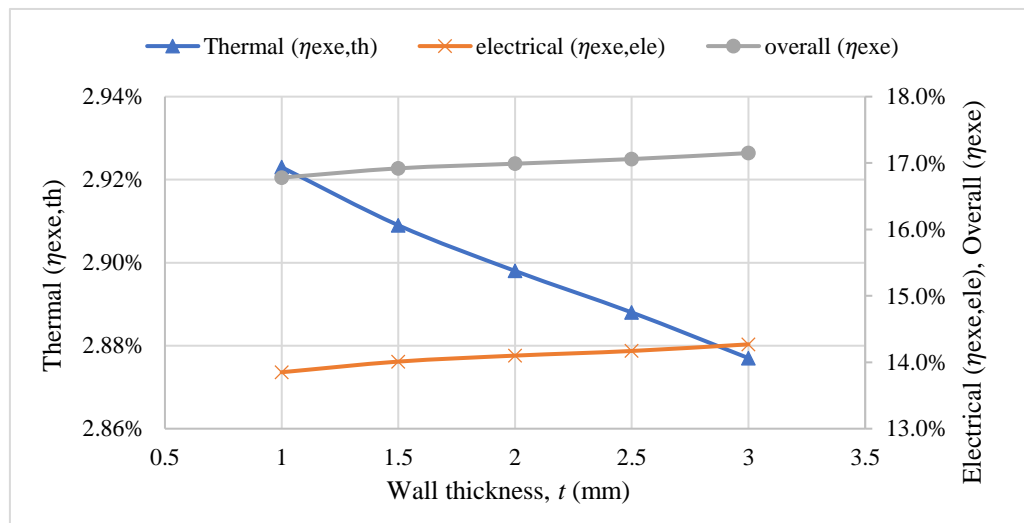


Figure 50. Exergy efficiency at different wall thickness, t (mm).

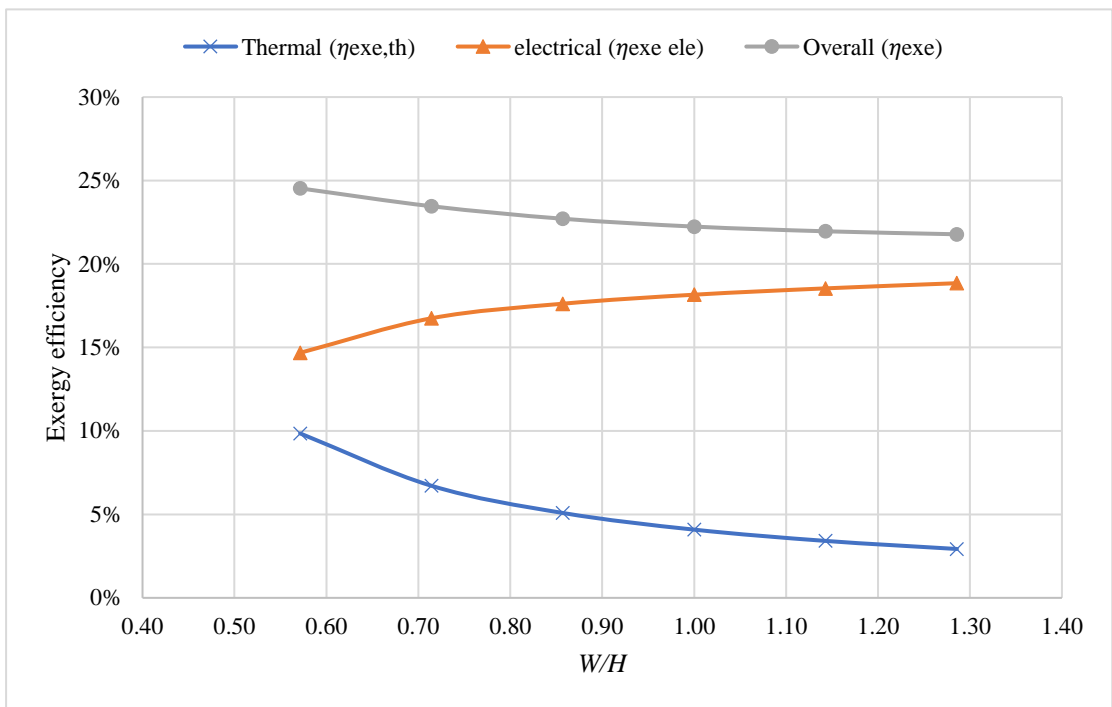


Figure 51. Exergy efficiency at different W/H .

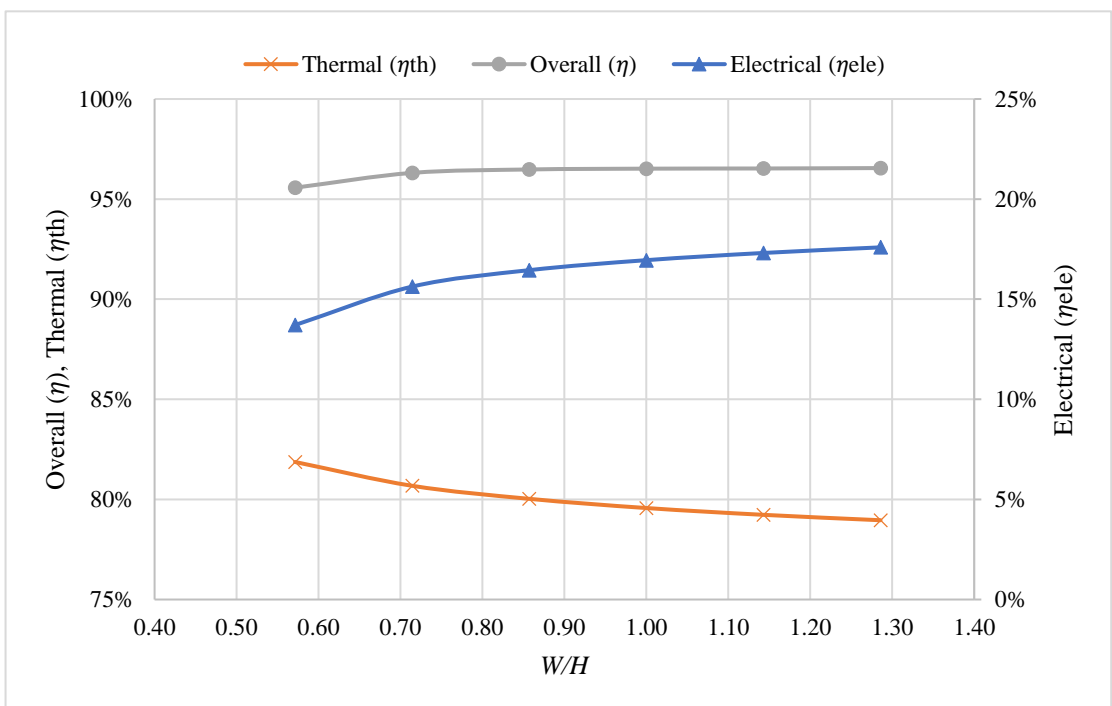


Figure 52. Energy efficiency at different W/H .

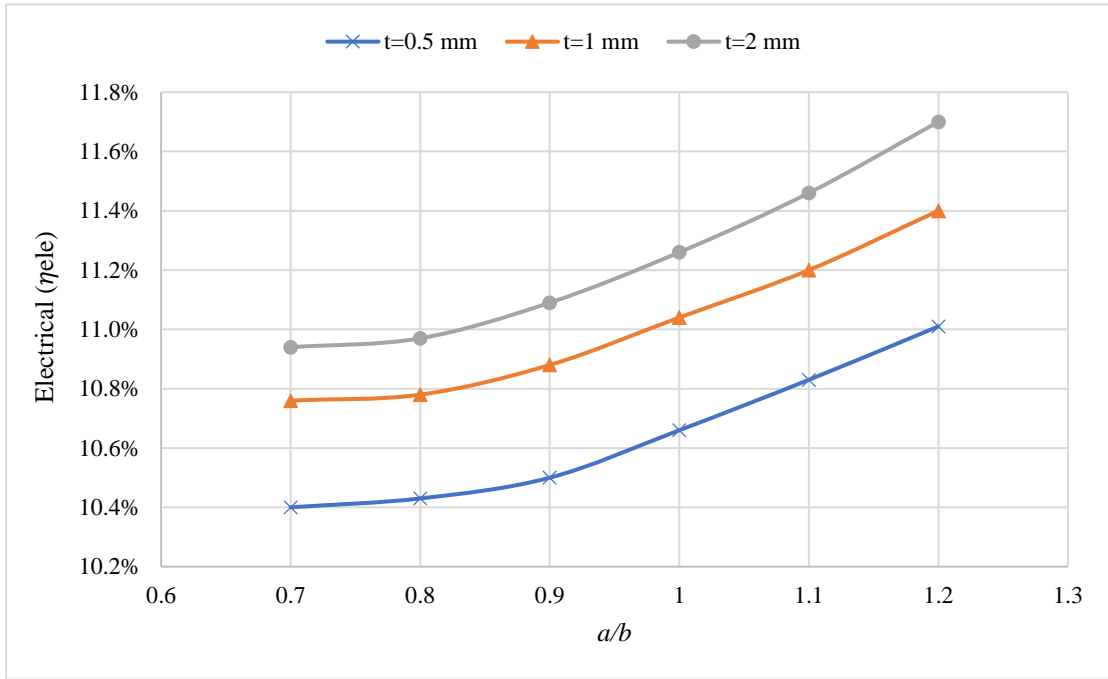


Figure 53. Electrical efficiency at different wall thickness (t) and a/b ratios.

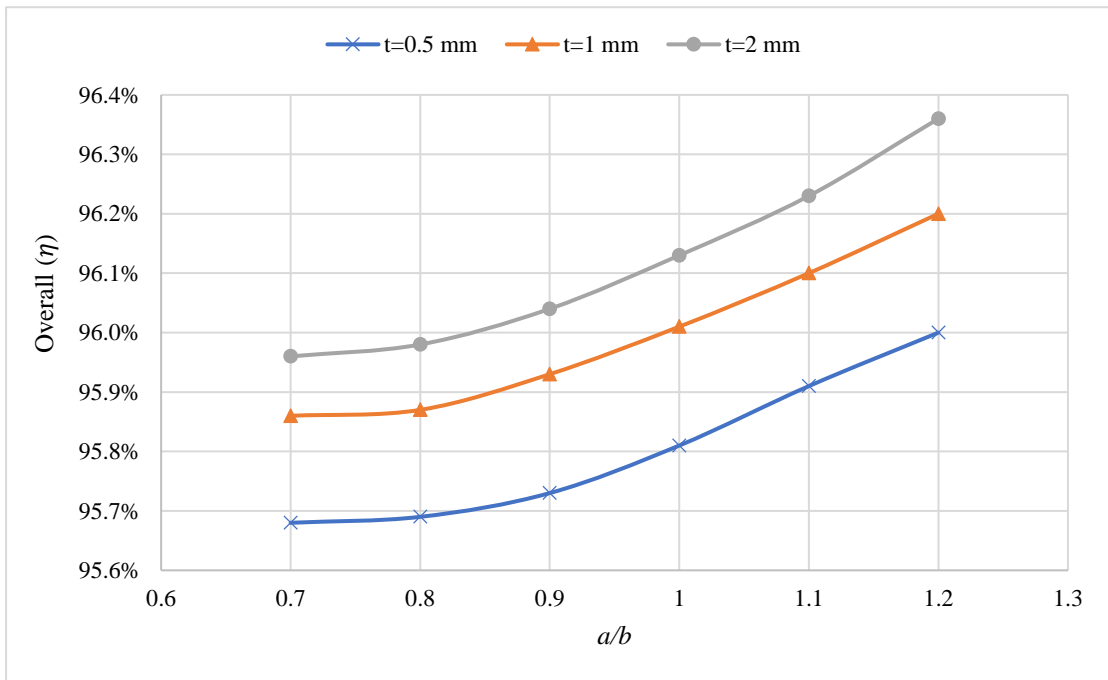


Figure 54. Overall efficiency at different wall thickness (t) and a/b ratios.

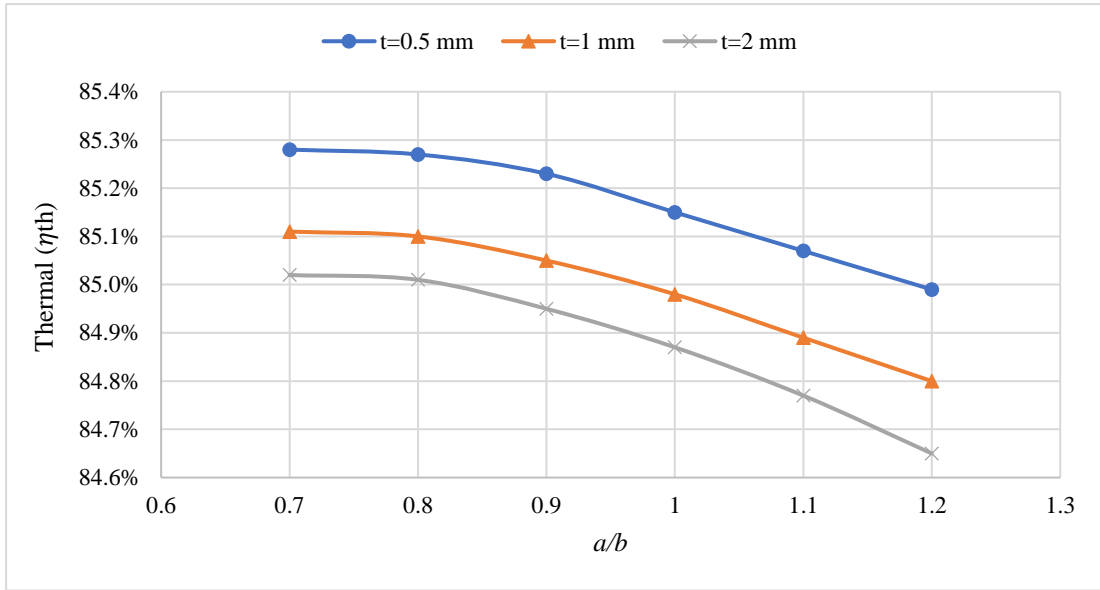


Figure 55. Thermal efficiency at different wall thickness (t) and a/b ratios.

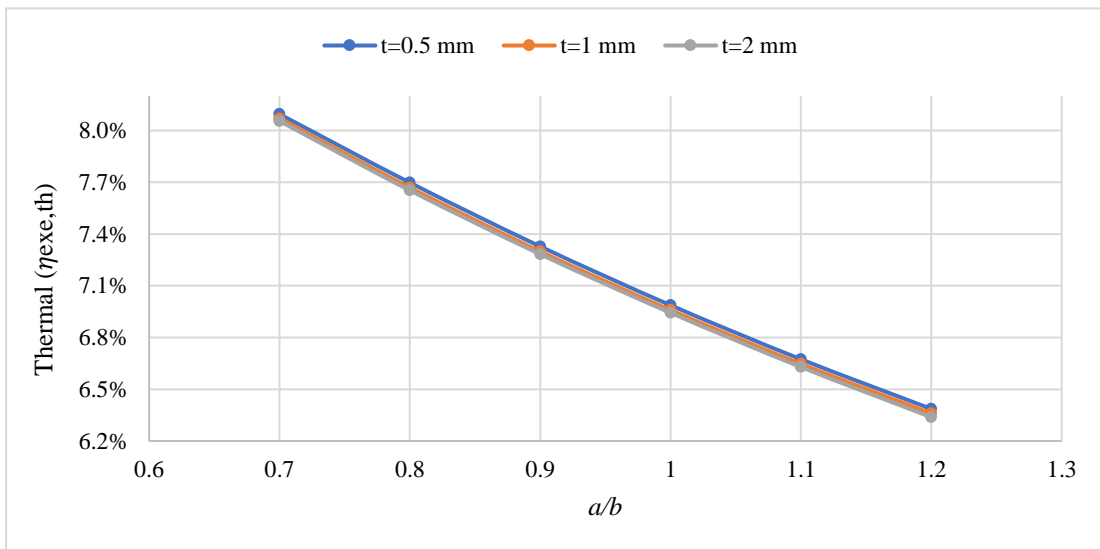


Figure 56 Thermal exergy at different wall thickness (t) and a/b ratios.

Figures 53-55 were conducted at Re , b , of 800 and 10 mm at different thickness, t , to show the effect of the a/b ratio on the PVT performance at different wall thickness. In order to maintain the same Reynolds number, the velocity is calculated at specified values of a/b by calculating the new hydraulic diameter, D_h . The results obtained in Figure 53 showed that the electrical energy increases as the a/b ratio increases at all wall thickness, t . At the same a/b ratio the electrical efficiency increases as the wall thickness increase. Whilst, the thermal efficiency showed a different relation as illustrated in Figure 55. The results showed a decrease in the thermal efficiency as the

a/b ratio increases, but at the same a/b ratio the thermal efficiency decreases as the wall thickness increases. Figure 54 depicts an increase in the overall efficiency with a/b ratio and at the same a/b value the overall efficiency increases as the wall thickness increase. The exergy analysis is investigated in Figures 56-58. Figure 56. Shows that the thermal exergy decreases as a/b increases but as the thickness changes with a/b the thermal exergy will approximately stay the same. The results obtained in Figure 57 showed an enhancement in electrical exergy as the a/b ratio increases. At the same a/b ratio the electrical exergy increased as the wall thickness (t) increases. Regarding the overall exergy, it is noticeable in Figure 58 that it decreases as the a/b ratio increase, but at the same a/b ratio it increases with the wall thickness (t).

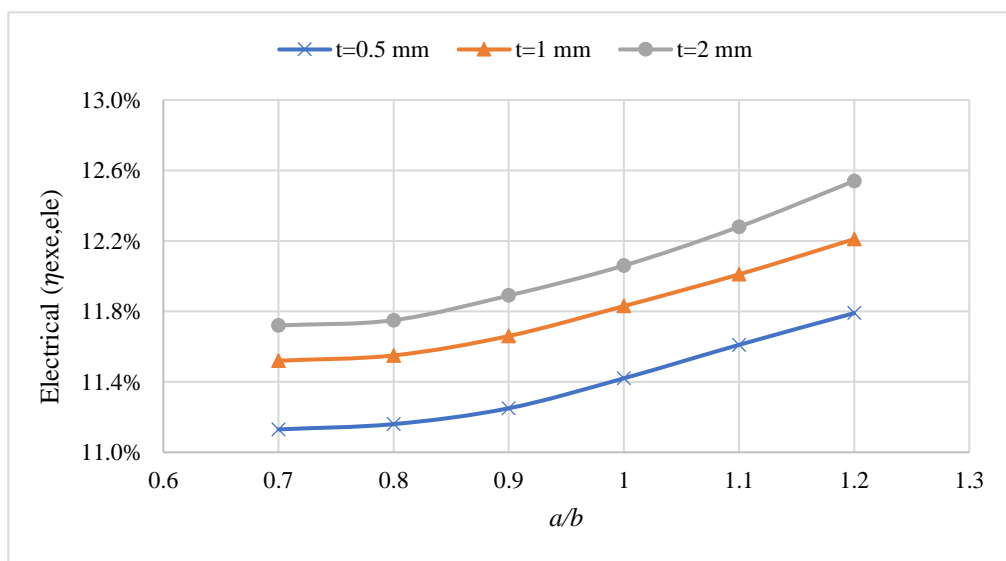


Figure 57. Electrical exergy at different wall thickness (t) and a/b ratios.

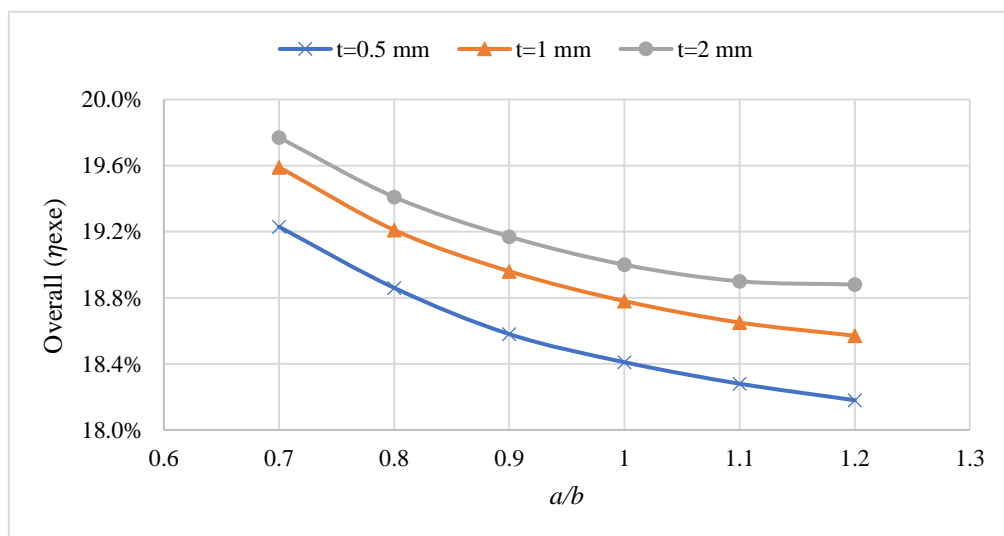


Figure 58. Overall exergy at different wall thickness (t) against different a/b ratios.

Chapter 6: Conclusions

The main purpose of using PVT hybrid systems is to convert the solar radiation into heat and electricity. Under normal solar radiation and conditions, PV cells temperature can be 30°C higher than the ambient temperature depending on how the PV cells are cooled. In this study, various designs of PVT systems and their advantages, disadvantages, type of fluid used, limitations, and applications has been presented. Also, a PVT system is designed and analyzed using CFD to reduce the PV cell temperature and enhance the overall efficiency. From the study it can be concluded that, to maximize PV performance, the heat removed from PV cell can be used in low-grade heat source that can be used as domestic hot water. Integrated PV with thermal collector improves the efficiency of the hybrid system. Different cooling techniques have shown validity in the field. The selection of cooling techniques depends on the added cost of implementation and maintenance of these systems. All cooling PVT hybrid system showed improvement in relative PV efficiency. The significance of improvement in relative efficiency needs to be weighted versus the added cost of the thermal collector.

The main objective of this study is to evaluate the performance of the collector using first and second law of thermodynamics. The effect of mass flow rate on the PVT performance is investigated. The results showed that the electrical efficiency of the PV increase when the temperature decrease. As the mass flow rate increase the PV temperature decrease nonlinearly. Also, the overall efficiency and the exergy efficiency of the PVT increase with the mass flow rate. The reason behind this outcome goes for the increase in the cooling factor for the PVT as the mass flow rate increases. Hence, the mass flow rate of the fluid indirectly affects PV unit cooling.

Nevertheless, the effect of the inlet water temperature was studied. According to the first law of thermodynamics, the overall efficiency obtained at lower inlet temperature is much greater than at high inlet water temperature. On the other hand, the adoption of second law of thermodynamics give an evaluation to the quality of energy, which indeed showed that it is not applicable to operate at low inlet temperatures. Also, the results showed an interesting outcome in which it is possible to indicate the optimum inlet temperature that maximize the overall exergy efficiency of the system.

Moreover, the PVT performance was tested at different thermal conductivity. The result showed an enhancement in the overall energy and exergy efficiency. It is noticeable from the results that the thermal and electrical efficiency had a small changes in their values after the thermal conductivity reaches 300 W/m.K, this indicates that it is not feasible to use material with higher thermal conductivity with a high cost. Also, the system performance was tested at different geometries in which it has a big contribution on the energy and exergy efficiency of the PVT.

References

- [1] M. Sumic, "Performance of a Solarus CPC-Thermal Collector," MS thesis, Dalarna University, Sweden, 2014.
- [2] C. J. Chen, *Physics of Solar Energy*. Hoboken, N.J: John Wiley & Sons, 2011, p. 326, 2011.
- [3] N. Martin, J.M. Ruiz, "Calculation of the PV modules angular losses under field conditions by means of an analytical model," *Solar Energy Materials and Solar Cells*, vol. 70, no. 1, pp. 25-38, 2001.
- [4] M. Q. Raza, M. Nadarajah, and C. Ekanayake, "On recent advances in PV output power forecast," *Solar Energy*, vol. 136, pp. 125-144, 2016.
- [5] A. Zervos, C. Lins, and J. Muth, "RE-thinking 2050: a 100% renewable energy vision for the European Union," European Renewable Energy Council (EREC), Belgium, Rep. no. 1, April 2010.
- [6] Z. Said, A. A. Alshehhi, and A. Mehmood, "Predictions of UAE's renewable energy mix in 2030," *Renewable Energy*, vol. 118, pp. 779–789, 2018.
- [7] H. Häberlin, *Photovoltaics: System Design and Practice*. Hoboken, NJ, USA: John Wiley & Sons, 2012, pp.1-24.
- [8] J.K. Tonui and Y. Tripanagnostopoulos, "Improved PVT solar collectors with heat extraction by forced or natural air circulation," *International Journal of Hydrogen Energy*, vol. 31, pp. 2137-2146, 2006.
- [9] E. Cuce, T. Bali, and S.A. Sekucoglu, "Effects of passive cooling on performance of silicon photovoltaic cells," *International Journal of Low-Carbon Technology*, vol. 6, no. 4, pp. 299-308, 2011.
- [10] R. Mazón-Hernández, J.R. García-Cascales, F. Vera-García, A.S. Káiser, and B. Zamora, "Improving the electrical parameters of a photovoltaic panel by means of an induced or forced air stream," *International Journal of Photoenergy*, vol. 2013, pp. 0-11, 2013.
- [11] A. Hasan, "Phase Change Materials for Thermal Regulation of Building Integrated Photovoltaics," PhD, Dublin Institute of Technology, Ireland, 2010.
- [12] S. Maiti, S. Banerjee, K. Vyas, P. Patel, and P. Ghosh. "Self regulation of photovoltaic module temperature in V-trough using a metal-wax composite phase change matrix. " *Solar Energy*, vol. 85, pp. 1805-1816, 2011.
- [13] M. Rosa-Clot, P. Rosa-Clot, G. Tina, and P. Scandura, "Submerged photovoltaic solar panel: SP2, " *Renewable Energy*, vol. 35, pp.1862-1865, 2010.
- [14] E. T. El-Shenawy, I. E. El-Seesy, and M. H. Ahmed, "Efficient design of hybrid PV/Hydrogen system," *World Applied Science Journal*, vol. 19, no. 9, pp. 1315-1321, 2012.
- [15] D. M Chandrasekar, S. Suresh, T. Senthilkumar, and M. Karthikeyan, "Passive cooling of standalone flat PV module with cotton wick structures, " *Energy Conversion and Management*, vol. 71, pp. 43-50, 2013.
- [16] X. Han, Y. Wang, and L. Zhu, "The performance and long-term stability of silicon concentrator solar cells immersed in dielectric liquids," *Energy Conversion Management*, vol. 66, pp. 189-198, 2013.
- [17] S.A. Abdulgafar, O.S. Omar, and K.M. Yousif, "Improving The Efficiency Of Polycrystalline Solar Panel Via Water Immersion Method," *International journal of Innovative Research in Science, Engineering and Technology*, vol. 3297, no. 1, pp. 8127-8132, 2007.
- [18] H.G. Teo, P.S. Lee, and M.N. Hawlader, "An active cooling system for

- photovoltaic modules,” *Applied Energy*, vol. 90, no. 1, pp. 309-315, 2012.
- [19] Z. Farhana, Y.M. Irwan, R.M. Azimmi, A.R. Razliana, and N. Gomesh, “Experimental investigation of photovoltaic modules cooling system,” in *Proc. IEEE Symposium Computers Informatics (ISCI)*, 2012, pp. 165-169.
- [20] R. Hosseini, N. Hosseini, and H. Khorasanizadeh, “An Experimental Study of Combining a Photovoltaic System with a Heating System,” *World Renewable Energy Congress*, 2011, pp. 2993-3000.
- [21] B. Du, E. Hu, and M. Kolhe, “Performance analysis of water cooled concentrated photovoltaic (CPV) system,” *Renewable and Sustainable Energy Reviews*, vol. 16, pp. 6732-6736, 2012.
- [22] H. Bahaidarah, A. Subhan, P. Gandhidasan, and S. Rehman, “Performance evaluation of a PV (photovoltaic) module by back surface water cooling for hot climatic conditions,” *Energy*, vol. 59, pp. 445-453, 2013.
- [23] L. Dorobanțu, M.O. Popescu, C.L. Popescu, and A. Crăciunescu, “Experimental Assessment of PV Panels Front Water Cooling Strategy,” *Renewable Energy and Power Quality Journal*, vol. 1, no. 11, pp. 1009-1012, 2013.
- [24] K. A. Moharram, M. S. Abd-Elhady, H. A. Kandil, and H. El-Sherif, “Enhancing the performance of photovoltaic panels by water cooling,” *Ain Shams Engineering Journal*, vol. 4, no. 4, pp. 869-877, 2013.
- [25] Y. Sun, Y. Wang, L. Zhu, B. Yin, H. Xiang, and Q. Huang, “Direct liquid-immersion cooling of concentrator silicon solar cells in a linear concentrating photovoltaic receiver,” *Energy*, vol. 65, pp. 264-271, 2014.
- [26] M.K. Smith *et al.*, “Water Cooling Method to Improve the Performance of Field-Mounted, Insulated, and Concentrating Photovoltaic Modules,” *Journal of Solar Energy Engineering*, vol. 136, no. 3, pp. 034503, 2014.
- [27] S. Nižetić, D. Čoko, A. Yadav, and F. Grubišić-Čabo, “Water spray cooling technique applied on a photovoltaic panel: The performance response,” *Energy Conversion Management*, vol. 108, pp. 287-296, 2016.
- [28] M. Rahimi, P. Valeh-e-Sheyda, M. Amin Parsamoghadam, M. Moein Masahi, and A. Alsairafi, “Design of a self-adjusted jet impingement system for cooling of photovoltaic cells,” *Energy Conversion and Management*, vol. 83, pp. 48-57, 2014.
- [29] H.A. Zondag, “Flat-plate PV-Thermal collectors and systems: A review,” *Renewable and Sustainable Energy Reviews*, vol. 12, no. 4, pp. 891-959, 2008.
- [30] A. K. Bhargava, H. P. Garg, and R. K. Agarwal, “Study of a hybrid solar system-solar air heater combined with solar cells,” *Energy Conversion and Management*, vol. 31, no. 5, pp. 471-479, 1991.
- [31] A.H Al-Waeli, K. Sopian, H.A. Kazem, and M.T. Chaichan, “Photovoltaic/Thermal (PVT) systems: Status and future prospects,” *Renewable and Sustainable Energy Reviews*, vol. 77, pp. 109-130, 2017.
- [32] F.P. Gasparin, A.J. Bühler, G.A. Rampinelli, and A. Krenzinger, “Statistical analysis of I-V curve parameters from photovoltaic modules,” *Solar Energy*, vol. 131, pp. 30-38, 2016.
- [33] B. Sandnes and J. Rekstad, “A photovoltaic/thermal (PVT) collector with a polymer absorber plate. Experimental study and analytical model,” *Solar Energy*, vol. 72, no. 1, pp. 63-73, 2002.
- [34] T.T. Chow, W. He, A.L. Chan, K.F. Fong, Z. Lin, and J. Ji, “Computer modeling and experimental validation of a building-integrated photovoltaic and water heating system,” *Applied Thermal Engineering*, vol. 28, no. 11-12, pp. 1356–

1364, 2008.

- [35] A. Naghdbishi, M. Sardarabadi, M. Passandideh Fard, and S. Zeinali Heris, "Computer Modelling and Experimental Validation of a Photovoltaic Thermal (PVT) Water Based Collector System," in *Proc. 2nd International Conference on Power and Energy Systems (ICPES)*, 2012, pp. 312-401.
- [36] A. Ibrahim, M.Y. Othman, M.H. Ruslan, S. Mat, and K. Sopian, "Recent advances in flat plate photovoltaic/thermal (PVT) solar collectors," *Renewable and Sustainable Energy Reviews*, vol. 15, no. 1, pp. 352-365, 2011.
- [37] W.T. An, and Y.F. Liu, "The study of PV Thermal integrated buildings solar system," *Applied Energy Technology*, vol. 23, no. 11, pp. 33-39, 2007.
- [38] N. Aste, G. Chiesa, and F. Verri, "Design, development and performance monitoring of a photovoltaic-thermal (PVT) air collector," *Renewable Energy*, vol. 33, no. 5, pp. 914-927, 2008.
- [39] H.A. Zondag, D.W. Vries, W.G. Helden, R.J. Zolingen, and A.A. Steenhoven, "The yield of different combined PV-thermal collector designs," *Solar Energy*, vol. 74, no. 3, pp. 253-269, 2003.
- [40] H.P. Garg and R.K. Agarwal, "Some aspects of a PVT collector/forced circulation flat plate solar water heater with solar cells," *Energy Conversion and Management*, vol. 36, no. 2, pp. 87-99, 1995.
- [41] D.L. Talavera, G. Nofuentes, J. Aguilera, and M. Fuentes, "Tables for the estimation of the internal rate of return of photovoltaic grid-connected systems," *Renewable and Sustainable Energy Reviews*, vol. 11, no. 3, pp. 447-466, 2007.
- [42] M.D. Bazilian, H. Kamalanathan, and D.K. Prasad, "Thermographic analysis of a building integrated photovoltaic system," *Renewable Energy*, vol. 26, no. 3, pp. 449-461, 2002.
- [43] H.A. Zondag, D.W. Vries, W. G Helden, R.J Zolingen, and A.A. Steenhoven, "The thermal and electrical yield of a PV-thermal collector," *Solar Energy*, vol. 72, no. 2, pp. 113-128, 2002.
- [44] A. Tiwari and M.S. Sodha, "Performance evaluation of solar PVT system: An experimental validation," *Solar Energy*, vol. 80, no. 7, pp. 751-759, 2006.
- [45] N. Christantonis, G. Vokas, and F. Skitides, "Simulation of hybrid Photovoltaic-Thermal Collector (PV-TC) Systems for domestic Heating and Cooling—Case Study: Island of Rhodes," *WSEAS Transactions on Circuits and Systems*, vol. 3, pp. 1228-1223, 2004.
- [46] R. Zakharchenko *et al.*, "Photovoltaic solar panel for a hybrid PVThermal system," *Solar Energy Materials and Solar Cells*, vol. 82, no. 1-2, pp. 253-261, 2004.
- [47] A. Ibrahim *et al.*, "Hybrid photovoltaic thermal (PVT) air and water based solar collectors suitable for building integrated applications," *American Journal of Environmental Sciences.*, vol. 5, no. 5, pp. 618-624, 2009.
- [48] V.V. Tyagi, S.C. Kaushik, and S.K. Tyagi, "Advancement in solar photovoltaic/thermal (PVT) hybrid collector technology," *Renewable and Sustainable Energy Reviews*, vol. 16, no. 3, pp. 1383-1398, 2012.
- [49] T.T. Chow, "Performance analysis of photovoltaic-thermal collector by explicit dynamic model," *Solar Energy*, vol. 75, no. 2, pp. 143-152, 2003.
- [50] X. Zhang, X. Zhao, S. Smith, J. Xu, and X. Yu, "Review of R&D progress and practical application of the solar photovoltaic/thermal (PV/T) technologies," *Renewable and Sustainable Energy Reviews*, vol. 16, no. 1, pp. 599-617, 2012.
- [51] Y. Tripanagnostopoulos, T. Nousia, M. Souliotis, and P. Yianoulis, "Hybrid

- photovoltaic/thermal solar systems,” *Solar Energy*, vol. 72, no. 3, pp. 217-234, 2002.
- [52] S. Kiran and U. Devadiga, “Performance Analysis of Hybrid Photovoltaic/Thermal Systems,” *International journal of emerging technology and advanced engineering*, vol. 4, no. 3, pp. 80-86, 2014.
- [53] S. Dubey and G.N. Tiwari, “Analysis of PVT flat plate water collectors connected in series,” *Solar Energy*, vol. 83, no. 9, pp. 1485-1498, 2009.
- [54] A. Ibrahim, A. Fudholi, K. Sopian, M. Othman, and M.H. Ruslan, “Efficiencies and improvement potential of building integrated photovoltaic thermal (BIPVT) system,” *Energy Conversion and Management*, vol. 77, pp. 527-534, 2014.
- [55] S.N. Jahromi, A. Vadiiee, and M. Yaghoubi, “Exergy and Economic Evaluation of a Commercially Available PVT Collector for Different Climates in Iran,” *Energy Procedia*, vol. 75, pp. 444-456, 2015.
- [56] V.N. Palaskar and S.P. Deshmukh, “Waste heat recovery study of spiral flow heat exchanger used in hybrid solar system with reflectors,” *International Journal of Energy Science*, vol. 5, no. 1, pp. 6-16, 2015.
- [57] A.A. Alzaabi, N.K. Badawiyeh, H.O. Hantoush, and A.K. Hamid, “Electrical/thermal performance of hybrid PVT system in Sharjah, UAE,” *International Journal of Smart Grid and Clean Energy*, vol. 3, no. 4, pp. 385-389, 2014.
- [58] H. Saitoh *et al.*, “Field experiments and analyses on a hybrid solar collector,” *Applied Thermal Engineering*, vol. 23, no. 16, pp. 2089-2105, 2003.
- [59] V.N. Palaskar and S.P. Deshmukh, “Performance analysis of a specially designed flow heat exchanger used in hybrid photovoltaic/thermal solar system,” *International Journal of Renewable Energy Research*, vol. 5, no. 2, pp. 476-482, 2015.
- [60] S.S. Mojumder, “Study of Hybrid Photovoltaic Thermal (PV/T) Solar System with Modification of Thin Metallic Sheet in the Air Channel,” *Journal of Energy Technologies and Policy*, vol. 3, no. 5, pp. 47-55, 2013.
- [61] S. Haddad, “Investigation of the Electrical and Thermal Performance of a PV/T Hybrid System,” in *Proc. tenth International Conference on Ecological Vehicles and Renewable Energies (EVER)*, 2015, pp. 220-310.
- [62] M. Rosa-Clot, P. Rosa-Clot, G.M. Tina, and C. Ventura, “Experimental photovoltaic-thermal Power Plants based on TESPI panel,” *Solar Energy*, vol. 133, pp. 305-314, 2016.
- [63] M.A. Al-Nimr and W.A. Al-Ammari, “A novel hybrid PV-distillation system,” *Solar Energy*, vol. 135, pp. 874-883, 2016.
- [64] R. Daghigh, M.H. Ruslan, A. Zaharim, and K. Sopian, “Monthly performance of a photovoltaic thermal (PVT) water heating system,” in *Proc. 6th IASME/WSEAS international conference on Energy & Environment*, 2011, pp. 298-303.
- [65] K.K. Tse, T.T. Chow, and Y. Su, “Performance evaluation and economic analysis of a full scale water-based photovoltaic/thermal (PVT) system in an office building,” *Energy and Buildings*, vol. 122, pp. 42-52, 2016.
- [66] L. Brottier, S. Naudin, V. Veaser, G. Terrom, and R. Bennacer, “Field Test Results of an Innovative PVT Collector for Solar Domestic Hot Water,” *Energy Procedia*, vol. 91, pp. 276-283, 2016.
- [67] F. Yazdanifard, E. Ebrahimnia-Bajestan, and M. Ameri, “Investigating the performance of a water-based photovoltaic/thermal (PVT) collector in laminar and turbulent flow regime,” *Renewable Energy*, vol. 99, pp. 295-306, 2016.

- [68] R. Daghigh, A. Ibrahim, G.L. Jin, M.H. Ruslan, and K. Sopian, "Predicting the performance of amorphous and crystalline silicon based photovoltaic solar thermal collectors," *Energy Conversion and Management*, vol. 52, no. 3, pp. 1741-1747, 2011.
- [69] A.R. Starke, J.M. Cardemil, R.A. Escobar, and S. Colle, "Assessing the performance of hybrid CSP + PV plants in northern Chile," *Solar Energy*, vol. 138, pp. 88-97, 2016.
- [70] Y. Khanjari, F. Pourfayaz, and A.B. Kasaeian, "Numerical investigation on using of nanofluid in a water-cooled photovoltaic thermal system," *Energy Conversion and Management*, vol. 122, pp. 263-278, 2016.
- [71] A. Fudholi, K. Sopian, M.H. Yazdi, M.H. Ruslan, A. Ibrahim, and H.A. Kazem, "Performance analysis of photovoltaic thermal (PVT) water collectors," *Energy Conversion and Management*, vol. 78, pp. 641-651, 2014.
- [72] S. Hassani, R. Saidur, S. Mekhilef, and R.A. Taylor, "Environmental and exergy benefit of nanofluid-based hybrid PVT systems," *Energy Conversion and Management*, vol. 123, pp. 431-444, 2016.
- [73] A.N. Al-Shamani *et al.*, "Nanofluids for improved efficiency in cooling solar collectors - A review," *Renewable and Sustainable. Energy Reviews*, vol. 38, pp. 348-367, 2014.
- [74] A.N. Al-Shamani, K. Sopian, S. Mat, H.A. Hasan, A.M. Abed, and M.H. Ruslan, "Experimental studies of rectangular tube absorber photovoltaic thermal collector with various types of nanofluids under the tropical climate conditions," *Energy Conversion and Management*, vol. 124, pp. 528-542, 2016.
- [75] H.A. Hussien, A.H. Numan, and A.R. Abdulmunem, "Improving of the photovoltaic / thermal system performance using water cooling technique," in *Proc. IOP Conference Series: Materials Science and Engineering*, 2015, pp. 012020
- [76] R. Nasrin, N.A. Rahim, H. Fayaz, and M. Hasanuzzaman, "Water/MWCNT nanofluid based cooling system of PVT: Experimental and numerical research," *Renewable Energy*, vol. 121, pp. 286-300, 2018.
- [77] O.K. Ahmed and S.M. Bawa, "Reflective mirrors effect on the performance of the hybrid PV/thermal water collector," *Energy for Sustainable Development*, vol. 43, pp. 235-246, 2018.
- [78] G. Evola and L. Marletta, "Exergy and thermoeconomic optimization of a water-cooled glazed hybrid photovoltaic/thermal (PVT) collector," *Solar Energy*, vol. 107, pp. 12-25, 2014.
- [79] J. Yazdanpanahi, F. Sarhaddi, and M.M. Adeli, "ScienceDirect Experimental investigation of exergy efficiency of a solar photovoltaic thermal (PVT) water collector based on exergy losses," *Solar Energy*, vol. 118, pp. 197-208, 2015.
- [80] S. Aberoumand, S. Ghamari, and B. Shabani, "Energy and exergy analysis of a photovoltaic thermal (PV/T) system using nano fluids : An experimental study," *Solar Energy*, vol. 165, pp. 167-177, 2018.
- [81] N. Arcuri, F. Reda, and M. De Simone, "Energy and thermo-fluid-dynamics evaluations of photovoltaic panels cooled by water and air," *Solar Energy*, vol. 105, pp. 147-156, 2014.
- [82] M.Y. Othman, K. Sopian, B. Yatim, and W.R. Daud, "Development of advanced solar assisted drying systems," *Renewable Energy*, vol. 31, no. 5, pp. 703-709, 2006.
- [83] A. Tiwari and M.S. Sodha, "Parametric study of various configurations of hybrid

- PV/thermal air collector: Experimental validation of theoretical model,” *Solar Energy Materials and Solar Cells*, vol. 91, no. 1, pp. 17-28, 2007.
- [84] S.C. Solanki, S. Dubey, and A. Tiwari, “Indoor simulation and testing of photovoltaic thermal (PV/T) air collectors,” *Applied Energy*, vol. 86, no. 11, pp. 2421-2428, 2009.
- [85] K. Sopian, K.S. Yigit, H.T. Liu, S. Kakaç, and T.N. Veziroglu, “Performance analysis of photovoltaic thermal air heaters,” *Energy Conversion and Management*, vol. 37, no. 11, pp. 1657-1670, 1996.
- [86] M.E. Alfegi, K. Sopian, M.Y. Othman, and B. Yatim, “Transient mathematical model of both side single pass photovoltaic thermal air collector,” *ARPJ Journal of Engineering and Applied Sciences*, vol. 2, no. 5, pp. 22-26, 2007.
- [87] M. E. A. Alfegi, K. Sopian, M. Y. H. Othman, and B. B. Yatim, “Experimental investigation of single pass, double duct photovoltaic thermal (PV/T) air collector with CPC and fins,” *American Journal of Applied Sciences*, vol. 5, no. 7, pp. 866–871, 2008.
- [88] G. L. Jin *et al.*, “Evaluation of single-pass photovoltaic-thermal air collector with rectangle tunnel absorber,” *American Journal of Applied Sciences*, vol. 7, no. 2, pp. 277–282, 2010.
- [89] K. Sopian, H.T. Liu, S. Kakac, and T.N. Veziroglu, “Performance of a double pass photovoltaic thermal solar collector suitable for solar drying systems,” *Energy Conversion and Management*, vol. 41, no. 4, pp. 353–365, 2000.
- [90] M.Y. Othman, B. Yatim, K. Sopian, and M.N. Bakar, “Double-pass photovoltaic thermal solar air collector with compound parabolic concentrator and fins,” *Journal of Energy Engineering.*, vol. 132, no. 3, pp. 116–120, 2006.
- [91] H.A. Zondag and W.G. Van Helden, “PV-thermal domestic systems,” in *Proc. of the 3rd World Conference on Photovoltaic Energy Conversion*, 2003, pp. 2000–2003.
- [92] J.K. Tonui and Y. Tripanagnostopoulos, “Air-cooled PVT solar collectors with low cost performance improvements,” *Solar Energy*, vol. 81, no. 4, pp. 498–511, 2007.
- [93] Y.B. Assoa and C. Ménézo, “Dynamic study of a new concept of photovoltaic-thermal hybrid collector,” *Solar Energy*, vol. 107, pp. 637–652, 2014.
- [94] G. Fraisse, C. Ménézo, and K. Johannes, “Energy performance of water hybrid PVT collectors applied to combisystems of Direct Solar Floor type,” *Solar Energy*, vol. 81, no. 11, pp. 1426–1438, 2007.
- [95] J. J. D. Anderson, “Governing Equations of Fluid Dynamics,” in *Computational Fluid Dynamics*, 3rd ed., vol. 2, J.F. Wendt, Ed. Belgium: Springer Science & Business Media, 2009, pp. 15–51.
- [96] Y.A. ÇENGEL, and A.J. GHAJAR, *Heat and Mass Transfer*, NY: McGraw-Hill, 2015, pp. 473-507.
- [97] H.P. Garg, *Advances in Solar Energy Technology*, Holland: Springer, 1987, pp. 259-348.
- [98] H.L. Tsai, C. Hsu, and B. Lin, “Design and evaluation of photovoltaic/thermal-assisted heat pump water heating system,” in *Proc. International and Symposium on Computer Consumer and Control (IS3C)*, 2014, pp. 59–62.
- [99] J.H. Wattmuff, “Solar and wind induced external coefficient for solar collectors,” *Coop. Mediterr. pour l’Energie Solaire, Rev. Int. d’Heliotechnique, 2nd Quart.*, 1977, pp. 56–60,
- [100] Z. Xu and C. Kleinstreuer, “Computational Analysis of Nanofluid Cooling of

- High Concentration Photovoltaic Cells,” *Journal of Thermal Science and Engineering Applications*, vol. 6, no. 3, pp. 031009, 2013.
- [101] S. Dubey, J.N. Sarvaiya, and B. Seshadri, “Temperature dependent photovoltaic (PV) efficiency and its effect on PV production in the world - A review,” *Energy Procedia*, vol. 33, pp. 311–321, 2013.
- [102] F. Yazdanifard and M. Ameri, “Exergetic advancement of photovoltaic/thermal systems (PVT): A review,” *Renewable and Sustainable Energy Reviews*, vol. 97, pp. 529-553, 2018.
- [103] R. Petela, “Exergy of Heat Radiation,” *Journal of Heat Transfer*, vol. 86, no. 2, pp. 187, 2012.
- [104] A. Bejan, G. Tsatsaronis, and M. Moran, *Thermal Design and Optimization*, NY: John Wiley and Sons, 1996, pp. 320-343.
- [105] T.T. Chow, G. Pei, K.F. Fong, Z. Lin, A.L. Chan, and J. Ji, “Energy and exergy analysis of photovoltaic-thermal collector with and without glass cover,” *Applied Energy*, vol. 86, no. 3, pp. 310-316, 2009.
- [106] M. Pons, “On the reference state for exergy when ambient temperature fluctuates,” *International Journal of Thermodynamics*, vol. 12, no. 3, pp. 113-121, 2009.

Vita

Marwan Hicham Osman was born in 1995 in Beirut, Lebanon. He received his secondary education in Sharjah, UAE. He received the B.Sc. degree in Mechanical Engineering from University of Sharjah in 2017. During the last semester in University of Sharjah, he worked as a part time Graphic Design Lab Assistant.

In September 2017, he joined the Mechanical Engineering master's program in the American University of Sharjah as a graduate teaching assistant.